The Cellular Physiology of Canine Chondrocytes: an *in-vitro* Study on Phenotype Regulation and Characteristics of Cell Death

(犬軟骨細胞の細胞生物学的態度：培養環境における分化調節と細胞死に関する研究**)**

Ekkapol Akaraphutiporn

HOKKAIDO UNIVERSITY

The Cellular Physiology of Canine Chondrocytes: an *in-vitro* Study on Phenotype Regulation and Characteristics of Cell Death

犬軟骨細胞の細胞生物学的態度：培養環境における分化調節と細胞死に関する研究

A Dissertation for the Degree of Doctor of Philosophy

Ekkapol Akaraphutiporn

Laboratory of Veterinary Surgery

Department of Veterinary Clinical Sciences

Graduate School of Veterinary Medicine

2020

Dissertation Examination Committee:

Professor Masahiro Okumura, Supervisor

Professor Kazuhiro Kimura

Professor Takashi Kimura

Associate Professor Atsushi Kobayashi

Assistant Professor Takafumi Sunaga

The Cellular Physiology of Canine Chondrocytes: an *in-vitro* Study on Phenotype Regulation and Characteristics of Cell Death

by

Ekkapol Akaraphutiporn

A dissertation submitted to the Graduate School of Veterinary Medicine of Hokkaido University in fulfillment of the requirements for the degree of Doctor of Philosophy

Hokkaido University

Japan

2020

Table of Contents

Table of Contents i

List of Publications Related to the Dissertation v

List of Abbreviations vi

List of Tables ix

List of Figures x

CHAPTER 1 General Introduction 1

CHAPTER 2 Alterations in characteristics of canine articular chondrocytes in non-passaged long-term monolayer culture: matter of differentiation, dedifferentiation and redifferentiation 9

2.1 Summary 10

2.2 Introduction 11

2.3 Material and Methods 14

2.3.1 Reagents 14

2.3.2 Chondrocytes isolation and culture 14

2.3.3 Chondrocytes treatment 15

2.3.4 Cell viability assay 15

2.3.5 Biochemical analysis 16

2.3.6 Identification of GAGs in ECM 16

2.3.7 RNA isolation and qPCR analysis 17

2.3.8 Ultrastructure analysis 17

2.3.9 Statistical analysis 18

2.4 Results 20

2.4.1 Effect of seeding density and culture time on the morphology of chondrocytes 20

2.4.2 Long-term monolayer cultured chondrocytes are able to resume proliferation after passage but have an altered morphology 20

2.4.3 Chondrocytes cultured with different initial seeding densities exhibit a similar pattern of proliferation curve, while cell number was decreased after maintained in the post-confluent condition 22

2.4.4 Quantification of total DNA and GAGs content 22

2.4.5 Long-term monolayer cultured chondrocytes synthesize abundant amount of ECM as indicated by GAGs content 23

2.4.6 Alteration in gene expression of long-term monolayer cultured chondrocytes 27

2.4.7 Long-term monolayer cultured causes cellular organelle abnormality 29

2.5 Discussion 31

CHAPTER 3 Effects of pentosan polysulfate on cell proliferation, cell cycle progression and cyclin-dependent kinases expression in canine articular chondrocytes 37

3.1 Summary 38

3.2 Introduction 39

3.3 Material and Methods 42

3.3.1 Reagents 42

3.3.2 Chondrocytes isolation and culture 42

3.3.3 Chondrocytes treatment 43

3.3.4 Cell viability assay 43

3.3.5 Cell apoptosis assay 44

3.3.6 Cell cycle analysis 44

3.3.7 Biochemical analysis 44

3.3.8 RNA isolation and qPCR analysis 45

3.3.9 Statistical analysis 46

3.4 Results 48

3.4.1 Effect of PPS on morphological appearance and confluency condition of cultured chondrocytes 48

3.4.2 PPS reduces chondrocyte viability 48

3.4.3 PPS has no cytotoxic effect on chondrocytes 50

3.4.4 PPS increases the proportion of chondrocytes in the G1 phase while reducing the proportion of chondrocytes in the S phase of the cell cycle 50

3.4.5 Effect of PPS on chondrocyte DNA and GAGs Content 51

3.4.6 PPS downregulates cell cycle regulator genes, while promotes Col2 expression 55

3.5 Discussion 57

CHAPTER 4 An insight into the role of apoptosis and autophagy in nitric oxide-induced chondrocyte cell death 62

4.1 Summary 63

4.2 Introduction 64

4.3 Material and Methods 67

4.3.1 Reagents and antibodies 67

4.3.2 Chondrocytes isolation and culture 68

4.3.3 Chondrocytes treatment 68

4.3.4 Cell viability assay 69

4.3.5 Cell apoptosis assay 69

4.3.6 Caspase-3 activity assay 69

4.3.7 Quantification of nitrite 70

4.3.8 Protein isolation and Western blot analysis 70

4.3.9 RNA isolation and qPCR analysis 71

4.3.10 Immunocytochemistry assay 71

4.3.11 Statistical analysis 72

4.4 Results 74

4.4.1 IL-1β and starvation condition enhances the effect of NO-induced cell death.....74

4.4.2 Co-treatment with SNP and IL-1β under nutrient-deprived condition exhibit low cell viability but express high autophagosome formation, as detected by LC3-II.....74

4.4.3 Activation of autophagy by rapamycin reduces cell apoptosis.....77

4.4.4 NO reduces activation of autophagy, autophagic flux and Atg mRNA expression77

4.4.5 NO generated by SNP is not directly related to cell death 79

4.4.6 NO reduces autophagy via promotion of the ERK, Akt and mTOR pathway.....79

4.4.7 Inhibition of mTOR/p70S6K pathway by rapamycin impairs NO-induced cell apoptosis 83

4.4.8 NO-induced cell apoptosis is predominantly through the caspase-independent pathway 83

4.5 Discussion 87

CHAPTER 5 General Conclusions.....91

References.....95

Abstract of the Dissertation 108

Acknowledgements.....110

List of Publications Related to the Dissertation

The contents of this dissertation are based on the following original publications and submitted manuscripts under review listed below by their Roman numeral I-VI of the research conducted during the period October 2016 - September 2020.

I. **Akaraphutiporn, E.**, Sunaga, T., Bwalya, E. C., Echigo, R. and Okumura, M. 2020. Alterations in characteristics of canine articular chondrocytes in non-passaged long-term monolayer culture: matter of differentiation, dedifferentiation and redifferentiation. J Vet Med Sci 82: 793-803.

II. **Akaraphutiporn, E.**, Bwalya, E. C., Kim, S., Sunaga, T., Echigo, R. and Okumura, M. Effects of Pentosan polysulfate on cell proliferation, cell cycle progression and cyclin-dependent kinases expression in canine articular chondrocytes. J Vet Med Sci. In press.

III. **Akaraphutiporn, E.**, Bwalya, E. C., Wang, Y., Mwale C., Sunaga, T. and Okumura, M. An insight into the role of apoptosis and autophagy in nitric oxide-induced chondrocyte cell death. Under review

List of Abbreviations

2D	Two-dimensional
3D	Three-dimensional
ACI	Autologous chondrocyte implantation
ADAMTS	A disintegrin and metalloproteinase with thrombospondin motifs
AIF	Apoptosis-inducing factor
Akt	Protein kinase B
ANOVA	Analysis of variance
CDK	Cyclin-dependent kinase
cDNA	Complementary deoxyribonucleic acid
Col1	Collagen type I
Col2	Collagen type II
Col3	Collagen type III
DAPI	4’,6-diamidino-2-phenylindole
DMEM	Dulbecco’s modified eagle’s medium
DMMB	Dimethylmethylene blue
DMOADs	Disease modifying osteoarthritic drugs
DMSO	Dimethyl sulfoxide
DNA	Deoxyribonucleic acid
ECM	Extracellular matrix
EDTA	Ethylenediaminetetraacetic acid
ERK	Extracellular signal-regulated kinase
FBS	Fetal bovine serum
FITC	Fluorescein isothiocyanate

GAGs	Glycosaminoglycans
GAPDH	Glyceraldehyde-3-phosphate dehydrogenase
HEPES	4-(2-hydroxyethyl)-1-piperazineethanesulfonic acid
HRP	Horseradish peroxidase
IL-1β	Interleukin-1 beta
iNOS	Inducible nitric oxide synthase
LC3	Microtubule-associated protein light chain 3
M-MLV	Murine leukemia virus reverse transcriptase
MMP	Matrix metalloproteinase
MSC	Mesenchymal stem cells
mRNA	Messenger ribonucleic acid
mTOR	Mammalian target of rapamycin
MTT	3-(4,5-dimehylthiazolyl-2)2,5-diphenyltetrazolium bromide
NCBI	National center for biotechnology information
NF-κB	Nuclear factor-kappa B
NO	Nitric oxide
NOS	Nitric oxide synthase
OA	Osteoarthritis
p62	Sequestosome-1
p70S6K	p70 ribosomal protein S6 kinase
PARP	Poly (ADP-ribose) polymerase
PBS	Phosphate-buffered saline
PBST	Phosphate-buffered saline with Tween 20
PGE2	Prostaglandin E2
PI	Propidium iodide

PPS	Pentosan polysulfate
PVDF	Polyvinylidene difluoride
qPCR	Quantitative real-time polymerase chain reaction
RA	Rheumatoid arthritis
RER	Rough endoplasmic reticulum
RIPA	Radioimmunoprecipitation assay
RNA	Ribonucleic acid
ROS	Reactive oxygen species
RT-PCR	Reverse transcription polymerase chain reaction
SDS-PAGE	Sodium dodecyl sulfate-polyacrylamide gel electrophoresis
SE	Standard error of the mean
SNP	Sodium nitroprusside
Sox9	SRY-Box transcription factor 9
TEM	Transmission electron microscopy

List of Tables

Table 1. The sequence of primers used for qPCR analysis to evaluate phenotypic stability of chondrocytes in long-term monolayer culture condition 19

Table 2. The sequence of primers used for qPCR analysis to evaluate cell cycle regulator genes and phenotypic stability of PPS treated chondrocytes 47

Table 3. Percentage of cells in each phase of cell cycle analyzed by the FlowJo software program using Watson Pragmatic model 54

Table 4. The sequence of primers used for qPCR analysis to evaluate autophagy-related genes in SNP treated chondrocytes 73

List of Figures

Figure 1. Morphological appearance and confluency condition of long-term monolayer cultured chondrocytes observed under a light microscope. 21

Figure 2. Chondrocytes cultured with different initial seeding densities exhibit a similar pattern of proliferation curve. 24

Figure 3. The number of cultured chondrocytes was decreased after maintained in post-confluent condition. 24

Figure 4. Long-term monolayer culture condition promotes GAGs synthesis but reduce DNA content of chondrocytes. 25

Figure 5. Long-term monolayer cultured chondrocytes synthesize an abundant amount of ECM as indicated by GAGs content.....26

Figure 6. Alteration in gene expression of long-term monolayer cultured chondrocytes. 28

Figure 7. Massively dilated RER was observed in chondrocytes after maintained in long-term monolayer culture conditions.....30

Figure 8. Morphological appearance and confluency condition of PPS treated chondrocytes observed under a light microscope. 49

Figure 9. Treatment with PPS resulted in reduced chondrocyte viability. 52

Figure 10. Treatment with PPS showed no cytotoxic effect on cultured chondrocytes. 52

Figure 11. PPS increases the proportion of chondrocytes distributed in the G1 phase while reducing the proportion of chondrocytes distributed in the S phase of the cell cycle. 53

Figure 12. Treatment with PPS promotes GAGs synthesis but reduces DNA content of chondrocytes in a concentration-dependent manner.....53

Figure 13. PPS downregulates cell cycle regulator genes, while promotes collagen type II expression. 56

Figure 14. Co-treatment with SNP and IL-1β under nutrient-deprived condition enhances the effect of NO-induced cell death. 75

Figure 15. Autophagosome formation was increased in the chondrocytes that pre-treated with IL-1β and stimulated with SNP under nutrient-deprived condition. 76

Figure 16. Activation of autophagy by rapamycin reduced cell apoptosis, whereas the inhibition of autophagy by bafilomycin had no effect on cell apoptosis. 80

Figure 17. Treatment with SNP resulted in reduction in autophagic activity, autophagic flux and Atg mRNA expression in chondrocytes. 81

Figure 18. Treatment with SNP resulted in reduction in cytoplasmic LC3-II puncta under the presence of bafilomycin. 82

Figure 19. The phosphorylation of ERK, Akt, mTOR and p70S6K were promoted in SNP treated chondrocytes. 85

Figure 20. The cleavage of PARP and caspase-3 activation in response to apoptosis was weakly detected, while AIF was highly expressed in SNP treated chondrocytes. 86

CHAPTER 1

General Introduction

Cartilage is a form of connective tissue found in various parts throughout the body that provides flexibility and supports other tissues. Cartilage has a unique structure in that it does not contain blood vessels, nerve supply or lymphatics and therefore relies only on diffusion for nutrient supply. In addition to this, it consists of only a single type of cellular component termed chondrocytes, which are embedded in the extracellular matrix (ECM) and play a crucial role in the cartilage homeostasis by maintaining ECM components (Hall, 2005; Sophia Fox et al., 2009; Athanasiou et al., 2013). Based on the differences in function and the molecular component, cartilage is commonly classified into three types; including hyaline cartilage, elastic cartilage and fibrocartilage (Hall, 2005; Athanasiou et al., 2013). Hyaline cartilage is the most abundant type of cartilage located on the articular surfaces of bone, between the ribs and some parts of the respiratory system. It has a smooth surface, bluish-white and shiny appearance, which is composed of dense ECM comprising primarily of water, collagens, proteoglycans and a lesser amount of other non-collagenous proteins (Responte et al., 2007; Sophia Fox et al., 2009; Athanasiou et al., 2013). Due to ECM structure and matrix components, hyaline cartilage is highly hydrated, with the water content accounting for 65-80% of the total cartilage weight (Responte et al., 2007; Sophia Fox et al., 2009; Xia et al., 2017). This large volume of water is retained within ECM, and together with its other components provide properties that enable the cartilage to withstand compressive, tensile and shear stresses during mechanical use, which is a unique physiological property of articular cartilage (Sophia Fox et al., 2009; Xia et al., 2017). Articular cartilage is a thin layer of hyaline cartilage that covers the ends of the bones where they articulate with each other and form a joint. It provides a smooth, low-friction gliding surface of synovial joints and takes a vital role in distributing mechanical loads generated during movement, which is obligatory for proper locomotion (Sophia Fox et al., 2009; Athanasiou et al., 2013; Yuan et al., 2015). Nevertheless, the structures of articular

cartilage could be easily damaged from a variety of causes and consequently leads to functional impairment in affected joints.

Osteoarthritis (OA) is the most common form of cartilage degenerative disease in both human and veterinary medicine, which involves all structures of the affected joints. It progressively causes impaired mobility, disability and pain, especially in the aging population worldwide (Yuan et al., 2015; Kapoor, 2015). This disease is characterized by a progressive loss of articular cartilage, together with the involvement of pathological change in the entire joint structures including the inflammation of synovial membrane, thickening of the joint capsule, degeneration of ligaments and subchondral bone remodeling, which subsequently results in the impaired mechanical function of the joint, limitation of movement and chronic pain (Poole, 2012; Loeser et al., 2012; Man and Mologhianu, 2014; Kapoor, 2015). Based on the clinical signs and physical findings, the prevalence of OA in a human population was previously estimated at 27 million adults in the US and 8.5 million adults in the UK, with a higher prevalence among the older population (Lawrence et al., 2008; Neogi, 2013). It is even reported that the total number of OA patients is more than 600 million people all around the world (Yuan et al., 2015). In veterinary medicine, it has been estimated that the prevalence of OA can be as high as 20% in the canine population with more than a year of age (Anderson et al., 2018). The consequent disability and chronic pain caused by OA is directly associated with both quality of life and economic burden. A recent study reveals that the estimated cost related to OA could be between 0.25-0.50% of a country's GDP (Puig-Junoy and Ruiz Zamora, 2015). Despite the high prevalence of OA and substantial economic impact, there are no current interventions proven to restore degraded articular cartilage or effectively prevent the progression of the disease (Athanasiou et al., 2013; Yuan et al., 2015; Kapoor, 2015; Mora et al., 2018). This is due to the poor capacity for self-regeneration of articular cartilage, together with the multifactorial etiology and complexity of OA pathogenesis, in which multiple joint

structures are involved (Man and Mologhianu, 2014; Kapoor, 2015; Xia et al., 2017). Even though several studies have identified the concept of OA pathogenesis, the underlying molecular mechanisms regulating OA initiation and progression are still not fully understood (Xia et al., 2017).

The limit in self-regeneration capacity of articular cartilage was related to the unique structure that has neither blood supply nor innervation, an extensively prolonged turnover rate of ECM and the low proliferative nature with a low density of chondrocytes (Walsh et al., 2003; Karuppal, 2017; Nam et al., 2018). Among the ECM components, the turnover rate of proteoglycans could take up to 25 years, whereas collagens could be longer than 100 years (Maroudas et al., 1998; Verzijl et al., 2000). While the articular cartilage mainly consists of ECM and water, it has a relatively low percentage of cellular components. The chondrocytes occupy approximately 1-5% of the total cartilage volume (Sophia Fox et al., 2009; Athanasiou et al., 2013). Furthermore, chondrocytes are recognized as quiescent cells that display very low mitotic activity under physiological conditions in adult articular cartilage (Sandell and Aigner, 2001; Hall, 2005; Goldring and Marcu, 2009; Kapoor, 2015). Nevertheless, these chondrocytes are an essential basic metabolic unit of cartilage that are responsible for maintaining matrix metabolism, which includes the synthesis of both matrix components and proteolytic enzymes for matrix degradation (Hall, 2005; Athanasiou et al., 2013; Akkiraju and Nohe, 2015). Several biochemical mediators that contribute to inflammation and catabolic pathways are produced by chondrocytes. Conversely, the metabolic activities of chondrocytes can be altered by their biochemical mediators as well as excessive mechanical stresses (Goldring and Berenbaum, 2004; Kapoor, 2015).

An imbalance between matrix synthesis and degradation is an apparent characteristic of osteoarthritic cartilage (Goldring and Marcu, 2009). During the course of OA, the metabolic activities of chondrocytes are altered, which results in the loss of cartilage homeostasis and

metabolic shift toward the catabolic reaction, leading to ECM degradation and cartilage destruction (Goldring and Marcu, 2009; Kapoor, 2015). The chondrocytes respond to the presence of inflammatory mediators, oxidative stress and a variety of physical stimuli by an increase in proteolytic enzymes secretion such as the matrix metalloproteinase (MMP) family and a disintegrin and metalloproteinase with thrombospondin motifs (ADAMTS), which potentially degrade the structure of proteoglycan and collagen in the cartilage ECM (Goldring and Marcu, 2009; Loeser et al., 2012; Man and Mologhianu, 2014; Akkiraju and Nohe, 2015). Apart from an alteration in metabolic activities, the progression of osteoarthritic cartilage also affects the characteristic of chondrocytes by altering cellular response. Under the pathological condition of degenerative articular cartilage, the chondrocytes that are normally resting in the post-mitotic state, which rarely proliferate, become more active and demonstrates the ability to reinitiate mitotic activity (Hulth et al., 1972; Rothwell and Bentley, 1973; Sandell and Aigner, 2001; Hall, 2005). This sudden change from resting to active chondrocytes, which should not occur in normal adult articular cartilage, could signify that the characteristic of differentiated chondrocytes was also changed. In fact, previous studies have shown that the cellular responses during OA progression could be classified into five categories: (1) phase of proliferation and cell death, (2) alteration in anabolic activity, (3) alteration in catabolic activity, (4) phenotypic shift, and (5) osteophyte formation (Sandell and Aigner, 2001). Among these classifications, the aims of this study is to focus on the alteration in chondrocyte phenotype, cell proliferation and mechanism of programmed cell death.

The degenerative condition and progressive loss of articular cartilage during the progression of OA is a major contributor to the inflammatory process, which results in swelling, pain and limited movement of joints (Poole, 2012; Loeser et al., 2012; Man and Mologhianu, 2014; Kapoor, 2015). Due to the limited self-regeneration capacity of articular cartilage, the damaged structures are unlikely to be restored. Thus, there is no cure for OA. Existing strategies

for OA treatment and prevention are mostly palliative, which are targeted towards pain control and halting disease progression, as well as to restore joint function (Anandacoomarasamy and March, 2010; Mobasheri, 2013; Mora et al., 2018; Zhang et al., 2019). The purposes of these management strategies are to improve the quality of life and retarding the necessity of surgical intervention as much as possible (Yu and Hunter, 2015). Currently, the available treatment options include physical approaches such as physiotherapy and rehabilitation, weight control, pharmacological management and surgical management (Henrotin et al., 2005; Yuan et al., 2015; Yu and Hunter, 2015). However, prolonged treatment with pharmacological intervention, particularly with anti-inflammatory drugs, could be associated with a variety of side effects (Henrotin et al., 2005; Yu and Hunter, 2015; Zhang et al., 2019; Ghouri and Conaghan, 2019). During the past decades, the development of novel pharmacological management for OA has focused on the disease progression by regenerating the original structure of cartilage, instead of only relieving the clinical symptoms (Mobasheri, 2013; Ghouri and Conaghan, 2019). Therefore, a particular type of drug that aims to prevent further damage on cartilage and reverse the pathological changes associated with OA progression has been developed under the terms of disease modifying osteoarthritic drugs (DMOADs) (Henrotin et al., 2005; Mobasheri, 2013; Ghouri and Conaghan, 2019). Up until now, a number of therapeutic agents have been proposed as DMOADs, whereas some of those are available and have been used in certain parts of the world. However, the mechanism of action of DMOADs on articular cartilage is yet to be fully explained (Anandacoomarasamy and March, 2010; Ghouri and Conaghan, 2019). While more clinical trials are needed, the understanding of molecular mechanisms involved in the pathogenesis of OA will be beneficial for the development of DMOADs as these drugs are targeted on the cartilage structures. In the most severe cases of OA with an inadequate response to either non-pharmacological or pharmacological treatment, the surgical approaches should be taken into consideration (Anandacoomarasamy and March, 2010; Katz et al., 2010; Yu and

Hunter, 2015). Regenerative medicine and tissue engineering are another prospective strategy that has developed rapidly in the last few decades (Luyten and Vanlauwe, 2012; Makris et al., 2015). Unlike the concept of a well-known surgical technique like total joint replacement, regenerative medicine and tissue engineering aim to provide an alternative solution to restore both cartilage structure and joint function by regenerating damaged tissues using cells-based approaches or enhance self-repair mechanisms (Zhang et al., 2009; Luyten and Vanlauwe, 2012; Makris et al., 2015). Current existing techniques for cartilage repair include microfracture, autografts transplantation and autologous chondrocyte implantation (ACI) (Zhang et al., 2009; Nam et al., 2018; Davies and Kuiper, 2019).

The cultivation of chondrocytes plays a vital role in both research purposes and therapeutic interventions, particularly in autologous cell-based approaches, which require a high quantity of cultured chondrocytes. Following the chondrocytes isolation from cartilage, monolayer culture is a culture method that is commonly used for cell expansion as it is simple, less time consuming and a large amount of cells could be obtained (Melero-Martin and Al-Rubeai, 2007; Isyar et al., 2016). Due to the nature of normal articular cartilage that contains low cellular components, the expansion process is rather necessary to achieve sufficient cells number. However, chondrocytes cultured in monolayer tend to rapidly dedifferentiate, especially after facing long expansion time and repeated culture (Darling and Athanasiou, 2005; Melero-Martin and Al-Rubeai, 2007; Caron et al., 2012). The dedifferentiation process of chondrocytes causes rapid phenotypic loss, which results in the morphological change from either round or polygonal to a fibroblastic-like appearance, together with an alteration in synthetic activities (Schulze-Tanzil et al., 2002; Darling and Athanasiou, 2005; Melero-Martin and Al-Rubeai, 2007; Caron et al., 2012). Under the normal condition, chondrocytes mainly synthesize high molecular weight proteoglycan as aggrecan and collagen type II (Col2), which are major matrix components in cartilage ECM and considered as a chondrocyte specific

marker (Melero-Martin and Al-Rubeai, 2007; Caron et al., 2012). While the synthetic activities of dedifferentiated chondrocytes are shifted from the chondrocyte specific marker to low molecular weight proteoglycan, collagen type I (Col1) and collagen type III (Col3) (Melero-Martin and Al-Rubeai, 2007; Caron et al., 2012). This dedifferentiation process of chondrocytes is a significant limitation on their use in both research and tissue engineering applications. To overcome the limitation of monolayer culture, which is also known as two-dimensional (2D) culture, several alternative culture models that could decelerate the dedifferentiation process has been established (Melero-Martin and Al-Rubeai, 2007; Otero et al., 2012; Caron et al., 2012). These alternative culture techniques include the use of additional culture supplements, using tissue-culture scaffolds, high cell density cultures and three-dimensional (3D) cultures (Melero-Martin and Al-Rubeai, 2007; Otero et al., 2012).

For this study, it was of interest to investigate the cellular physiology of canine articular chondrocytes that contribute to phenotypic stability and molecular mechanism of programmed cell death in the monolayer culture system, since the phenotypic stability of chondrocytes and cell death has played an essential role in both physiological and pathological conditions of articular cartilage. Consequently, understanding the precise mechanisms of these events will undoubtedly provide insight into the manipulation of chondrocytes, which could be beneficial for cartilage degenerative disease treatment. This study was classified into three sections: First, it presents the strategy of expanding isolated chondrocytes using a specific culture model to preserve phenotypic stability. Second, the effects of certain DMOADs was evaluated on the phenotypic stability and proliferative activity of chondrocytes, particularly in cell cycle modulation. In the last section, the molecular mechanisms regulating apoptosis and autophagy in nitric oxide (NO) -induced chondrocyte cell death were investigated.

CHAPTER 2

Alterations in characteristics of canine articular chondrocytes in non-passaged long-term monolayer culture: matter of differentiation, dedifferentiation and redifferentiation

2.1 Summary

The purpose of the study was to investigate the effects of culture time on phenotypic stability of canine articular chondrocytes in non-passaged long-term monolayer culture conditions. Canine articular chondrocytes were isolated and cultured from femoral head cartilages of four dogs. Third passage chondrocytes were seeded at three different initial seeding densities (2,000, 10,000 and 50,000 cells/cm^2) and maintained in monolayer culture condition up to 8 weeks without undergoing subculture after confluence. The evaluation was performed on the characteristic changes of chondrocytes based on the morphological appearance, proliferation capability, DNA content, glycosaminoglycans (GAGs) content, mRNA expression and ultrastructure of chondrocytes. Our results from MTT colorimetric assay and Hoechst assay reveal that cultured chondrocytes maintained under post-confluence condition could become stratified, while exhibited a capability to proliferate up to 4 weeks. The accumulation of GAGs content was increased in a time-dependent manner from 2 to 8 weeks as determined dimethylmethylene blue (DMMB) assay and alcian blue staining. The chondrocyte mRNA expression profile analyzed by quantitative real-time polymerase chain reaction (qPCR) was drastically affected by prolonged culture time. Col2, aggrecan, Sox9 and MMP-13 mRNA expression were significantly upregulated, whereas Col1 mRNA expression was downregulated. In addition, the ultrastructure of chondrocytes observed by transmission electron microscopy (TEM) indicated the dilation of rough endoplasmic reticulum (RER). These findings suggest that the chondrocytes cultured in non-passaged long-term monolayer culture conditions could be partially redifferentiated through the spontaneous redifferentiation process using only standard culture media without the addition of chondrogenic supplements or tissue-culture scaffolds.

2.2 Introduction

Articular cartilage is a thin layer of hyaline cartilage that anatomically covers the articular surfaces of bones, which provides a smooth, low-friction gliding and load-bearing surface in the synovial joint (Sophia Fox et al., 2009; Athanasiou et al., 2013; Yuan et al., 2015). It basically comprises two major fractions, including the cellular portion and ECM components. The cartilage structures were supported by ECM, whereas the ECM is directly responsible for the mechanical load in a joint and also provides biochemical support to the cellular component (Gao et al., 2014). On the other hand, the only cellular component embedded in cartilage named chondrocytes is responsible for synthesizing and maintenance the components of ECM (Hall, 2005; Sophia Fox et al., 2009; Athanasiou et al., 2013). Chondrocytes are highly specialized cells that originated from mesenchymal stem cells (MSC) and undergo various stages of differentiation and occupied in cartilage as a resting cell in a small amount compared to the total cartilage volume (Archer and Francis-West, 2003; Athanasiou et al., 2013; Phull et al., 2016). Despite the small fraction and low proliferative nature of chondrocytes, its existence was the most vital factor in maintaining healthy cartilage tissue by involved in the homeostasis of ECM (Hall, 2005; Athanasiou et al., 2013). Therefore, chondrocytes isolated from various sources are the most desirable cell used for both research purposes and therapeutic interventions.

The cultivation of chondrocytes was widely used and could be considered as the most powerful technique for investigating the cellular mechanism associated with the phenotypic stability of chondrocytes. Generally, chondrocytes used for the *in-vitro* study were obtained from primary articular chondrocytes that were enzymatically released from the cartilage ECM and expanded in monolayer culture until an appropriate number of chondrocytes were acquired (Isyar et al., 2016). Although several culture models have currently existed, the 2D monolayer

culture may be the most suitable method for chondrocytes expansion *in-vitro*, as it is simple, less equipment is need, less time consuming and capable for produce a large amount of cell. However, expanding chondrocytes in 2D monolayer has a great disadvantage as it involved in the dedifferentiation process of chondrocytes (Stewart et al., 2000; Darling and Athanasiou, 2005; Lin et al., 2008; Caron et al., 2012). It is well known that chondrocytes culture through multiple passaging and long expansion period are unable to maintain their phenotype and rapidly dedifferentiate to a fibroblast-like chondrocytes. As a result, the morphological appearance of chondrocytes become more elongated, fibroblast-like instead of rounded, polygonal morphology (Darling and Athanasiou, 2005; Melero-Martin and Al-Rubeai, 2007; Takahashi et al., 2007; Caron et al., 2012). Furthermore, the expression of major matrix components in cartilage ECM particularly Col2 and aggrecan are drastically reduced, while the expression of a fibroblastic phenotype is increased (Melero-Martin and Al-Rubeai, 2007; Caron et al., 2012). This limited in cell number and dedifferentiation process during expansion are the most significant issues that challenge the tissue engineering applications.

Currently, there are several culture models that proved their benefit on phenotypic stability of chondrocytes such as high cell density cultures, 3D cultures and using biocompatible materials as tissue-culture scaffolds. Unlike conventional 2D monolayer culture, these culture models are capable of preventing the dedifferentiation process as well as support the redifferentiation process of dedifferentiated chondrocytes (Watt, 1988; Schulze-Tanzil et al., 2002; Lin et al., 2008; Otero et al., 2012). The principle behind these culture models is the environmental condition that enables to promote cell-cell and cell-matrix interactions, which mimic the microenvironment of chondrocytes that resided in native articular cartilage ECM (Takahashi et al., 2007; Schulze-Tanzil, 2009; Gao et al., 2014). However, although these approaches drastically improve the quality of chondrocytes as indicated by phenotypic stability,

it potentially limits cell proliferation, compared to conventional 2D monolayer culture. In addition, it is much more time consuming, requires more handling techniques and may need an additional cost (Villar-Suárez et al., 2004; Otero et al., 2012; Mhanna et al., 2014). Thus, on many occasions, the expanded chondrocytes from 2D monolayer culture are passaging again in 3D culture to encourage the redifferentiation process, which will maximize both the quality and quantity of cultured chondrocytes.

The present study focused on a strategy for canine articular chondrocytes expansion using conventional 2D monolayer culture with prolonged culture time. It is commonly known that due to the contact inhibition phenomenon, which could terminate cell proliferation, cultured cells should be passage before it became too confluent. However, this study attempts to stimulate the contact inhibition phenomenon by prolonging the culture time beyond the confluence condition for two purposes. First, we intentionally use the effect of contact inhibition to turn the chondrocytes back to their low proliferative nature. Second, we aim to create a condition of high cell density to promote ECM synthesis. This is due to the synthetic activities of chondrocytes that are inversely related to proliferative activities. We expected to use post-mitotic state chondrocytes and self-synthesis ECM from high-density culture to mimic a cartilage-like microenvironment *in-vitro*. Our hypothesis is that long-term conventional 2D monolayer conditions could promote the redifferentiation process of isolated canine articular chondrocytes. The purpose of this study was to investigate the effects of culture time on phenotypic stability of canine articular chondrocytes in non-passaged long-term monolayer culture conditions.

2.3 Material and Methods

2.3.1 Reagents

The sources of materials used were as follows: Dulbecco's modified Eagle's medium (DMEM) was purchased from Gibco (Grand Island, NY, USA); Fetal bovine serum (FBS) was purchased from Nichirei Biosciences Inc. (Tokyo, Japan); HEPES and MTT were purchased from Dojindo (Kumamoto, Japan); Papain, calf thymus DNA, DMMB, alcian blue, uranyl acetate and lead citrate were purchased from Sigma-Aldrich (St. Louis, MO, USA); KAPA SYBR FAST qPCR kit was purchased from KAPA Biosystems (Woburn, MA, USA); Epon resin and 200 mesh copper grid were purchased from Nisshin EM (Tokyo, Japan); TRIZol reagent and M-MLV RT kit were purchased from Invitrogen (Carlsbad, CA, USA); Culture dishes and culture plates were purchased from Corning (Lowell, MA, USA). All other reagents were purchased from Wako Pure Chemicals Industries (Osaka, Japan) unless stated otherwise.

2.3.2 Chondrocytes isolation and culture

The use of animal samples was in accordance with Hokkaido University Institutional Animal Care and Use Committee guidelines (approval #12–0059). Healthy canine articular cartilage tissue samples were isolated from the femoral head of four dogs (2-11 years old) at Hokkaido University Veterinary Teaching Hospital. The first two dogs were experimental Beagle dogs that were euthanized at the end of an experimental study not related to this study, while another two dogs were Pomeranian and Shetland sheepdog that were undergoing femoral head and neck ostectomy due to traumatic coxofemoral luxation. Briefly, articular cartilage tissue samples were harvested and dissected into small sections. Then the digestion process was performed in DMEM supplemented with 0.3% collagenase type I for 18 h at 37°C in a 5% CO_2 incubator. The released chondrocytes were separated by filtering through a 40 μm nylon

filter and primary chondrocytes were expanded at a density of 10,000 cells/cm^2. Chondrocytes were passaged at 80-90% confluence by washed twice with phosphate-buffered saline (PBS) and released from culture dishes using 0.05% trypsin with 0.02% ethylenediaminetetraacetic acid (EDTA) in PBS. The culture media used in this study was DMEM containing 10 mM HEPES, 25 mM $NaHCO_3$, 100 U/ml penicillin G potassium and 73 U/ml streptomycin sulfate.

2.3.3 Chondrocytes treatment

Unless specified otherwise, all cultured chondrocytes used in this study were seeded in 12-well polystyrene culture plates in DMEM containing 10% FBS and maintained at 37°C in a 5% CO_2 incubator. The third passage of chondrocytes was seeded and cultured as a monolayer at different initial seeding densities of 2,000 (Low seeding density; LD), 10,000 (Normal seeding density; ND) and 50,000 cells/cm^2 (High seeding density; HD). The culture media was changed twice per week, while cultured chondrocytes were maintained in monolayer conditions up to 8 weeks without passaging. After culture for 8 weeks, chondrocytes were passaging once to the fourth passage to confirm proliferation capability at a density of 10,000 cells/cm^2. Total cell number and cell viability were evaluated by trypan blue exclusion test once every 4 weeks. Cell morphology and confluency condition of cultured chondrocytes were observed under a light microscope.

2.3.4 Cell viability assay

Chondrocytes were seeded into 96-well polystyrene culture plates and cultured up to 168 h. The proliferation curve was generated by performing MTT colorimetric assay every 24 h. Briefly, the cells were washed once with PBS, then 0.5 mg/ml MTT solution prepared in DMEM was added into each well and incubated for 4 h at 37°C in a 5% CO_2 incubator. The MTT solution was then removed and dimethyl sulfoxide (DMSO) was added to dissolve

formazan crystals. The absorbance was measured using a Multiskan FC microplate reader (Thermo Scientific, Vantaa, Finland) at 570 nm.

2.3.5 Biochemical analysis

Cell lysates of cultured chondrocytes were collected every 2 weeks during the culture period. To perform cell digestion, the cells were washed once with PBS, then 300 µg/ml papain solution containing 20 mM Na_2HPO_4, 2 mM dithiothreitol and 1 mM EDTA was added into each well and incubated for 18 h at 60°C. The quantification of DNA content was performed by Hoechst assay with calf thymus DNA as a standard. In brief, cell lysates were mixed with 1 µg/ml Hoechst solution containing 10 mM Tris-HCl, 100 mM NaCl and 1 mM EDTA, then incubated for 10 min at room temperature and the measurement was performed using 350/460 nm filter set. The quantification of GAGs content was performed by DMMB assay with chondroitin sulfate as a standard. To quantified GAGs accumulation and GAGs released in culture media, both cell lysate and culture media were used. In brief, cell lysates or culture media were mixed with 15 µg/ml DMMB solution containing 40.5 mM glycine, 27.5 mM NaCl and 0.1 M acetic acid, then incubated for 1 min at room temperature and the absorbance was measured at 525 nm. The results were normalized with DNA content. Both assays were measured using an Infinite M200 Pro microplate reader (Tecan, Männedorf, Switzerland).

2.3.6 Identification of GAGs in ECM

The accumulation of GAGs content in ECM was identified by alcian blue staining every 2 weeks during the culture period. To perform alcian blue staining, the cells were washed once with PBS, then fixed with 4% formaldehyde in PBS for 30 min at room temperature. The formaldehyde solution was then removed and the solution of 1% alcian blue prepared in distilled water was added into culture plates and incubated for 30 min at room temperature.

After staining, cells were washed thrice with 0.1 N HCl and once with distilled water to neutralize the acidity of HCl. The accumulation of GAGs was observed on both visual inspections and under a light microscope.

2.3.7 RNA isolation and qPCR analysis

Total RNA was extracted from cultured chondrocytes every week up to 8 weeks using TRIZol reagent, according to the manufacturer's instructions. The RNA concentration was measured by spectrophotometry at 260 nm, while the absorbance ratio at 260/280 and 260/230 nm were used to evaluate the quality of RNA. The RNA concentration from each sample was adjusted to 1 µg and reverse transcribed into cDNA with Oligo(dt)15 primer using M-MLV RT kit according to the manufacturer's recommended protocol. The synthesized cDNA was then used to perform qPCR analysis on the Rotor-gene Q instrument (Qiagen, Hilden, Germany) using KAPA SYBR FAST qPCR kit. The relative mRNA expression levels of each gene were quantified by delta-delta Ct method and normalized against the reference gene, glyceraldehyde-3-phosphate dehydrogenase (GAPDH). While the expression of Col1, Col2, aggrecan, Sox9 and MMP-13 were used to evaluate the phenotypic stability of chondrocytes. The sequence of primers used in the experiment was designed according to the data published on the National Center for Biotechnology Information (NCBI) website using Primer-BLAST programs, whereas the specificity of primers was validated by a single band on gel electrophoresis and confirmed by a single peak in the melting curve analysis. The sequence, amplicon length and accession number for each of primers are indicated in Table 1.

2.3.8 Ultrastructure analysis

The ultrastructure of chondrocytes was observed by TEM and compared between week 1 and 8 of culture using chondrocytes in ND group. For the sample preparation, the cells were

washed once with PBS, then fixed with 2.5% glutaraldehyde in 0.1 M sodium cacodylate buffer for 30 min at 4°C and post fixed with 1% osmium tetra oxide in the same buffer for 1 h at 4°C. Fixed samples were then dehydrated through a series of ethanol solutions in ascending concentrations up to 99.5%. After dehydration, the samples were washed thrice with propylene oxide, then immersed in the mixture of propylene oxide and epon resin for 3 h at room temperature and embedded in epon resin for 48 h at 60°C. Ultrathin sections at the thickness of 60 nm were obtained using a Reichert Ultracut S ultramicrotome (Leica Microsystems, Vienna, Austria) and collected on 200 mesh copper grids. The sections were double-stained with uranyl acetate and lead citrate and examined under a JEM-1400 plus TEM (JEOL Ltd., Tokyo, Japan) at 80 kV.

2.3.9 Statistical analysis

Quantitative data analysis was performed using GraphPad Prism software (GraphPad Software Inc., La Jolla, CA, USA). All quantitative results are presented as mean ± standard error of the mean (SE). Friedman's test and Dunn's multiple comparison test were used to evaluate significant differences in the gene expression results, while all other statistical comparisons were performed using analysis of variance (ANOVA) and Dunnett's multiple comparison test. *P*-value less than 0.05 was considered significant.

Table 1. The sequence of primers used for qPCR analysis to evaluate phenotypic stability of chondrocytes in long-term monolayer culture condition

Gene	Primer sequence (5'-3')	Amplicon length (bp)	Accession number
GAPDH	Forward: CTGAACGGGAAGCTCACTGG'	129	NM_001003142.1
	Reverse: CGATGCCTGCTTCACTACCT		
Collagen type I	Forward: CATCCCAGCCAAGAACTGGT	139	NM_001003187.1
	Reverse: GAAGGCGAGTTGAGTAGCCA		
Collagen type II	Forward: CACTGCCAACGTCCAGATGA	215	NM_001006951.1
	Reverse: GTTTCGTGCAGCCATCCTTC		
Aggrecan	Forward: ACTTCCGCTGGTCAGATGGA	111	NM_001113455.1
	Reverse: TCTCGTGCCAGATCATCACC		
Sox9	Forward: GCCGAGGAGGCCACCGAACA	179	NM_001002978.1
	Reverse: CCCGGCTGCACGTCGGTTTT		
MMP-13	Forward: GGCTTAGAGGTCACTGGCAAAC	118	XM_022418390.1
	Reverse: TGGACCACTTGAGAGTTCGGG		

2.4 Results

2.4.1 Effect of seeding density and culture time on the morphology of chondrocytes

Morphological appearance and confluency of cultured chondrocytes were evaluated under a light microscopy during the 8 weeks culture period. The chondrocytes were reached 100% confluence within 11 days (range 10-12) in LD group, 8 days (range 7-9) in ND group and 4 days (range 3-4) in HD group. As shown in Figure 1A, during the beginning of culture period chondrocytes exhibited a polygonal morphology only in HD group, whereas an elongated, fibroblast-like morphology was observed in ND and LD group. However, the morphological difference between each group ceased after 4 weeks. In HD and ND group, an accumulation of ECM as indicated by an opaque spot on culture plates was more clearly detected compared to LD group. At the end of an experiment, chondrocytes in all culture plates were tightly packed and broad opaque regions were identified in all groups.

2.4.2 Long-term monolayer cultured chondrocytes are able to resume proliferation after passage but have an altered morphology

As shown in Figure 1B, the proliferation capability of fourth passage chondrocytes passaging from third passage long-term monolayer culture condition was well-maintained. However, the morphological difference between each passage was observed. After culture for 1 week, third passage chondrocytes exhibited a typical elongated, fibroblast-like morphology found in monolayer culture. In contrast, the fourth passage chondrocytes exhibited a polygonal morphology with an increase in basal cellular area compared to third passage.

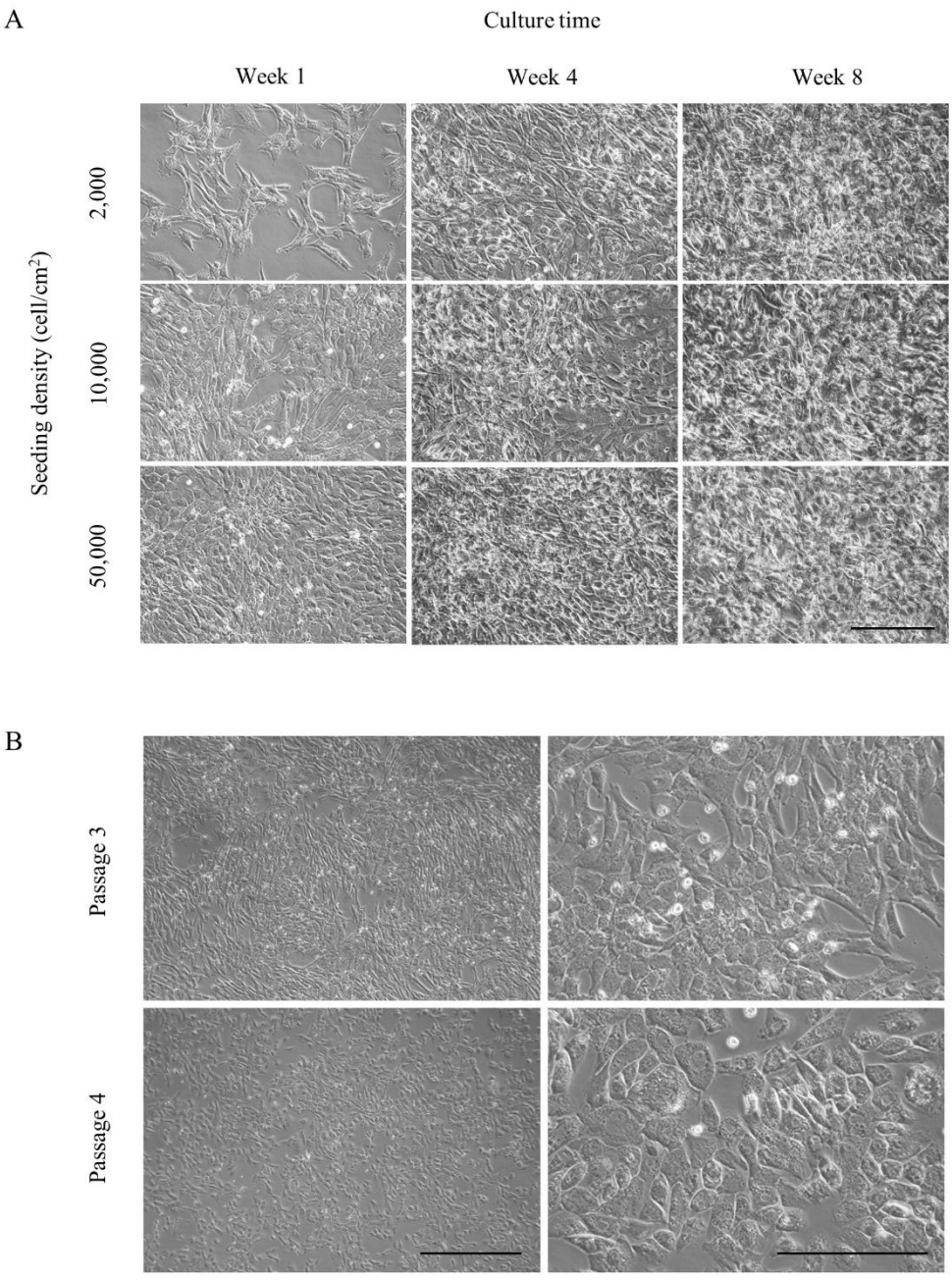

Figure 1. Morphological appearance and confluency condition of long-term monolayer cultured chondrocytes observed under a light microscope.

Chondrocytes were seeded and cultured as a monolayer at different initial seeding densities of 2,000, 10,000 and 50,000 cells/cm^2 and maintained over a period of 8 weeks. After culture for 8 weeks, chondrocytes were passaging once to fourth passage to confirm proliferation capability. **(A)** Images were captured from chondrocytes cultured at week 1, 4 and 8 of culture period. Opaque regions which indicated an accumulation of ECM were observed at week 8 of culture. Scale bar = 200 μm. **(B)** Third and fourth passage (passage from long-term culture) of chondrocytes in monolayer culture seeded with 10,000 cells/cm^2 observed at week 1. The basal area of chondrocytes in fourth passage was drastically increased while exhibited a spherical or polygonal morphology. Scale bar = 500 μm. (left), 200 μm. (right)

2.4.3 Chondrocytes cultured with different initial seeding densities exhibit a similar pattern of proliferation curve, while cell number was decreased after maintained in the post-confluent condition

The proliferation curve from day 1 to day 7 generated by MTT colorimetric assay indicates a similar pattern of cell growth between chondrocytes cultured with different initial seeding densities (Figure 2). While the results from trypan blue exclusion test reveal that the total cell number was decreased under the post-confluent condition. As shown in Figure 3, the highest cell number was observed at week 4, then significantly decreased at week 8 in all groups; LD (130,000 ± 2,900 decreased to 108,000 ± 3,300 cells/cm^2, P = 0.009), ND (146,000 ± 4,700 decreased to 120,500 ± 2,500 cells/cm^2, P = 0.02) and HD (168,800 ± 5,300 decreased to 143,000 ± 7,500 cells/cm^2, P = 0.017). In addition, the total cell number observed at week 4 was increased at 68.4, 14.6 and 3.4-fold in LD, ND and HD group, respectively compared to initial seeding density.

2.4.4 Quantification of total DNA and GAGs content

Total DNA and GAGs content of cultured chondrocytes were evaluated by biochemical analysis every 2 weeks during the culture period. As shown in Figure 4, biochemical analysis results from chondrocytes cultured with different initial seeding densities showed a similar tendency. Quantified from cell lysates, the results from Hoechst assay indicated the highest DNA content at week 4 then steadily decreased until week 8 in all group with a significant difference in DNA content found between week 2 and 4 in two groups (Figure 4A); LD (7.85 ± 1.39 versus 11.08 ± 1.75 µg/ml, P = 0.022) and HD (15.18 ± 0.97 versus 18.08 ± 3.37 µg/ml, P = 0.008). In addition, the results from DMMB assay revealed that GAGs content in cell lysates was commenced to increase at week 6 and the highest amount of GAGs content was

observed at week 8. There was a significant difference in GAGs content between week 2 and 8 in all groups (Figure 4B); LD (0.9 ± 0.14 versus 1.68 ± 0.73 µg/µg of DNA, $P = 0.001$), ND (0.86 ± 0.11 versus 1.33 ± 0.43 µg/µg of DNA, $P = 0.003$) and HD (0.55 ± 0.07 versus 1.23 ± 0.16 µg/µg of DNA, $P = 0.015$). On the other hand, the significant difference of GAGs content in culture media was observed only between week 2 and 8 in LD group (Figure 4C) (0.66 ± 0.09 versus 0.92 ± 0.17 µg/µg of DNA, $P < 0.001$).

2.4.5 Long-term monolayer cultured chondrocytes synthesize abundant amount of ECM as indicated by GAGs content

An abundant amount of ECM was synthesized during long-term culture, as indicated by alcian blue staining on GAGs content, which is the main ECM component of cartilage (Figure 5). The staining intensities of alcian blue in cultured chondrocytes was increased in a time-dependent manner during long-term culture. The positive alcian blue stain was detected in ND and HD group as early as week 2, compared to LD group which showed weaker alcian blue stain. However, there was no difference in staining intensities observed between each group after week 2 until the end of an experiment. Notably, strong alcian blue positive stain indicating increased GAGs deposition could be observed at week 6 and 8 in all groups.

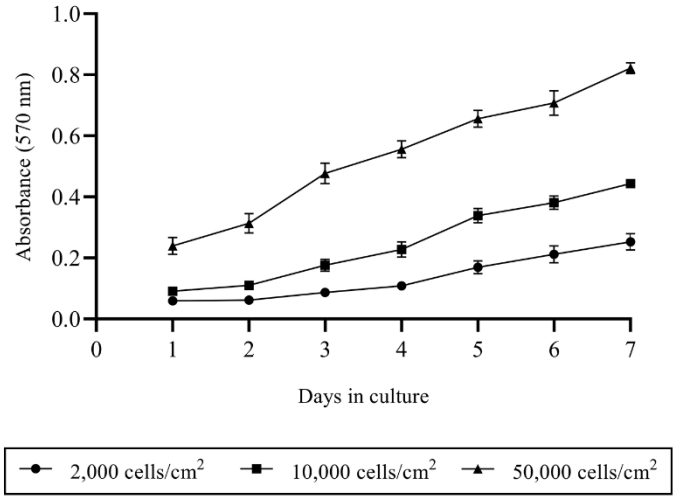

Figure 2. Chondrocytes cultured with different initial seeding densities exhibit a similar pattern of proliferation curve.

Chondrocytes were seeded and cultured as a monolayer at different initial seeding densities of 2,000, 10,000 and 50,000 cells/cm^2 and maintained over a period of 8 weeks. The proliferation curve of cultured chondrocytes was analyzed by MTT assay during the first 7 days.

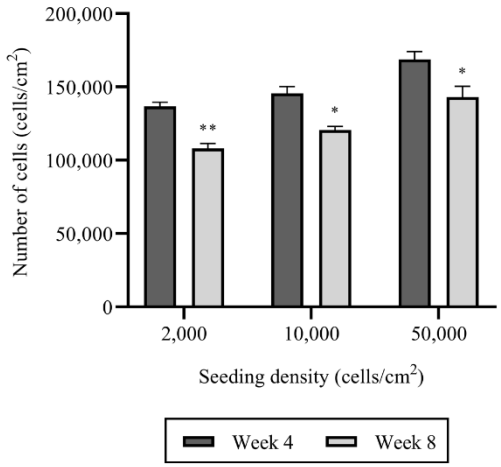

Figure 3. The number of cultured chondrocytes was decreased after maintained in post-confluent condition.

Chondrocytes were seeded and cultured as a monolayer at different initial seeding densities of 2,000, 10,000 and 50,000 cells/cm^2 and maintained over a period of 8 weeks. Total cell number and cell viability were evaluated by trypan blue exclusion test once every 4 weeks. The number of chondrocytes was significantly decreased after week 4 in all groups. The data are represented as the mean ± SE. (compared to week 4: *P < 0.05 and **P < 0.01)

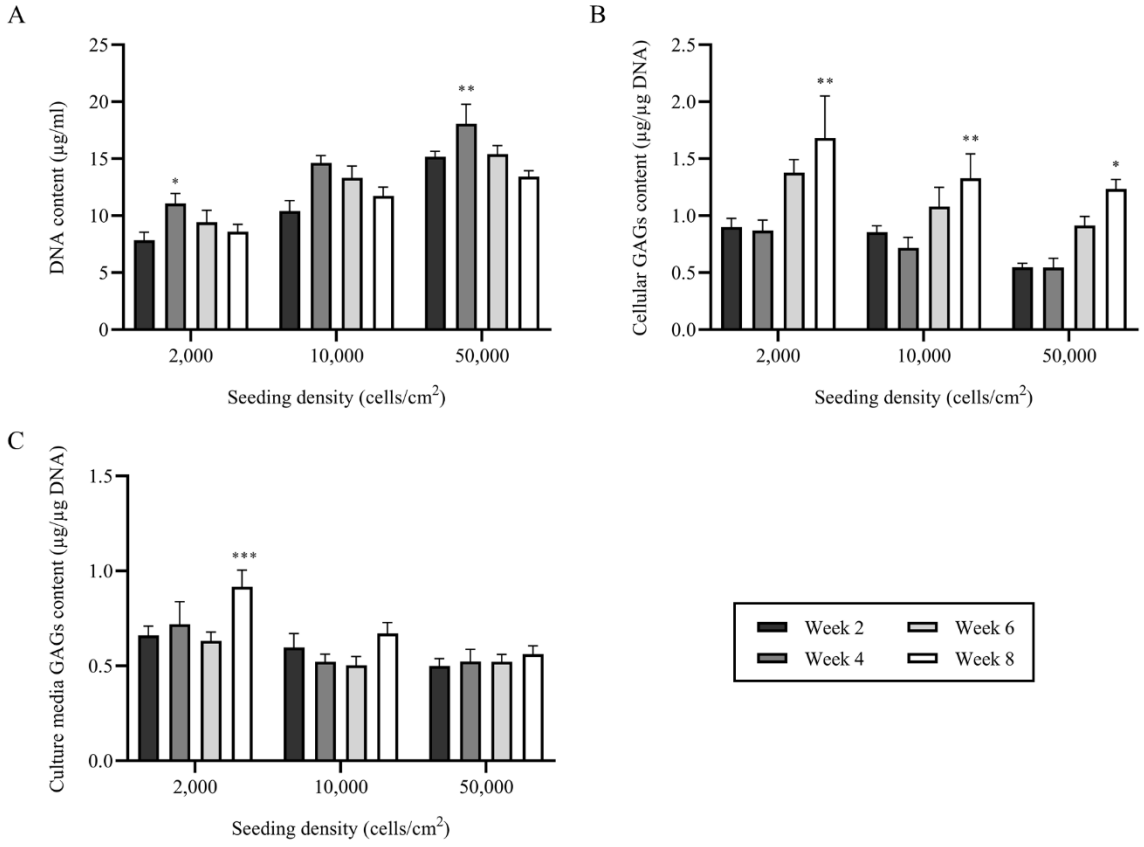

Figure 4. Long-term monolayer culture condition promotes GAGs synthesis but reduce DNA content of chondrocytes.

Chondrocytes were seeded and cultured as a monolayer at different initial seeding densities of 2,000, 10,000 and 50,000 cells/cm^2 and maintained over a period of 8 weeks. Biochemical analysis was performed every 2 weeks during the cultured period. **(A)** Quantification of DNA content in cell lysates by Hoechst assay. **(B and C)** Quantification of GAGs content (normalized with DNA content) by DMMB assay in cell lysates and culture media, respectively. The data are represented as the mean ± SE. (compared to week 2: *$P < 0.05$, **$P < 0.01$ and ***$P < 0.001$)

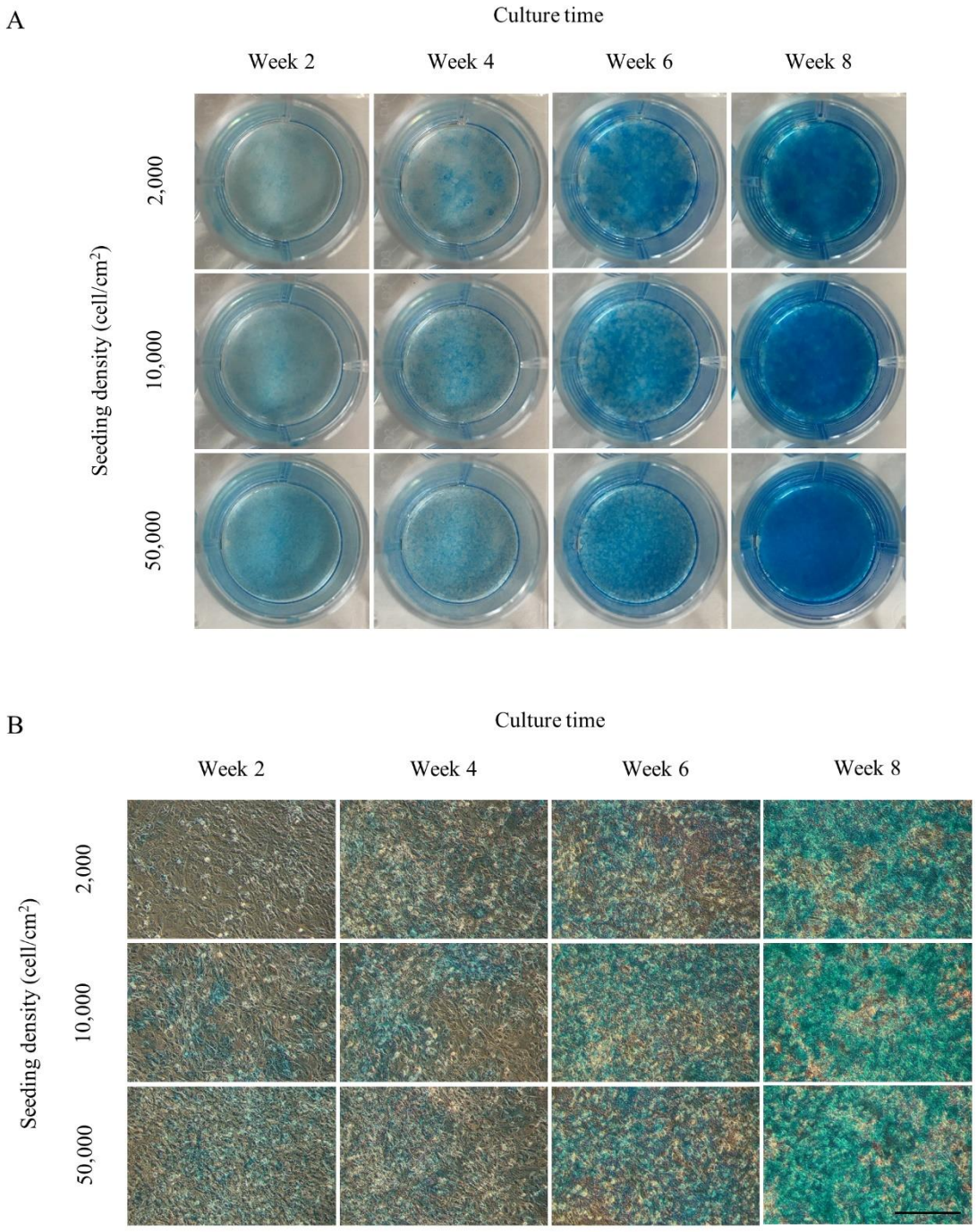

Figure 5. Long-term monolayer cultured chondrocytes synthesize an abundant amount of ECM as indicated by GAGs content.

Chondrocytes were seeded and cultured as a monolayer at different initial seeding densities of 2,000, 10,000 and 50,000 cells/cm^2 and maintained over a period of 8 weeks. Alcian blue staining for GAGs was performed in 12-well polystyrene culture plates every 2 weeks during the cultured period. Alcian blue-stained images of long-term monolayer cultured chondrocytes **(A)** observed on culture plates and **(B)** observed under the light microscope. Scale bar = 200 μm.

2.4.6 Alteration in gene expression of long-term monolayer cultured chondrocytes

The chondrocyte mRNA expression profile analyzed by qPCR in each group was statistically compared to week 1 as the control. Our finding revealed that the phenotypic stability of cultured chondrocytes was drastically affected by long-term culture. The mRNA expression of Col1 was downregulated after week 1 and showed the lowest expression during week 5 and 6. The lowest expression of Col1 was observed at week 6 in ND group, which downregulated more than 8-fold ($P = 0.001$) compared to week 1 (Figure 6A). While the mRNA expression level of main ECM components, Col2 and aggrecan were both upregulated in a time-dependent manner with the highest expression observed in HD group. Precisely, the mRNA expression of Col2 and aggrecan at week 8 were upregulated more than 350-fold ($P < 0.001$) and 40-fold ($P = 0.002$), respectively compared to week 1 (Figure 6B and 6C). Similarly, the highest mRNA expression of Sox9 was detected at week 8 but in ND group which was upregulated more than 180-fold ($P < 0.001$) compared to week 1 (Figure 6D). Interestingly, the mRNA expression of proteolytic enzymes MMP-13 was found to be similar to ECM components with the highest expression observed at week 7 in HD group by 1000-fold ($P = 0.03$) compared to week 1 (Figure 6E).

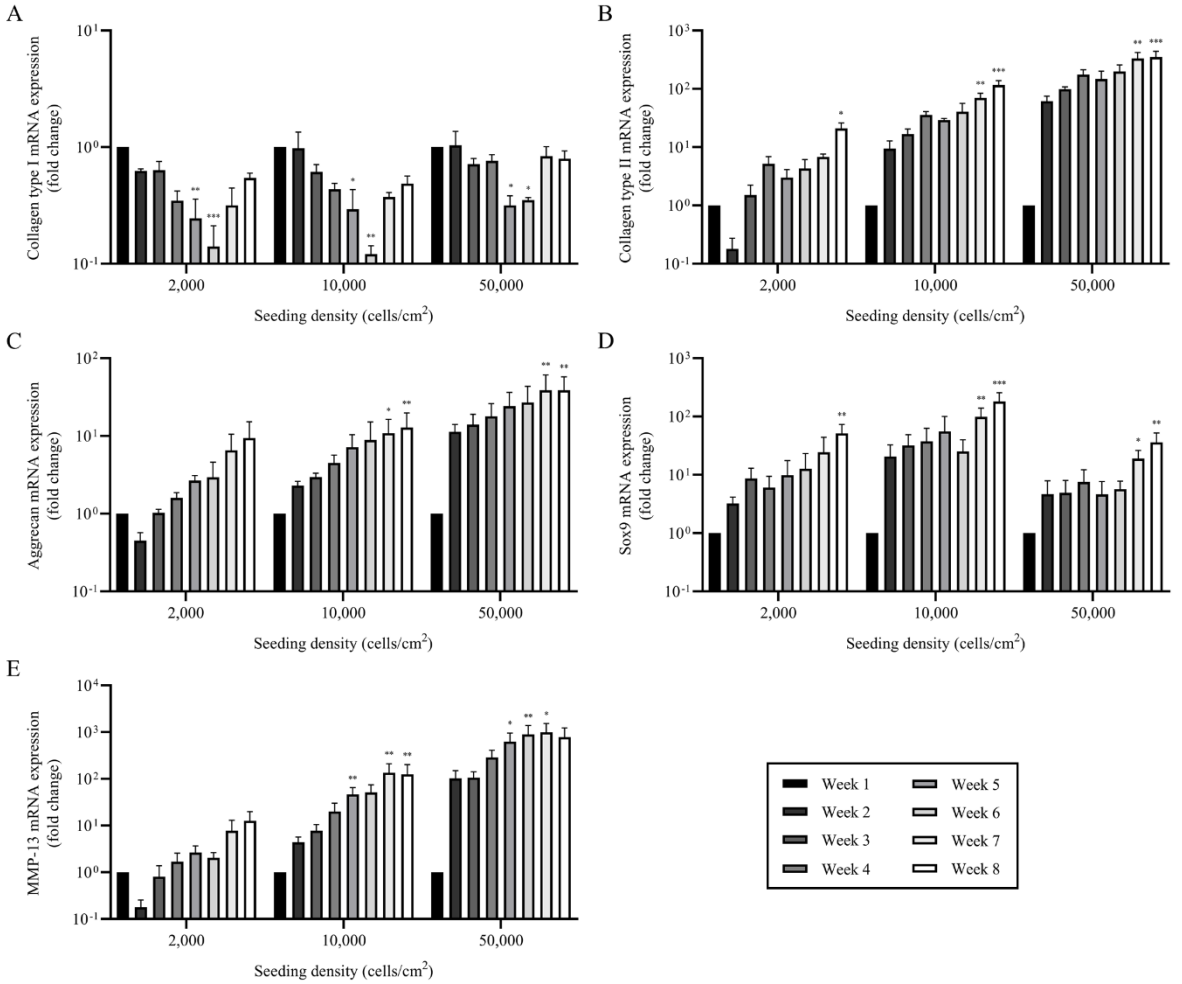

Figure 6. Alteration in gene expression of long-term monolayer cultured chondrocytes.

Chondrocytes were seeded and cultured as a monolayer at different initial seeding densities of 2,000, 10,000 and 50,000 cells/cm^2 and maintained over a period of 8 weeks. Relative mRNA expression of chondrocytes was evaluated by qPCR analysis every week during the culture period. The relative mRNA expression of **(A)** collagen type I, **(B)** collagen type II, **(C)** aggrecan, **(D)** Sox9 and **(E)** MMP-13 were normalized to the housekeeping gene, GAPDH. The data are represented as the mean ± SE. (compared to week 1: *P < 0.05, **P < 0.01 and ***P < 0.001)

2.4.7 Long-term monolayer cultured causes cellular organelle abnormality

The cellular structure and organelles of chondrocytes in long-term monolayer culture conditions were observed under TEM. As shown in Figure 7, chondrocytes from week 1 (Figure 7A-C) and 8 (Figure 7D-F) both contained abundant RER and mitochondria. Dilated RER has commonly observed in both week 1 and 8 chondrocytes cultures but with differenced degrees of dilation. The chondrocytes from week 1 were typically contained dilated RER at mild degree (Figure 7B), whereas the massively dilated RER was indicated in week 8 chondrocytes cultures (Figure 7E). Although autophagic vacuoles could be observed in both week 1 and 8 chondrocytes cultures (Figure 7B, 7E), the number and size of autophagic vacuoles were slightly increased in week 8 compared to week 1. Furthermore, the cell volume of chondrocytes from week 8 was drastically increase compared to week 1, which indicated the hypertrophic change of chondrocytes.

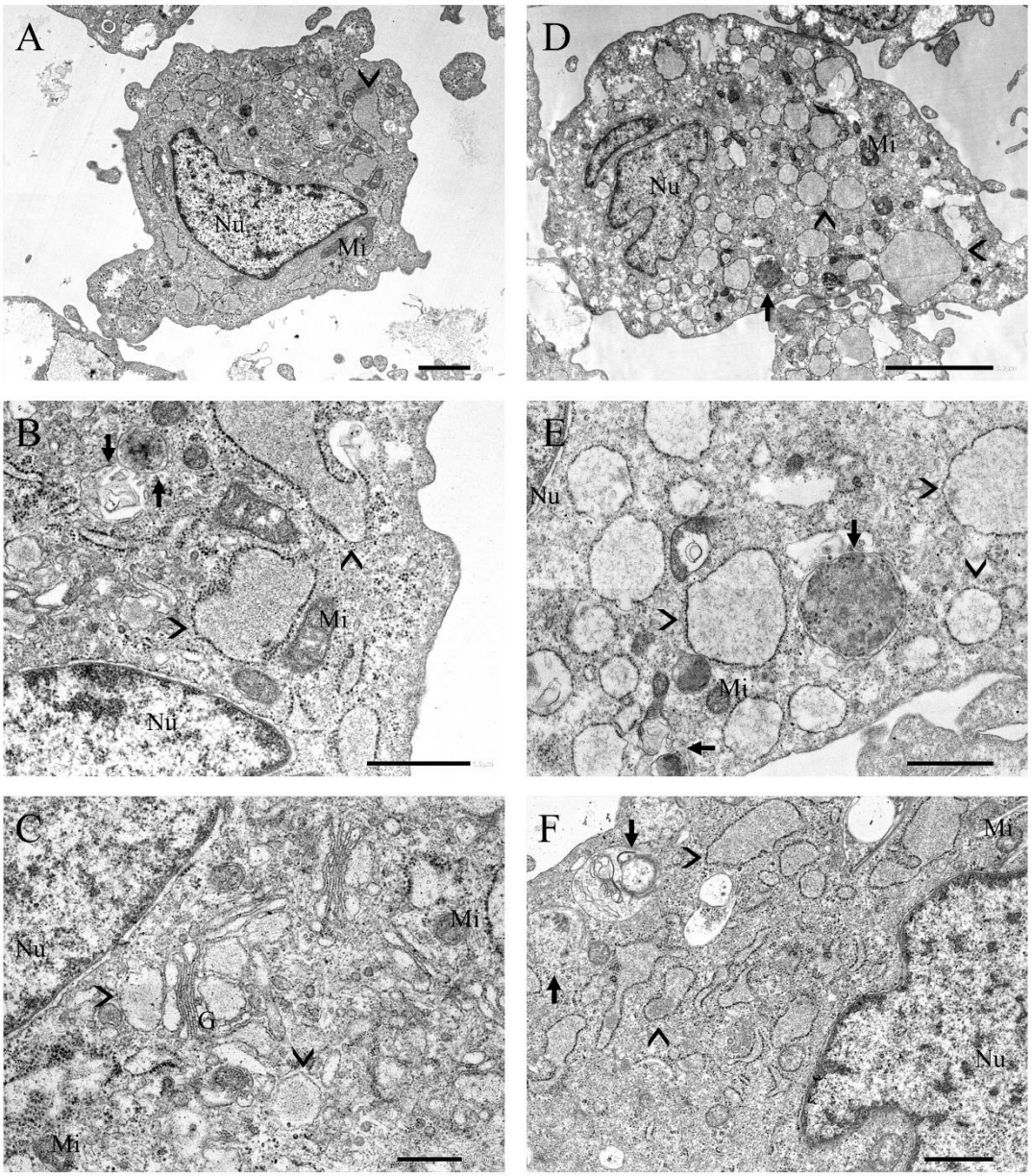

Figure 7. Massively dilated RER was observed in chondrocytes after maintained in long-term monolayer culture conditions.

TEM analysis of chondrocytes ultrastructure in long-term monolayer culture seeded with 10,000 cells/cm^2 compared between week 1 **(A-C)** and 8 **(D-F)**. **(A and D)** Chondrocytes from both week 1 and 8 contained abundant RER (arrowhead) and mitochondria (Mi). Dilated RER was observed in both samples with different dilation degrees, whereas **(B)** mildly dilated RER was observed in week 1 and **(E)** massively dilated RER was observed in week 8. The autophagic activity of chondrocytes was indicated by the presence of autophagic vacuole (arrow). **(E and F)** Chondrocytes maintained in long-term culture showed an increase in the number and size of autophagic vacuoles compared to chondrocytes in week 1. Other cellular organelles presented in the images are including, nucleus (Nu) and golgi apparatus (G). All images are from 60 nm-thick epon resin ultrathin section double-stained with uranyl acetate and lead citrate and examined under a TEM at 80 kV. Scale bar = 2 µm (A); 1 µm (B, E, F); 500 nm (C); 5 µm (D).

2.5 Discussion

Conventional 2D monolayer culture is the most common method used for chondrocytes expansion. Due to the large number of cells needed for both cartilage tissue engineering and research purposes, the expansion of chondrocytes is an unavoidable process that required to achieve sufficient cell number. Although conventional 2D monolayer culture is simple and capable for large scale chondrocyte expansion, the expanded chondrocytes are low in quality as it was unable to maintain their phenotype (Melero-Martin and Al-Rubeai, 2007). The major problem of chondrocytes expanding *in-vitro* is the dedifferentiation process, which is characterized by the gradual change from the chondrocyte phenotype to fibroblast-like phenotype (Darling and Athanasiou, 2005; Lin et al., 2008; Caron et al., 2012). In this study, we describe the characteristic changes of canine articular chondrocytes during non-passaged long-term monolayer culture conditions. Our findings demonstrate that the phenotypic loss of dedifferentiated chondrocytes cultured in conventional 2D monolayer could be spontaneously, but partially restored by an appropriate culture time in standard culture media without the addition of known chondrogenic supplements or using tissue-culture scaffolds.

The phenotypic stability of cultured chondrocytes is influenced to some extent by initial seeding density (Watt, 1988; Schulze-Tanzil et al., 2002; Otero et al., 2012). Compared to low seeding density, high seeding density are more capable to stabilizes the chondrocyte phenotype as it was able to reduce cell division rounds needed to reach confluence (López-Alcorocho et al., 2019). Moreover, the high cell density condition also supports cell-cell interactions, which enhances the expression of cell adhesion molecules N-cadherin (DeMara et al., 2011; Gao et al., 2014; Costa et al., 2018). Consistent to our findings on morphological appearance, which indicates that chondrocytes cultured with lower seeding density are more likely to exhibit fibroblast-like morphology, particularly during the early stage of cell expansion (Melero-

Martin and Al-Rubeai, 2007). However, the morphological difference between chondrocytes cultured with high and low seeding density could not be observed after culture for 4 weeks. The chondrocytes' appearance in all groups is similar with an observed polygonal morphology. Despite the differences in initial seeding densities, the proliferation curve of chondrocytes cultured in monolayer generated by MTT colorimetric assay indicates a similar pattern of cell growth. Interestingly, the proliferation curve of chondrocytes from HD group indicated cell proliferation even after cells were observed at 100% confluence on day 4. This result is consistent with what has been reported in previous studies which demonstrated that chondrocytes cultured in monolayer could form a layer and became stratified under post-confluence condition (Patti et al., 1999; Gartland et al., 2005; Hendriks et al., 2006). Nevertheless, the limit of cell proliferation after confluence condition has existed. Our results reveal that the cell number and DNA content of chondrocytes maintained in conventional 2D monolayer cultures have increased but terminated at week 4, then gradually declines until the end of an experiment. We suggest that the proliferative capability of chondrocytes was well-maintained even in a high cell density environment, which allows stratified culture to become possible in the post-confluence condition. However, the high number of cells will eventually trigger the contact inhibition mechanism and terminates chondrocyte proliferation (Isyar et al., 2016). This finding indicates the possibility of stratified culture, the limit of cell proliferation and maximum cell number gain in monolayer culture.

The post-confluence condition maintained in this study was intended to trigger contact inhibition phenomenon to turn the chondrocytes back to their post-mitotic state and promote ECM synthesis (Gelse et al., 2012; Otero et al., 2012). These preparations were to create a culture condition that resembles native cartilage microenvironment, we aim to use self-synthesis ECM from high-density chondrocytes culture to establish a cartilage-like

microenvironment on culture plates, which may support chondrocyte expansion *in-vitro* (Schulze-Tanzil, 2009; García-Carvajal et al., 2013). Our results from GAGs quantification and alcian blue staining confirm that chondrocytes in long-term monolayer cultured condition synthesize an abundant amount of ECM, especially after week 4, in which cell proliferation is terminated as indicated by cell number and DNA content. This has been previously suggested to be due to proliferative and synthetic activities of chondrocytes being inversely related (Patti et al., 1999; Otero et al., 2012). Another promising finding is that chondrocytes passage from the long-term monolayer conditions were able to resume proliferation with altered cell morphology. The chondrocytes passaging from long-term culture exhibited a polygonal morphology instead of a typical, fibroblast-like morphology. Furthermore, the basal area of these chondrocytes was observed to be drastically increased compared to the previous passage, which may indicate hypertrophic differentiation (Gratal et al., 2019).

The phenotypic stability of chondrocytes in long-term monolayer culture conditions is drastically affected by culture time, as indicated by mRNA expression profiles. Our results from the qPCR analysis revealed that at the end of an experiment, the mRNA expression of chondrocyte specific markers; Col2 and aggrecan, chondrogenic marker; Sox9 and hypertrophic marker; MMP-13 were upregulated, while fibroblast specific marker; Col1 was downregulated (Lin et al., 2008; Mao et al., 2018; Ripmeester et al., 2018). The upregulation of Col2 and aggrecan, together with the downregulation of Col1 have corresponded with transcription factor Sox9 expression, which is a crucial factor in cartilage formation that could activate several chondrocyte specific markers and represses Col1 expression (Akiyama et al., 2004; Dreier, 2010; Caron et al., 2012; Shi et al., 2015). In addition, the high expression of Col2 was in consistent with a previous study, which found that Col2 was upregulated in chondrocytes that maintained long-term post-confluence monolayer (Binette et al., 1998).

Taken together, we suggest that prolonged culture under post-confluence conditions allows chondrocytes to proliferate to its maximum potential, which resulted in a very densely packed and stratified culture condition. This high cell density condition is able to promote more cell-cell interaction, enhances ECM synthesis and enforces a rounded chondrocyte morphology (Takahashi et al., 2007; Schulze-Tanzil, 2009; Gao et al., 2014). Contrary to the high expression of a negative regulator of chondrocyte hypertrophy Sox9, an increase in MMP-13 expression was observed (Dreier, 2010; Martinez-Sanchez et al., 2012). We speculate that the upregulation of MMP-13, which is considered as the chondrocyte hypertrophic marker and major Col2 degrading collagenase, could be related to cellular response due to the vast amount of ECM synthesized, especially at week 6 and 8 as the MMP-13 is necessary for ECM remodeling to permit cell enlargement. However, this could also be an indication of a mixed population of chondrocytes, which correlated to the TEM result that observed an increase in cell volume (D'Angelo et al., 2000). The long-term monolayer culture condition used in this study showed the remarkable capability to support ECM synthesis and promote the expression of chondrocyte specific markers, compared to conventional 2D monolayer culture, which chondrocytes trend to rapidly dedifferentiate.

In this study, dilated RER was typically observed in both week 1 (sub-confluent) and week 8 (post-confluent) chondrocytes culture but with different degrees of dilation. As the main function of RER is responsible for protein synthesis, the dilated RER indicates highly synthetic activity of chondrocytes and could occur to some extent in healthy chondrocytes (Roy and Meachim, 1968; Ovalle and Nahirney, 2007; Shapiro, 2015). Unlike the chondrocytes in post-confluent condition, the RER observed in sub-confluent condition were mostly dilated only at mild degree, which reflects the regular synthesis function. We suggest that the abnormally massive dilated RER that observed in post-confluent chondrocytes culture was

associated with hypertrophic chondrocytes found in the epiphyseal plate (Anderson, 1967; Oakes et al., 1977; Hall, 2012). Moreover, in the present study we detected several autophagic vacuoles in chondrocytes, which indicates a self-digesting mechanism called autophagy. Autophagy is the physiological cellular mechanism that occurred to maintain cellular function and survival by degrades macromolecules and organelles to sustain cellular metabolism. In the low turnover rate cell such as chondrocytes, autophagy is considered as an essential mechanism that promotes cell survival through an unfavorable condition (Caramés et al., 2010; Chang et al., 2013; Luo et al., 2019). While a decrease in the autophagic activity of chondrocytes is associated with the pathogenesis of OA (Caramés et al., 2010; Chang et al., 2013). Our results indicate that the autophagic activity of chondrocytes is well-maintained even in the long-term culture condition.

In conclusion, the study presented in this chapter demonstrates that the alteration in characteristics of canine articular chondrocytes in monolayer culture is mainly contingent on culture time. The long-term monolayer culture condition allows chondrocytes to proliferate to their maximum capacity, leading to extremely high cell density with the stratified condition, which subsequently promotes ECM synthesis. Thus, the culture condition that resembles native articular cartilage microenvironment could promote phenotypic stability and enhance the redifferentiation process, as evidenced by mRNA expression and GAGs deposition profile. However, the redifferentiation process could be considered only partially due to some characteristics of hypertrophic differentiated chondrocytes that were also observed in these long-term monolayer cultures. In addition, these long-term monolayer cultured chondrocytes can be passaged and exhibit a decent proliferative capability displaying a polygonal as opposed to a typical fibroblastic-like morphology. Therefore, the long-term monolayer culture model

might serve as an excellent *in-vitro* model for cartilage research due to the ECM-rich condition with post-mitotic state chondrocytes.

CHAPTER 3

Effects of pentosan polysulfate on cell proliferation, cell cycle progression and cyclin-dependent kinases expression in canine articular chondrocytes

3.1 Summary

The purpose of the study was to investigate the effects of pentosan polysulfate (PPS) on cell proliferation, particularly in cell cycle modulation and phenotype promotion of canine articular chondrocytes. Canine articular chondrocytes were isolated and cultured from femoral head cartilages of four dogs. The second passage chondrocytes were cultured in monolayer conditions for 24 h. Thereafter, chondrocytes were treated with PPS (0-80 µg/ml) for a further 72 h. The effects of PPS on chondrocytes were evaluated based on morphological appearance, cell viability, cell cycle distribution, DNA content, GAGs content and mRNA expression. Our results from MTT colorimetric assay, Hoechst assay and cell apoptosis assay reveal that PPS reduced chondrocyte viability in a concentration- and time-dependent manner, however, not related to cell death. Consistent with the results from cell cycle analysis, which indicates that PPS significantly reduced chondrocyte proliferation through cell cycle modulation particularly by maintaining a significantly higher proportion of chondrocytes in G1 phase and a significantly lower proportion in the S phase of the cell cycle in a similar manner. Together with the chondrocyte mRNA expression profile analyzed by qPCR, the high proportion of chondrocytes in G1 phase corresponded with the significant downregulation of cyclin-dependent kinase (CDK) 1 and 4. In addition, our study further confirms that PPS promotes the phenotype of canine articular chondrocytes through significant upregulation of Col2 mRNA expression and GAGs synthesis. These findings suggest that the effect of PPS on the inhibition of chondrocyte proliferation while promoting a chondrocyte phenotype may be beneficial on therapeutic treatment during the early stages of OA progression, which transient increase in proliferative activity of chondrocytes with subsequent phenotypic shift and less productive in an essential component of ECM is observed.

3.2 Introduction

In the articular cartilage, chondrocytes are the sole resident cell that occupies less than 5% of the total cartilage volume but plays a fundamental role in cartilage homeostasis by synthesizing and maintaining the components of ECM (Hall, 2005; Sophia Fox et al., 2009; Athanasiou et al., 2013). Chondrocytes are a unique cell type that can function in a low oxygen environment within avascular structure of articular cartilage while relies on the nutrients primarily from a synovial fluid by diffusion through the ECM (Archer and Francis-West, 2003; Athanasiou et al., 2013). Under the physiological conditions, the mature chondrocytes resided in the articular cartilage are remain as resting cells, which are typically quiescent and do not divide after skeletal maturity is attained (Sandell and Aigner, 2001; Hall, 2005; Goldring and Marcu, 2009). Due to these circumstances, chondrocytes maintain the ECM structure in a relatively low turnover state (Sophia Fox et al., 2009; Otero et al., 2012). Nevertheless, these resting chondrocytes could rapidly become phenotypically unstable and resume their proliferative activities under the pathological conditions (Sandell and Aigner, 2001).

The degenerative joint disease, also known as OA, is the most common type of arthritis that involves the entire joint structure, including articular cartilage, synovial membrane, ligaments, joint capsule and subchondral bones (Dreier, 2010; Goldring, 2012; Maldonado and Nam, 2013). Osteoarthritic cartilage is characterized by an imbalance in cartilage homeostasis from the failure of chondrocytes to maintain the metabolic activities between synthesis and degradation of ECM components (García-Carvajal et al., 2013). Chondrocytes in osteoarthritic cartilage were prone to shift towards a catabolic state and actively produce various kinds of proteolytic enzymes, especially the MMPs family that is responsible for the breakdown of the cartilage matrix components (Goldring and Marcu, 2009; Kapoor, 2015). During the initial stage of OA progression, the usually resting chondrocytes are undergoing a phenotypic shift

and become activated chondrocytes, which results in a transient increase in proliferative activity, followed by cell accumulation and cluster formation which is a characteristic feature of osteoarthritic cartilage (Sandell and Aigner, 2001; Maldonado and Nam, 2013; Charlier et al., 2016). Some previous studies had suggested that the sudden change in chondrocyte activity might due to better access to various factors in synovial fluid through the fissuring, loosening or damaged collagen network (Sandell and Aigner, 2001).

Interestingly, a similar situation of this phenotypic shift can be observed from chondrocytes in monolayer culture conditions, in which the resting chondrocytes embedded in articular cartilage were isolated and seeded on culture plates. This sudden change from the condition of native cartilage microenvironment to the 2D condition on culture plate, where both nutrients and oxygen are easier to access allows chondrocytes to be active and rapidly proliferate (Otero et al., 2012). Moreover, due to the repetition of the proliferation process, these proliferated chondrocytes are gradually losing their phenotype and capability to proliferate, similar to the chondrocytes in osteoarthritic cartilage (Lin et al., 2008; VanderKraan and van den Berg, 2012). Although the molecular mechanisms and final outcomes of metabolic alterations, phenotypic shift and cell proliferation are different as the isolated chondrocytes are going through a dedifferentiation process, while the osteoarthritic chondrocytes are terminally differentiated to hypertrophic chondrocytes (Melero-Martin and Al-Rubeai, 2007; Zhong et al., 2016; Charlier et al., 2019). However, a recent study has revealed that a variety of degenerated phenotypes could be presented during the onset of OA, including the dedifferentiated-like phenotype observed in the monolayer culture condition (Charlier et al., 2019). We believed that intervening in these events might provide us more understanding in chondrocyte physiology, disease progression and therapeutic targets for OA treatment.

The currently available treatment options for OA are mostly palliative and are unable to completely cease disease progression (Mobasheri, 2013). However, the development of pharmacological therapies during recent years has aimed towards modifying the original structure of cartilage instead of only at relieving the symptoms. These novel drugs, which promote cartilage regeneration concurrent with halting further damage of joints, are classified as DMOADs (Henrotin et al., 2005; Mobasheri, 2013; Ghouri and Conaghan, 2019).

PPS is a semi-synthetic drug with a low molecular weight heparin-like structure manufactured from beech-wood hemicellulose. It has a property similar to heparin, which contains both anticoagulant and fibrinolytic effects but much weaker (Ghosh et al., 2009; Kumagai et al., 2010). PPS has been shown to demonstrate a chondroprotective effect on articular cartilage as it reduces cartilage matrix degradation, improves blood flow and stimulates hyaluronan and proteoglycan synthesis (Ghosh et al., 2009; Kumagai et al., 2010; Bwalya et al., 2017). The efficacy of PPS on osteoarthritic joint has been demonstrated in both *in-vitro* and *in-vivo* studies, while it has been proposed as a potential DMOADs (Sunaga et al., 2012; Bwalya et al., 2017; Bwalya et al., 2018). However, the mechanism of action of PPS on articular cartilage remains to be fully explained, especially the effects of PPS on chondrocyte proliferation and cell cycle, which have not yet been implemented. Our hypothesis is that the benefits of PPS on OA treatment could be related to the disturbance on the resting state of chondrocytes and phenotypic shift. Therefore, the purpose of this study was to investigate the effects of PPS on cell proliferation, particularly in cell cycle modulation and phenotype promotion of canine articular chondrocytes under monolayer culture conditions.

3.3 Material and Methods

3.3.1 Reagents

The sources of materials used were as follows: DMEM was purchased from Gibco; FBS was purchased from Nichirei Biosciences Inc.; HEPES and MTT were purchased from Dojindo; Papain, calf thymus DNA and DMMB were purchased from Sigma-Aldrich; KAPA SYBR FAST qPCR kit was purchased from KAPA Biosystems; PPS was purchased from Biopharm Australia (NSW, Australia); FITC annexin V apoptosis detection kit I was purchased from BD Bioscience (Heidelberg, Germany); NucleoSpin RNA purification kit was purchased from Macherey-Nagel (Dürren, Germany); TRIZol reagent and M-MLV RT kit were purchased from Invitrogen; Culture dishes and culture plates were purchased from Corning. All other reagents were purchased from Wako Pure Chemicals Industries unless stated otherwise.

3.3.2 Chondrocytes isolation and culture

The use of animal samples was in accordance with Hokkaido University Institutional Animal Care and Use Committee guidelines (approval #12–0059). Healthy canine articular cartilage tissue samples were isolated from the femoral head of four dogs (4-11 years old) at Hokkaido University Veterinary Teaching Hospital. The first dog was experimental Beagle dogs that were euthanized at the end of an experimental study not related to this study, while another three dogs were Toy poodle, Pomeranian and Shetland sheepdog that were undergoing femoral head and neck ostectomy due to traumatic coxofemoral luxation. Briefly, articular cartilage tissue samples were harvested and dissected into small sections. Then the digestion process was performed in DMEM supplemented with 0.3% collagenase type I for 18 h at 37°C in a 5% CO_2 incubator. The released chondrocytes were separated by filtering through a 40 μm

nylon filter and primary chondrocytes were expanded at a density of 10,000 cells/cm^2. Chondrocytes were passaged at 80-90% confluence by washed twice with PBS and released from culture dishes using 0.05% trypsin with 0.02% EDTA in PBS. Following the above procedure, the second passage chondrocytes at a density of 12,000 cells/cm^2 were used for any further experiments. The culture media used in this study was DMEM containing 10 mM HEPES, 25 mM $NaHCO_3$, 100 U/ml penicillin G potassium and 73 U/ml streptomycin sulfate.

3.3.3 Chondrocytes treatment

Unless specified otherwise, all cultured chondrocytes used in this study were seeded in 60 mm polystyrene culture dishes in DMEM containing 10% FBS and incubated for 24 h at 37°C in a 5% CO_2 incubator. Thereafter, the culture media was removed, and chondrocytes were incubated in the presence (5, 10, 20, 40 and 80 µg/ml) or absence (Control) of PPS for a further 72 h. Cell morphology, confluency condition and cell attachment on culture surfaces were observed under a light microscope.

3.3.4 Cell viability assay

Chondrocytes were seeded into 96-well polystyrene culture plates and treated as described above. Cell viability was evaluated by MTT colorimetric assay every 24 h during the treatment period. Briefly, the cells were washed once with PBS, then 0.5 mg/ml MTT solution prepared in DMEM was added into each well and incubated for 4 h at 37°C in a 5% CO_2 incubator. The MTT solution was then removed and DMSO was added to dissolve formazan crystals. The absorbance was measured using a Multiskan FC microplate reader at 570 nm.

3.3.5 Cell apoptosis assay

The chondrocyte apoptosis was evaluated with annexin V and propidium iodide (PI) stained using FITC annexin V apoptosis detection kit I in accordance with the manufacturer's protocol. In brief, the cells were harvested and washed twice with PBS, then resuspended in binding buffer. FITC-annexin V and PI were added into the cell suspension, then incubated for 15 min in darkness at room temperature. The samples were analyzed using a FACS Verse flow cytometer (BD Biosciences).

3.3.6 Cell cycle analysis

The effect of PPS on cell cycle was assessed through PI staining using flow cytometry analysis. In brief, the cells were harvested and washed twice with PBS, then fixed with cold 70% ethanol overnight at -20°C. Fixed cells were treated with 100 μg/ml RNase A in PBS for 30 min at 37°C prior to incubating with 50 μg/ml PI for 10 min at room temperature with light protection. The samples were analyzed using a FACS Verse flow cytometer and the cell distribution results were evaluated by the FlowJo software program (Treestar, Ashland, OR, USA) using Watson Pragmatic model.

3.3.7 Biochemical analysis

Cell lysates of cultured chondrocytes were used for biochemical analysis. To perform cell digestion, the cells were washed once with PBS, then 300 μg/ml papain solution containing 20 mM Na_2HPO_4, 2 mM dithiothreitol and 1 mM EDTA was added into each well and incubated for 18 h at 60°C. The quantification of DNA content was performed by Hoechst assay with calf thymus DNA as a standard. In brief, cell lysates were mixed with 1 μg/ml Hoechst solution containing 10 mM Tris-HCl, 100 mM NaCl and 1 mM EDTA, then incubated

for 10 min at room temperature and the measurement was performed using 350/460 nm filter set. The quantification of GAGs content was performed by DMMB assay with chondroitin sulfate as a standard. In brief, cell lysates were mixed with 15 µg/ml DMMB solution containing 40.5 mM glycine, 27.5 mM NaCl and 0.1 M acetic acid, then incubated for 1 min at room temperature and the absorbance was measured at 525 nm. The results were normalized with DNA content. Both assays were measured using an Infinite M200 Pro microplate reader.

3.3.8 RNA isolation and qPCR analysis

To evaluate the effect of PPS on gene expression, chondrocytes were seeded in 60 mm polystyrene culture dishes and incubated for 24 h as described above. Thereafter, the culture media was removed, and chondrocytes were treated with 0 (control), 5, 20 and 80 µg/ml of PPS for 24 and 72 h. Total RNA was extracted from cultured chondrocytes using TRIZol reagent and purified with NucleoSpin RNA purification kit, according to the manufacturer's instructions. The RNA concentration was measured by spectrophotometry at 260 nm, while the absorbance ratio at 260/280 and 260/230 nm were used to evaluate the quality of RNA. The RNA concentration from each sample was adjusted to 1 µg and reverse transcribed into cDNA with Oligo(dt)15 primer using M-MLV RT kit according to the manufacturer's recommended protocol. The synthesized cDNA was then used to perform qPCR analysis on the Rotor-gene Q instrument using KAPA SYBR FAST qPCR kit. The relative mRNA expression levels of each gene were quantified by delta-delta Ct method and normalized against the reference gene, GAPDH. The expression of Col2 and MMP-13 were used to evaluate the chondrocyte phenotype, while the expression of CDK family including CDK1, 2, 4 and 6 were used to evaluate the cell cycle regulation. The sequence of primers used in the experiment was designed according to the data published on the NCBI website using Primer-BLAST programs, whereas the specificity of primers was validated by a single band on gel electrophoresis and confirmed

by a single peak in the melting curve analysis. The sequence, amplicon length and accession number for each of primers are indicated in Table 2.

3.3.9 Statistical analysis

Quantitative data analysis was performed using GraphPad Prism software (GraphPad Software Inc., La Jolla, CA, USA). All quantitative results are presented as mean ± SE. Correlation between PPS concentration, cell viability and cell cycle distribution were calculated using Pearson correlation coefficient, while all other statistical comparisons were performed using ANOVA with a Dunnett's multiple comparison test to compare between groups. *P*-value less than 0.05 was considered significant.

Table 2. The sequence of primers used for qPCR analysis to evaluate cell cycle regulator genes and phenotypic stability of PPS treated chondrocytes

Gene	Primer sequence (5'-3')	Amplicon length (bp)	Accession number
GAPDH	Forward: CTGAACGGGAAGCTCACTGG	129	NM_001003142.1
	Reverse: CGATGCCTGCTTCACTACCT		
CDK1	Forward: TGTATGTGCTGTGCCATCGG	150	XM_003639013.4
	Reverse: GCCTCCAGGTCTTTGAAGCA		
CDK2	Forward: CTCTAGCGCTTGCTTCATGG	72	XM_005625479.3
	Reverse: TACACAACTCCGTACGTGCC		
CDK4	Forward: TAGCTTGCGGCCTGTCTATG	145	XM_844780.5
	Reverse: CAGAGAAGACCCTCACTCGG		
CDK6	Forward: AGCCAAACGTCCCTAGAAGC	121	XM_022427346.1
	Reverse: GAGAGATGCCTGGTAGACGC		
Collagen type II	Forward: CACTGCCAACGTCCAGATGA	215	NM_001006951.1
	Reverse: GTTTCGTGCAGCCATCCTTC		
MMP-13	Forward: GGCTTAGAGGTCACTGGCAAAC	118	XM_022418390.1
	Reverse: TGGACCACTTGAGAGTTCGGG		

3.4 Results

3.4.1 Effect of PPS on morphological appearance and confluency condition of cultured chondrocytes

Morphological appearance and confluency condition of cultured chondrocytes were evaluated under light microscopy after treated with PPS for 72 h. As shown in Figure 8, the chondrocytes that treated with various concentrations of PPS show a different degree of confluency. Compared to untreated chondrocytes, a reduction in cell confluency percentage could be observed at PPS concentration of 20 µg/ml and was evident with higher concentrations of PPS at 40 and 80 µg/ml. In addition, there was no morphological difference observed between each treatment conditions, whereas chondrocytes in all treatment condition exhibited the typical elongated, fibroblast-like morphology that observed in monolayer culture.

3.4.2 PPS reduces chondrocyte viability

The chondrocyte viability was evaluated by MTT colorimetric assay after treated with PPS for 24, 48 and 72 h. Our results indicated that chondrocyte viability was reduced by PPS in a concentration-dependent manner (Figure 9). There was a significant negative correlation between PPS concentration and chondrocyte viability at 24 ($r = -0.839$; $P = 0.037$), 48 ($r = -0.959$; $P = 0.003$) and 72 h ($r = -0.945$; $P = 0.005$). Even though the significant reduction in chondrocyte viability was only observed after 72 h of treatment with the concentrations of PPS at 40 ($P = 0.045$) and 80 µg/ml ($P = 0.007$). Treatment with PPS for 72 h at the concentration of 5, 10, 20, 40 and 80 µg/ml reduced relative chondrocyte viability to 96.56 ± 4.6, 94.11 ± 4.23, 87.41 ± 3.36, 79.27 ± 2.91 and 71.42 ± 2.38%, respectively compared to control (100%). According to these results, the cytotoxic effect of PPS was suspected and required further investigation.

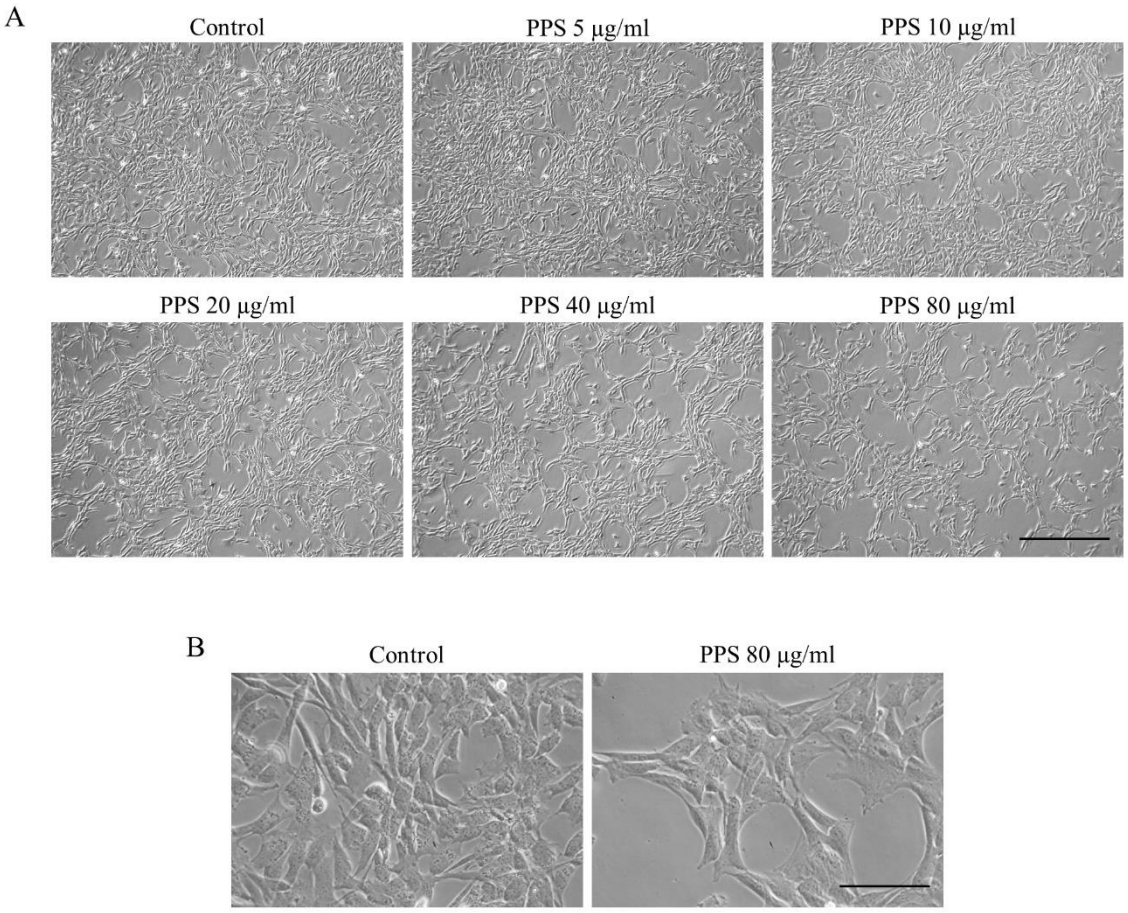

Figure 8. Morphological appearance and confluency condition of PPS treated chondrocytes observed under a light microscope.

Chondrocytes were cultured as a monolayer for 24 h prior to the treatment with various concentrations of PPS (0, 5, 10, 20, 40 and 80 µg/ml) for 72 h. **(A)** Magnification: x40, Scale bar: 500 µm. **(B)** Magnification: x200, Scale bar: 100 µm.

3.4.3 PPS has no cytotoxic effect on chondrocytes

The cytotoxic effect of PPS on chondrocytes was evaluated by cell apoptosis assay using flow cytometry analysis with annexin V and PI staining. As shown in Figure 10, the results from flow cytometry analysis at 72 h after treatment revealed a similar pattern of cell distribution among chondrocytes exposed to various concentrations of PPS and the control. The proportion of viable cells and non-viable cells (including early apoptotic, late apoptotic and necrotic cells) showed no significant difference ($P > 0.05$) between the groups. The percentage of viable cells after treated with PPS for 72 h at the concentration of 5, 10, 20, 40 and 80 µg/ml were 95.9 ± 0.6, 96.3 ± 0.4, 95.9 ± 0.8, 96.1 ± 0.8 and 96.1 ± 0.8%, respectively compared to control (94.2 ± 0.7%). These results suggested that reduce in chondrocyte viability by PPS was not related to cell death.

3.4.4 PPS increases the proportion of chondrocytes in the G1 phase while reducing the proportion of chondrocytes in the S phase of the cell cycle

The effect of PPS on chondrocyte viability was further investigated by cell cycle distribution using flow cytometry analysis with PI staining (Figure 11). Compared to untreated chondrocytes, after 24 h of PPS treatment, chondrocytes in G1 phase were significantly increased ($P = 0.001$) only at 80 µg/ml of PPS. While chondrocytes in S phase were significantly reduced at 20 ($P = 0.007$), 40 ($P = 0.005$) and 80 µg/ml ($P < 0.001$) of PPS after 24 h treatment (Table 3). Similarly, after 48 h of PPS treatment; chondrocytes in S phase were significantly reduced at 40 ($P = 0.002$) and 80 µg/ml ($P < 0.001$) of PPS (Table 3). There was a strong positive correlation observed between the PPS concentration and number of chondrocytes distributed in G1 phase at 24 ($r = 0.986$, $P < 0.001$) and 48 h ($r = 0.923$, $P < 0.001$) after treatment. In contrast, chondrocytes in S phase demonstrated a strong negative

correlation between the PPS concentration and number of chondrocytes distributed in S phase at 24 (r = -0.981, $P < 0.001$) and 48 h (r = -0.973, $P = 0.001$) after treatment. However, there was no significant correlation ($P > 0.05$) on both G1 and S phase after treatment with PPS at 72 h. In addition, there was a significant negative correlation between the PPS concentration and chondrocytes distribution in G2 phase at 48 h (r = -0.858, $P = 0.029$) and a significant positive correlation at 72 h (r = 0.815, $P = 0.048$) after treatment.

3.4.5 Effect of PPS on chondrocyte DNA and GAGs Content

Total DNA and GAGs content of cultured chondrocytes were evaluated by biochemical analysis after treated with PPS for 72 h. The results from Hoechst assay indicated the decrease in the content of DNA in cell lysates with a significant difference observed at the PPS concentrations of 40 and 80 µg/ml compared to control (Figure 12A). Total DNA content of chondrocytes treated with PPS at 40 and 80 µg/ml for 72 h was significantly decreased to 2.086 ± 0.175 ($P = 0.01$) and 1.834 ± 0.128 µg/ml ($P = 0.001$), respectively compared to control (3.101 ± 0.268 µg/ml). In addition, the results from DMMB assay revealed that higher content of GAGs was synthesized in PPS treated chondrocytes in a concentration-dependent manner (Figure 12B), although a significant increase in GAGs content was only observed with higher concentrations of PPS at 40 ($P = 0.049$) and 80 µg/ml ($P = 0.016$) compared to control. Total GAGs content normalized with DNA content evaluated after 72 h of treatment with the concentrations of PPS at 5, 10, 20, 40 and 80 µg/ml were 0.91 ± 0.12, 1.02 ± 0.11, 1.12 ± 0.12, 1.21 ± 0.12 and 1.30 ± 0.19 µg/µg DNA, respectively compared to control (0.69 ± 0.15 µg/µg DNA).

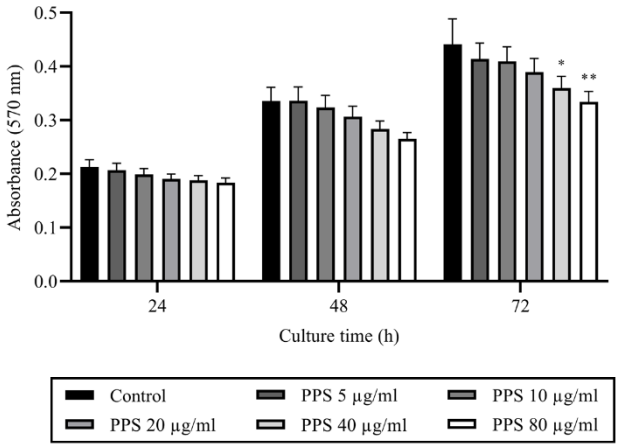

Figure 9. Treatment with PPS resulted in reduced chondrocyte viability.

Chondrocytes were cultured as a monolayer for 24 h prior to the treatment with various concentrations of PPS (0, 5, 10, 20, 40 and 80 µg/ml) for 72 h. The cell viability of cultured chondrocytes was analyzed by MTT assay at 24, 48 and 72 h during PPS treatment. The data are represented as the mean ± SE. (compared to control: **P* < 0.05 and ***P* < 0.01)

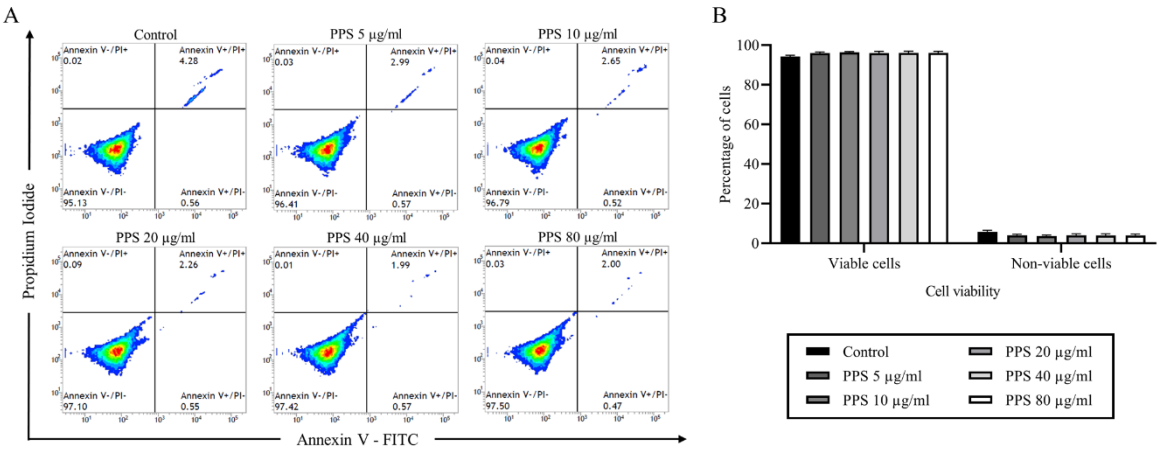

Figure 10. Treatment with PPS showed no cytotoxic effect on cultured chondrocytes.

Chondrocytes were cultured as a monolayer for 24 h prior to the treatment with various concentrations of PPS (0, 5, 10, 20, 40 and 80 µg/ml) for 72 h. Cell apoptosis was evaluated by flow cytometry analysis with annexin V and PI staining at 72 h after exposure to PPS. **(A)** Flow cytometry results showed the percentage of cells binding to annexin V and PI. Each quadrant is indicated for: upper left, necrotic cells; upper right, late apoptotic cells; lower left, live cells; and lower right, early apoptotic cells. **(B)** The bar graph represents percentage of viable and non-viable cells.

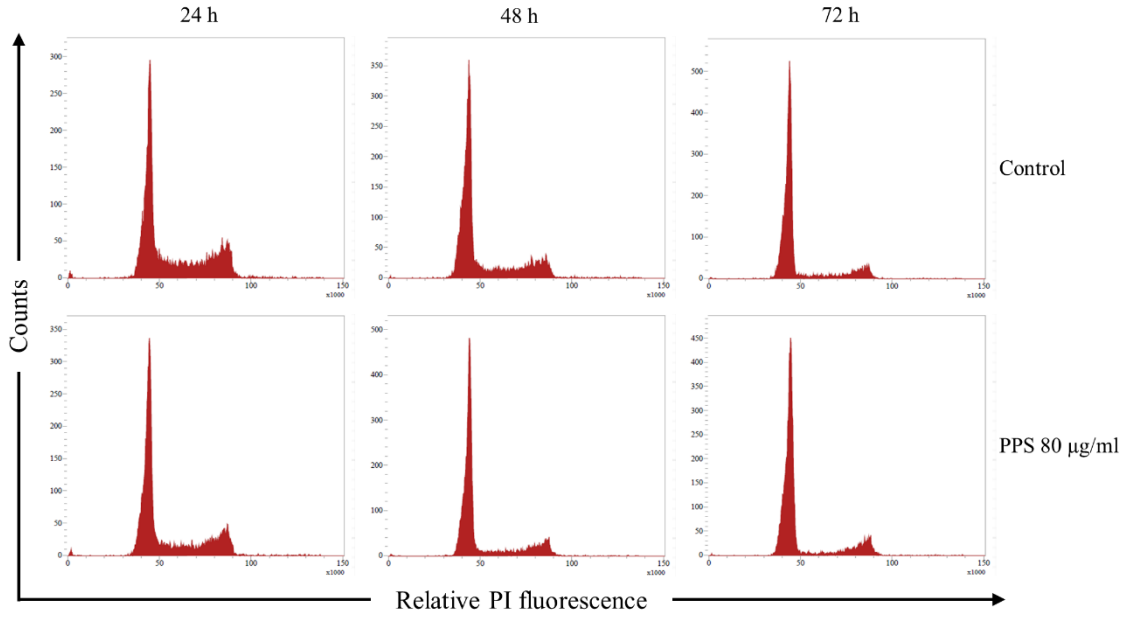

Figure 11. PPS increases the proportion of chondrocytes distributed in the G1 phase while reducing the proportion of chondrocytes distributed in the S phase of the cell cycle.

Chondrocytes were cultured as a monolayer for 24 h prior to the treatment with various concentrations of PPS (0, 5, 10, 20, 40 and 80 µg/ml) for 72 h. The cell cycle was analyzed by flow cytometry and PI staining at 24, 48 and 72 h during PPS treatment. A represents histogram showing the cell distribution pattern between control and treatment PPS at 80 µg/ml. The results were analyzed by the FlowJo software program using Watson Pragmatic model.

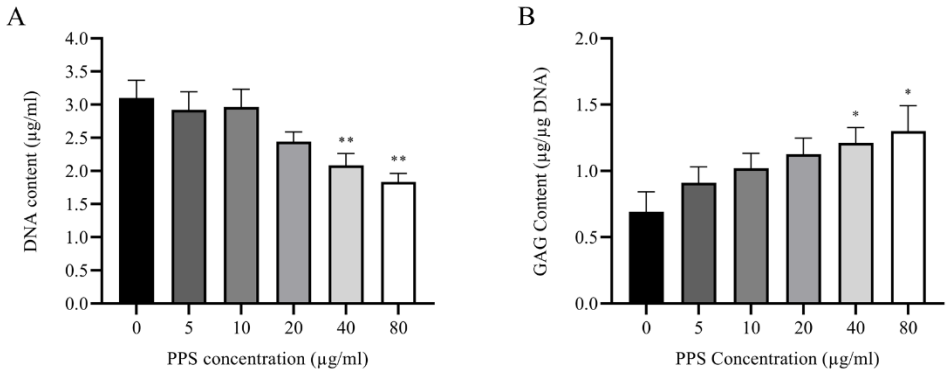

Figure 12. Treatment with PPS promotes GAGs synthesis but reduces DNA content of chondrocytes in a concentration-dependent manner.

Chondrocytes were cultured as a monolayer for 24 h prior to the treatment with various concentrations of PPS (0, 5, 10, 20, 40 and 80 µg/ml) for 72 h. Biochemical analysis was performed at 72 h after exposure to PPS. **(A)** Quantification of DNA content in cell lysates by Hoechst assay. **(B)** Quantification of GAGs content (normalized with DNA content) by DMMB assay in cell lysates. The data are represented as the mean ± SE. (compared to control: **P* < 0.05 and ***P* < 0.01)

Table 3. Percentage of cells in each phase of cell cycle analyzed by the FlowJo software program using Watson Pragmatic model

Cell cycle phase	PPS Concentration (μg/ml)					
	0	**5**	**10**	**20**	**40**	**80**
24 h						
G1 (%)	56.33 ± 2.37	56.65 ± 2.34	57.26 ± 1.95	59.14 ± 2.06	60.03 ± 2.23	63.41 ± 2.39**
S (%)	30.36 ± 1.67	30.31 ± 1.66	29.11 ± 1.45	27.75 ± 1.48**	26.23 ± 1.41**	23.54 ± 1.44***
G2 (%)	10.41 ± 0.67	10.43 ± 0.60	10.79 ± 0.63	10.25 ± 0.51	10.14 ± 0.74	9.93 ± 0.50
48 h						
G1 (%)	67.29 ± 2.21	66.30 ± 2.85	67.25 ± 3.18	68.49 ± ±2.67	70.81 ± 3.20	71.54 ± 3.06
S (%)	21.86 ± 1.93	21.98 ± 2.17	21.79 ± 2.35	20.53 ± 2.14	18.30 ± 2.27**	16.79 ± 2.18***
G2 (%)	7.95 ± 0.57	8.57 ± 0.60	7.99 ± 0.43	8.08 ± 0.50	7.85 ± 0.60	7.22 ± 0.65
72 h						
G1 (%)	77.91 ± 1.85	80.76 ± 0.90	81.49 ± 1.30	80.13 ± 1.45	80.44 ± 1.60	78.14 ± 1.51
S (%)	11.95 ± 1.28	9.66 ± 0.86	10.45 ± 0.96	10.95 ± 0.92	10.82 ± 0.96	11.16 ± 0.90
G2 (%)	6.15 ± 0.44	6.20 ± 0.43	6.53 ± 0.36	6.90 ± 0.44	7.39 ± 0.53	7.23 ± 0.57

The data are expressed as the mean ± SE. (**$P < 0.01$ and ***$P < 0.001$)

3.4.6 PPS downregulates cell cycle regulator genes, while promotes Col2 expression

The chondrocyte mRNA expression profile was analyzed by qPCR after treated with PPS at the concentration of 0 (control), 5, 20 and 80 µg/ml for 24 and 72 h. Our finding revealed a marked decrease in the mRNA expression of CDK1 and 4 in chondrocytes that treated with 40 ($P = 0.013$ and $P < 0.001$, respectively) and 80 µg/ml of PPS ($P = 0.005$ and $P = 0.033$, respectively) at 24 h compared to control (Figure 13A and 13C). However, the mRNA expression of CDK2 and 6 remained unchanged within the same treatments except in chondrocytes that treated with PPS at the concentration of 5 µg/ml in which both genes were significantly upregulated ($P < 0.05$) (Figure 13B and 13D). Notably, at 72 h after treatment, the mRNA expression of CDK2 remained significantly upregulated ($P < 0.05$) with the PPS concentration at 5 and 80 µg/ml. Conversely, at the same time point, CDK6 mRNA expression was significantly downregulated ($P < 0.001$) at all PPS concentrations. The mRNA expression of CDK1 was decreased in chondrocytes that treated with PPS at the concentration of 5 and 20 µg/ml ($P < 0.001$ and $P = 0.008$, respectively), while significantly increased with the PPS concentration at 80 µg/ml ($P = 0.024$) compared to control at 72 h of treatment. On the other hand, there was no significant difference ($P > 0.05$) in CDK4 mRNA expression between the groups at the same time point. In addition, the chondrocyte specific marker Col2 was expressed by chondrocytes in all culture groups. Although our results demonstrated a significant decrease ($P < 0.001$) in Col2 mRNA expression after treated with PPS for 24 h at the concentration of 5 and 20 µg/ml compared to the control. There was a concentration-dependent upregulation of Col2 mRNA expression at 72 h of PPS treatment with a significant difference being observed at the concentration of 20 ($P = 0.011$) and 80 µg/ml ($P = 0.009$) compared to the control (Figure 13E). Nevertheless, there was no significant difference in the mRNA expression for MMP-13 between PPS treated chondrocytes and the control at all treatment times (Figure 13F).

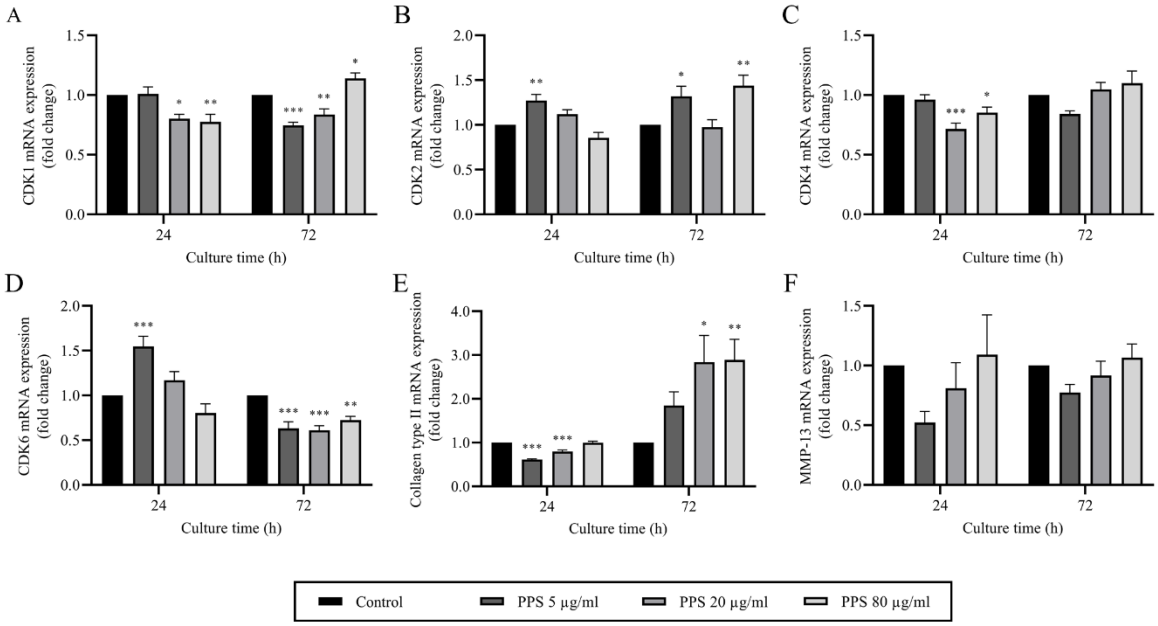

Figure 13. PPS downregulates cell cycle regulator genes, while promotes collagen type II expression. Chondrocytes were cultured as a monolayer for 24 h prior to the treatment with various concentrations of PPS (0, 5, 20 and 80 µg/ml) for 72 h. Relative mRNA expression of chondrocytes was evaluated by qPCR analysis at 24 and 72 h during PPS treatment. The relative mRNA expression of **(A)** CDK1, **(B)** CDK2, **(C)** CDK4, **(D)** CDK6, **(E)** collagen type II and **(F)** MMP-13 were normalized to the housekeeping gene, GAPDH. The data are represented as the mean ± SE. (compared to control: $*P < 0.05$, $**P < 0.01$ and $***P < 0.001$)

3.5 Discussion

It is well known that a variety of cellular responses could be observed from chondrocytes in osteoarthritic cartilage. Interestingly, the quiescent cells that lack proliferative activity as chondrocytes were able to reacquire the ability to proliferate once again during the early stages of OA progression. Although an increase in proliferative activity of chondrocytes was transient, the hallmark of proliferated chondrocytes was evidently observed by cell accumulation and cluster formation within the OA joint (Gartland et al., 2005; Goldring and Marcu, 2009; Charlier et al., 2019). We suggested that the isolated chondrocytes in monolayer culture, which prominent in proliferative activity and exhibit dedifferentiated phenotype could serve as a good research model that imitated the condition of an initial stage of OA progression. While previous studies have demonstrated an ability to promote anabolic activities and anti-inflammatory effects of PPS, to the best of our knowledge, this is the first study to demonstrate its effects on cell proliferation as a cell cycle regulator. In this study, we used canine articular chondrocytes cultured in the monolayer to demonstrates that PPS reduces chondrocyte viability not through PPS-induced cell death but by reduces proliferative activity during the early stages of monolayer culture (24 h). Our findings further demonstrate that the modulation of cell cycle by PPS appears to be through the short-term inhibition of cell cycle regulator genes, particularly CDK1 and 4. Consistent with previous findings, our results validate the use of PPS as a chondrocyte phenotype promoter as evidenced by the significant upregulation of chondrocyte specific markers, Col2 and GAGs synthesis (Ghosh et al., 2009; Bwalya et al., 2018).

According to MTT colorimetric assay and Hoechst assay, chondrocyte viability in monolayer culture treated with PPS was reduced in a concentration- and time-dependent manner. The treatment with a higher concentration of PPS at 40 and 80 µg/ml for 72 h demonstrated significantly lower cell viability compared to the control but with no significant

difference observed between the treatments at 24 and 48 h of culture. In contrast to our findings, a previous study demonstrated that PPS possessed the ability to promote proliferation and chondrogenic differentiation in MSC (Sørensen et al., 2008; Ghosh et al., 2009). We speculated that the disparity in cellular response between chondrocytes and MSC was related to their diversity in cell properties and expression patterns (Karlsson et al., 2007; Bernstein et al., 2010). Further investigation by flow cytometry analysis with annexin V and PI staining revealed that reduces in chondrocyte viability by PPS was not due to PPS-induced cell death as confirmed by the similar pattern of cell distribution among chondrocytes exposed to various concentration of PPS and the control, which showed no significant difference on both viable and non-viable cells between the groups. Consistent with other related studies on PPS, our findings clearly indicate the safety of PPS on chondrocytes even at high concentration (Ghosh, 1999; Bwalya et al., 2017; Bwalya et al., 2018).

The cause of a reduction in chondrocyte viability was uncovered by the results from cell cycle analysis, which indicated that treatment with PPS at different time points affected the proportion of chondrocytes distributed in each phase of cell cycle. Cell cycle analysis showed that PPS significantly increased the proportion of cells distributed in the G1 phase while reducing the proportion of cells distributed in the S phase. However, the effect of PPS on cell cycle distribution was only observed during the high proliferative stage of monolayer culture at 24 and 48 h with no significant difference observed at 72 h. Precisely, after chondrocytes were treated with PPS for 24 and 48 h, our results indicated a strong positive correlation between the PPS concentration and the proportion of cells distributed in G1 phase, while there was a strong negative correlation between PPS concentration and the proportion of cells distributed in S phase. These correlations on both G1 and S phase were not observed at 72 h of treatment. In addition, the relationship between PPS concentration and the proportion

of cells distributed in G2 phase of cell cycle was a negative correlation at 48 h and a positive correlation at 72 h. Taken together, this finding suggests that the treatment with PPS in monolayer cultured chondrocytes could increase the proportion of cells distributed in the G1 phase while reducing the number of cells distributed in S and G2 phases of the cell cycle. However, this concentration-dependent effect of PPS was observed only at 24 and 48 h after treatment, which considered a transient effect. We speculate that an increase in cell density on culture plates during the late proliferative stage might trigger contact inhibition phenomenon, causing mediation from various pathways that are involved in cell cycle (Gérard and Goldbeter, 2014).

Among several proteins involved in cell cycle control, CDKs are the most important regulator that drive the events of the cell cycle by phosphorylating the target proteins. During cell division, CDK4/Cyclin D and CDK6/Cyclin D complex phosphorylate the retinoblastoma protein and allow cell cycle progression through G1, while CDK2/Cyclin A and CDK2/Cyclin E complex activate DNA synthesis (LuValle, 2000; Gérard and Goldbeter, 2014; Berridge, 2014). The activation of CDK1/Cyclin B control cell mitosis, and together, CDK1 is a major kinase that could form a complex with Cyclin D, E and A, instead of CDK2, 4 and 6 for correct progression in the cell cycle (Berridge, 2014). In this study, the mRNA expression of CDK1, 2, 4 and 6 were evaluated by qPCR analysis. During the high proliferative stage of chondrocytes (24 h), an increase in the proportion of cells distributed in G1 phase and subsequently reduce in S phase has corresponded to the downregulation of CDK1 and 4 mRNA expression. However, the mRNA expression of CDK2 and 6 were significantly upregulated in the presence of PPS at low concentration. Although the mRNA expression of CDK1, 2 and 4 at a low proliferative stage of chondrocytes (72 h) were directly proportional to PPS concentration, the proportion of cells distributed in each phase of cell cycle was unaffected.

Judging from these results, we speculate that PPS modulates the cell cycle progression in monolayer cultured chondrocytes mainly through the major kinase CDK1, together with CDK4. While the downregulation of CDK1 and 4 mRNA expression observed in this study could be consistent with the inhibitory effects of PPS on nuclear factor-kappa B (NF-κB) nuclear translocation in chondrocytes culture that has been previously reported (Sunaga et al., 2012; Bwalya et al., 2017). As the reduction in NF-κB activation could affect cell cycle progression, particularly in the early stage of cell cycle (Joyce et al., 2001; Jhou et al., 2009).

Consistent with a previous study, our results indicate significantly higher expression of chondrocyte specific markers Col2 as well as a higher GAGs synthesis from the cultured chondrocytes that treated with PPS compared to untreated (Ghosh et al., 2009; Bwalya et al., 2018). Interestingly, the relationship between Col2 and CDK6 mRNA expression were inversely correlated at both early and late proliferative stage. We suggest that the low mRNA expression of Col2 observed in this study was due to the high mRNA expression of CDK6, which has been shown to induce c-Jun phosphorylation that could lead to the suppression of Col2 and Sox9 (Hwang et al., 2007). Furthermore, previous studies have demonstrated that an increase in the proliferation rate of chondrocytes in osteoarthritic cartilage is directly related to higher gene expression of cell cycle regulators, CDK6 and Cyclin D compared to normal chondrocytes (DeAndrés et al., 2016). On the other hand, the treatment with PPS showed no significant effect on the mRNA expression of proteolytic enzymes MMP-13 in cultured chondrocytes. Although a previous study has shown that PPS can downregulate interleukin-1 beta (IL-1β) -induced MMP-13 upregulation in canine articular chondrocytes *in-vitro* (Bwalya et al., 2017). This finding might demonstrate the unique selective inhibitory effect of PPS only on cytokine-induced MMP-13 upregulation but not on the constitutively expressed MMP-13,

which is required for the normal articular cartilage to maintain regular ECM turnover (Yamamoto et al., 2016).

In conclusion, the study presented in this chapter demonstrates that PPS reduces cell viability of canine articular chondrocytes in monolayer culture by reduces proliferative activity during the early stages of culture, while indicating the safety of PPS on chondrocytes. The treatment with PPS modulates cell cycle progression of cultured chondrocytes by maintaining a significantly higher proportion of cells distributed in the G1 phase and a significantly lower proportion of cells distributed in the S phase in a concentration- and time-dependent manner. The inhibition on proliferative activity of cultured chondrocytes appears to be through the short-term inhibition of cell cycle regulator genes, particularly CDK1 and 4. In addition, our results further validate the use of PPS as a chondrocyte phenotype promoter due to the significant upregulation of Col2 mRNA expression and GAGs synthesis. Therefore, the effect of PPS on the inhibition of chondrocyte proliferation while promoting a chondrocyte phenotype may be beneficial on therapeutic treatment during the early stages of OA progression, which transient increase in proliferative activity of chondrocytes with subsequent phenotypic shift and less productive in an essential component of ECM is observed.

CHAPTER 4

An insight into the role of apoptosis and autophagy in nitric oxide-induced chondrocyte cell death

4.1 Summary

The purpose of the study was to investigate the roles and characterize the molecular mechanisms regulating apoptosis and autophagy in NO-induced chondrocyte cell death. Canine articular chondrocytes were isolated and cultured from femoral head cartilages of three dogs. The second passage chondrocytes were cultured in monolayer conditions for 24 h. Thereafter, chondrocytes were treated with sodium nitroprusside (SNP) combined with the presence or absence of IL-1β and nutrient-deprived conditions. The effects of SNP on chondrocytes were evaluated based on cell viability, NO production, autophagic activity and apoptotic event. Our results show that co-treatment with IL-1β under nutrient-deprived condition potentially enhanced the effect of NO-induced cell death. While the treatment with SNP significantly reduced autophagic activity, autophagic flux and multiple autophagy-related genes expression of chondrocytes as confirmed by immunocytochemistry, Western blot and qPCR analysis. These findings were associated with an increase in the ERK, Akt and mTOR phosphorylation, whereas autophagy induction through mTOR/p70S6K inhibition by rapamycin significantly reduced NO-induced cell apoptosis. Furthermore, the cleavage of poly (ADP-ribose) polymerase (PARP) and caspase-3 activation in response to apoptosis was weakly detected. These results corresponded with a significantly increase in apoptosis-inducing factor (AIF) expression, suggesting the involvement of the caspase-independent pathway. These findings suggest that NO inhibits autophagy and induces chondrocyte apoptosis mainly, but not entirely through the caspase-independent pathway. Our data indicates that autophagy is a protective mechanism in the pathogenesis of OA and could be proposed as a valuable therapeutic target for the treatment of degenerative joint diseases.

4.2 Introduction

OA was previously defined as a prototypical degenerative disease resulting from wear and tear processes, which leads to loss of articular cartilage. However, many recent studies have shown that several biochemical mediators were contributed to the initiation and progression of OA through the inflammatory conditions and further involved in the metabolic condition of chondrocytes, causing an imbalance between anabolic and catabolic pathway (Krasnokutsky et al., 2008; Man and Mologhianu, 2014; Rahmati et al., 2016). It has been well demonstrated that several inflammatory mediators and cytokines could be observed with a relatively high level from both synovial fluid and serum samples in patients with OA or rheumatoid arthritis (RA) (Sokolove and Lepus, 2013; Robinson et al., 2016). Under the pathological condition, activated chondrocytes, as well as inflamed synoviocytes, are a potential source of biochemical mediators in the pathophysiology of OA. The excessive levels of mediators released from these cells include MMPs, pro-inflammatory cytokines (e.g., IL-1β, IL-6, IL-15, IL-17, TNF-α), prostaglandin E2 (PGE2), reactive oxygen species (ROS) and NO (Abramson, 2008a; Miller et al., 2014; Rahmati et al., 2016).

Among numerous inflammatory mediators associated with the pathological condition of OA and RA, NO is a major biochemical mediator that mainly responsible for the catabolic activity of chondrocytes (Fermor et al., 2007; Vuolteenaho et al., 2007; Abramson, 2008a). Generally, NO is a cellular signaling molecule that spontaneously and constitutively produced during the conversion of L-arginine to L-citrulline by the enzyme nitric oxide synthase (NOS) (Abramson, 2008a). In healthy articular cartilage, a small amount of NO is existed and implicated in the physiological function of chondrocytes, including proliferation, differentiation, and even in protective mechanism (Stichtenoth and Frölich, 1998; Nishida et al., 2000; Del Carlo and Loeser, 2002). Although a small amount of NO was considered as

harmless and even played an important role in cellular signaling to maintain physiological homeostasis, the overproduction of NO by osteoarthritic chondrocytes is associated with the development and maintenance of OA (Fermor et al., 2007; Vuolteenaho et al., 2007; Rahmati et al., 2016). While the previous study has shown that NOS inhibitors could reduce the severity of arthritis in an animal model (Fermor et al., 2007). An excessive amount of NO was involved in the inflammatory condition, cartilage destruction, mitochondrial dysfunction, inhibition of chondrocyte proliferation and induction of apoptotic cell death (Mazzetti et al., 2001; Abramson, 2008b). The death of chondrocytes that occurred in OA progression is associated with progressive cartilage degradation and considered as a central feature of advanced stages in osteoarthritic cartilage (Sandell and Aigner, 2001; Musumeci et al., 2015). Depend on cellular features, chondrocyte cell death could be classified into autophagy, apoptosis, chondroptosis, necrosis or even a combination of these processes (Charlier et al., 2016).

One of the most widely studied exogenous NO donors that used to demonstrate the biological role of NO is SNP. Although chondrocyte cell death could be induce by several factors and occurred through a variety of molecular pathways, it has been shown that a strong correlation exists between the cytotoxicity of NO and apoptotic cell death (Blanco et al., 1995; Kühn and Lotz, 2003; Kühn et al., 2004). Apoptosis is a form of programmed cell death that undergoes through an orderly and highly regulated process, which leads to cell death. In fact, apoptosis is an essential process to maintain the homeostasis of various tissues, whereas dysregulation in apoptosis is associated with a variety of diseases (Elmore, 2007; Hwang and Kim, 2015). Nevertheless, the molecular mechanisms of NO-induced chondrocyte apoptosis are remains to be fully explained and several studies suggest that the outcome depended on each experimental condition (Kühn et al., 2004; Charlier et al., 2016). On the other hand, autophagy is another form of programmed cell death characterized by the presence of double-

membrane cytoplasmic vesicles called autophagosomes that use for the self-digesting process. Autophagy is the physiological cellular mechanism used to maintain cellular function by degrading organelles and proteins which promotes cell survival through the unfavorable conditions (Chang et al., 2013; Luo et al., 2019). While excessive autophagy could lead to cell death, a decrease in autophagy is also related to several pathological conditions, including OA (Caramés et al., 2010; Musumeci et al., 2015). Despite the fact that the effects of NO regulating autophagy in chondrocytes have been previously reported, the results are still unclear and further studies are required to confirm the role of autophagy in NO-induced chondrocyte cell death (Sarkar et al., 2011; Sasaki et al., 2012; Shen et al., 2014).

Both apoptosis and autophagy are essential cellular degradation mechanisms that influence the homeostasis and survivability of chondrocytes. Further investigation on the mutual relationship and interaction between these two pathways will undoubtedly provide valuable information on the pathophysiology and therapeutic approaches for OA. Our hypothesis is that NO synthesized in SNP treated chondrocytes could potentially reduce chondrocyte viability through the apoptosis process, whereas autophagy plays a survival role against NO-induced chondrocyte cell death. Therefore, the purpose of this study was to investigate the roles and characterize the molecular mechanisms regulating apoptosis and autophagy in NO-induced chondrocyte cell death.

4.3 Material and Methods

4.3.1 Reagents and antibodies

The sources of materials used were as follows: Antibodies against microtubule-associated protein light chain 3 (LC3) and sequestosome-1 (p62/SQSTM1) were purchased from Novus Biologicals (Littleton, CO, USA); Antibodies against β-actin, AIF, cleaved caspase-3, PARP, ERK1/2, phospho-ERK1/2, Akt, phospho-Akt, mammalian target of rapamycin (mTOR), phospho-mTOR, p70 ribosomal protein S6 kinase (p70S6K), phospho-p70S6K, HRP conjugated anti-rabbit IgG and bafilomycin A1 were purchased from Cell Signaling Technology (Danvers, MA, USA); Rapamycin was purchased from Invivogen (San Diego, CA, USA); Recombinant canine IL-1β was purchased from Kingfisher Biotech (Saint Paul, MN, USA); Protein quantification assay kit was purchased from Macherey-Nagel; Radioimmunoprecipitation assay (RIPA) buffer and protease inhibitor cocktail were purchased from Sigma-Aldrich; Caspase-3 assay kit was purchased from Abcam (Cambridge, UK); NucBlue Fixed Cell ReadyProbes and ProLong Gold Antifade reagent were purchased from Thermo Fisher Scientific (Eugene, OR, USA); DMEM was purchased from Gibco; FBS was purchased from Nichirei Biosciences Inc.; HEPES and MTT were purchased from Dojindo; KAPA SYBR FAST qPCR kit was purchased from KAPA Biosystems; FITC annexin V apoptosis detection kit I was purchased from BD Bioscience; TRIZol reagent, M-MLV RT kit and FITC conjugated anti-rabbit IgG were purchased from Invitrogen; Culture dishes and culture plates were purchased from Corning. All other reagents were purchased from Wako Pure Chemicals Industries unless stated otherwise.

4.3.2 Chondrocytes isolation and culture

The use of animal samples was in accordance with Hokkaido University Institutional Animal Care and Use Committee guidelines (approval #12–0059). Healthy canine articular cartilage tissue samples were isolated from the femoral head of three dogs (3-4 years old) at Hokkaido University Veterinary Teaching Hospital. These three dogs were experimental Beagle dogs that were euthanized at the end of an experimental study not related to this study. Briefly, articular cartilage tissue samples were harvested and dissected into small sections. Then the digestion process was performed in DMEM supplemented with 0.3% collagenase type I for 18 h at 37°C in a 5% CO_2 incubator. The released chondrocytes were separated by filtering through a 40 μm nylon filter and primary chondrocytes were expanded at a density of 15,000 cells/cm^2. Chondrocytes were passaged at 80-90% confluence by washed once with PBS and released from culture dishes using 0.05% trypsin with 0.02% EDTA in PBS. Following the above procedure, the second passage chondrocytes were used for any further experiments. The culture media used in this study was DMEM containing 10 mM HEPES, 25 mM $NaHCO_3$, 100 U/ml penicillin G potassium and 73 U/ml streptomycin sulfate.

4.3.3 Chondrocytes treatment

Unless specified otherwise, all cultured chondrocytes used in this study were seeded in 60 mm polystyrene culture dishes in DMEM containing 10% FBS and incubated for 24 h at 37°C in a 5% CO_2 incubator. Thereafter, the culture media was removed, and chondrocytes were either not treated or treated with 10 ng/ml IL-1β in DMEM containing 10% FBS for 72 h. Then the culture media was changed to either DMEM containing 10% FBS or serum-free DMEM with the presence or absence of 100 μM SNP and incubated for a further 8 h. The effect of autophagic activity on cultured chondrocytes was evaluated by treating with 10 μM

rapamycin during this last 8 h of treatment. While 100 nM bafilomycin was added at 4 h before the end of the treatment to assess the autophagic flux.

4.3.4 Cell viability assay

Chondrocytes were seeded into 96-well polystyrene culture plates and treated as described above with various concentrations of SNP (0, 25, 50, 100 and 200 μM) for 24 h. Cell viability was evaluated by MTT colorimetric assay. Briefly, the cells were washed once with PBS, then 0.5 mg/ml MTT solution prepared in DMEM was added into each well and incubated for 4 h at 37°C in a 5% CO_2 incubator. The MTT solution was then removed and DMSO was added to dissolve formazan crystals. The absorbance was measured using a Multiskan FC microplate reader at 570 nm.

4.3.5 Cell apoptosis assay

Chondrocyte apoptosis was evaluated with annexin V and PI stain using FITC annexin V apoptosis detection kit I in accordance with the manufacturer's protocol. Co-treatment with autophagy inducer (10 μM rapamycin) or inhibitor (100 nM bafilomycin) during the last 8 h of SNP treatment was used to evaluate the roles of autophagy in cultured chondrocytes. In brief, the cells were harvested and washed twice with PBS, then resuspended in binding buffer. FITC-annexin V and PI were added into the cell suspension, then incubated for 15 min in darkness at room temperature. The samples were analyzed using a FACS Verse flow cytometer.

4.3.6 Caspase-3 activity assay

Caspase-3 activity was determined using a caspase-3 assay kit according to the manufacturer's instructions. Briefly, chondrocytes were harvested, washed once with PBS and resuspended in chilled cell lysis buffer for 10 min on ice. The protein concentration of each

sample was measured by protein quantification assay kit and adjust to 2 µg/µl, then DEVD-pNA substrate and reaction buffer containing DTT was added. Samples were incubated for 2 h at 37°C and the absorbance was measured using a Multiskan FC microplate reader at 405 nm.

4.3.7 Quantification of nitrite

The concentration of nitrite accumulated in the cell culture supernatants was determined by Griess reaction with sodium nitrite as standard. After treatment, 50 µl of cell culture supernatants were collected and mixed with an equal amount of Griess reagent containing 0.1% N-(1-Naphthyl)-ethylenediamine dihydrochloride and 1% sulfanilamide in 5% H_3PO_4, then incubated for 10 min in darkness at room temperature. The absorbance was measured with a Multiskan FC microplate reader at 540 nm.

4.3.8 Protein isolation and Western blot analysis

Total proteins were extracted from cultured chondrocytes using chilled RIPA buffer supplemented with protease inhibitor cocktail and cell debris was removed by centrifugation at 12,000 rpm for 20 min at 4°C. The protein concentration was measured by protein quantification assay kit, then adjusted and 4 µg of protein from each sample was separate on 4-12% sodium dodecyl sulfate-polyacrylamide gel electrophoresis (SDS-PAGE) for 60 min at 140 V, then transfer onto polyvinylidene difluoride (PVDF) membranes for 90 min at 75 V. Membranes were blocked with 10% skim milk in PBS supplemented with 0.1% Tween 20 (PBST) for 1 h and incubated with primary antibodies in 1:1,500 (1:4,000 for β-actin) dilution overnight at 4°C. After incubation, membranes were washed thrice with PBST at 5 min interval on the shaker. Subsequently, membranes were incubated with HRP conjugated anti-rabbit IgG at a dilution of 1:3,000 (1:8,000 for β-actin) for 1 h then washed thrice with PBST at 5 min interval on the shaker. Finally, membranes were incubated in HRP substrate for 5 min. The

results of Western blot were visualized using Image Quant LAS 4000 (GE Healthcare, Buckinghamshire, UK) and the intensity of each protein bands were quantified using ImageJ software (NIH, Bethesda, MD, USA). Quantified values were normalized by β-actin as a loading control, while phosphorylated proteins were normalized by the corresponding total proteins.

4.3.9 RNA isolation and qPCR analysis

Total RNA was extracted from cultured chondrocytes using TRIZol reagent, according to the manufacturer's instructions. The RNA concentration was measured by spectrophotometry at 260 nm, while the absorbance ratio at 260/280 and 260/230 nm were used to evaluate the quality of RNA. The RNA concentration from each sample was adjusted to 1 μg and reverse transcribed into cDNA with Oligo(dt)15 primer using M-MLV RT kit according to the manufacturer's recommended protocol. The synthesized cDNA was then used to perform qPCR analysis on the Rotor-gene Q instrument using KAPA SYBR FAST qPCR kit. The relative mRNA expression levels of each gene were quantified by delta-delta Ct method and normalized against the reference gene, GAPDH. While the expression of Atg5, beclin-1, Atg7, LC3 and p62 were used to verify the effects of NO on autophagy at the gene transcription level. The sequence of primers used in the experiment was designed using BLAST programs, which available on the NCBI website, whereas the specificity of primers was validated by a single peak in the melting curve analysis. The sequence, amplicon length and accession number for each of primers are indicated in Table 4.

4.3.10 Immunocytochemistry assay

Immunocytochemistry was performed on chondrocytes grown on 8-well chamber slides. After treatment, chondrocytes were washed once with PBS and fixed in 4%

paraformaldehyde for 10 min, incubated with 0.1 M glycine in PBS for 10 min, permeabilized with 0.05% digitonin in PBS for 5 min, then washed thrice with PBS at 5 min interval on the shaker. Non-specific antibody binding was blocked by incubation with 5% FBS in PBS for 30 min. The fixed cells were incubated with LC3 antibody (MBL, Nagoya, Japan) in 1:500 dilution overnight at 4°C. After incubation, cells were washed thrice with PBS at 5 min interval on the shaker. Subsequently, cells were incubated with FITC conjugated anti-rabbit IgG at a dilution of 1:1,000 for 1 h in darkness. NucBlue Fixed Cell ReadyProbes was used to stain the nucleus, while ProLong Gold Antifade reagent was used to mount the slides. The fluorescent images were captured using LSM 700 laser scanning confocal microscope and ZEN software (Carl Zeiss, Jena, Germany).

4.3.11 Statistical analysis

Quantitative data analysis was performed using GraphPad Prism software (GraphPad Software Inc., La Jolla, CA, USA). All quantitative results are presented as mean ± SE. Statistical comparisons were performed using ANOVA, with a Dunnett's multiple comparison test to compare between groups. *P*-value less than 0.05 was considered significant.

Table 4. The sequence of primers used for qPCR analysis to evaluate autophagy-related genes in SNP treated chondrocytes

Gene	Primer sequence (5'-3')	Amplicon length (bp)	Accession number
GAPDH	Forward: CTGAACGGGAAGCTCACTGG	129	NM_001003142.1
	Reverse: CGATGCCTGCTTCACTACCT		
Atg5	Forward: GAGGTGTCAGTTCCTCGCAA	105	XM_005627675.3
	Reverse: TCTGATCACTGTTCCACGGG		
Beclin-1	Forward: TGTCTGCCCTACAGGATGGA	163	XM_005624442.3
	Reverse: AAGACACCCAAGCAAGACCC		
Atg7	Forward: GAGTCCCAGCGCTACCATAC	144	XM_022406362.1
	Reverse: GCTGCGCTAAGTTACAGGGA		
LC3	Forward: TGGCTCCTGAACTGAACTGC	135	XM_005634951.2
	Reverse: CCAGGAGGGCATCCCTAACA		
p62	Forward: GCCCGAGATGGAGTCTGATA	97	XM_022425090.1
	Reverse: AGACTGCAGTTCACCTGTGG		

4.4 Results

4.4.1 IL-1β and starvation condition enhances the effect of NO-induced cell death

The chondrocyte viability was evaluated by MTT colorimetric assay after treated with various concentrations of SNP. As shown in Figure 14, the treatment condition that pre-incubated with IL-1β and treated with SNP under serum starvation could reduce chondrocyte viability with a lower concentration of SNP at 50 µM. While the chondrocyte viability in other treatment conditions was reduced by SNP at the concentration of 200 µM. Our results suggested that IL-1β and nutrient-deprived conditions are able to enhance the effect of NO-induced cell death. According to these results, the impairment of autophagic activity was suspected and required further investigation.

4.4.2 Co-treatment with SNP and IL-1β under nutrient-deprived condition exhibit low cell viability but express high autophagosome formation, as detected by LC3-II

The conversion of LC3-I to LC3-II (LC3 lipidation) detected by Western blot analysis (Figure 15A) was used to observe a number of autophagosome formation presented in chondrocytes. Despite the presence of IL-1β and SNP, the protein expression of LC3-II in serum-starved chondrocytes was increased in all groups (Figure 15B). Even though the significant increase in autophagosome formation was only observed in the chondrocytes that pre-incubated with IL-1β and treated with SNP ($P < 0.001$). Our results also reveal that protein expression of p62 was significantly decreased only in untreated with serum-starved chondrocytes ($P = 0.041$) (Figure 15C). These results revealed that high autophagosome formation was observed in the treatment conditions that showed the lowest cell viability.

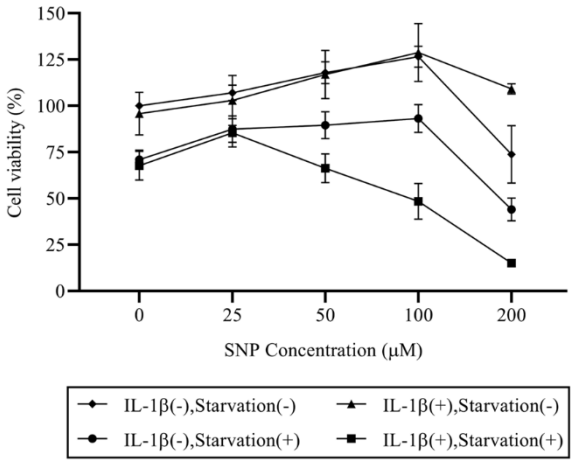

Figure 14. Co-treatment with SNP and IL-1β under nutrient-deprived condition enhances the effect of NO-induced cell death.

Chondrocytes were either not treated or treated with 10 ng/ml IL-1β for 72 h prior to the stimulation with various concentrations of SNP (0, 25, 50, 100 and 200 μM) in the culture media with the presence or absence of serum supplement for 24 h. Reduction in cell viability as evaluated by MTT assay was observed at 200 μM SNP in three groups, except the chondrocytes that pre-treated with IL-1β and stimulated with SNP in the culture media without serum supplement in which cell viability reduction commenced with the lower concentration of SNP at 50 μM. The data are represented as the mean ± SE.

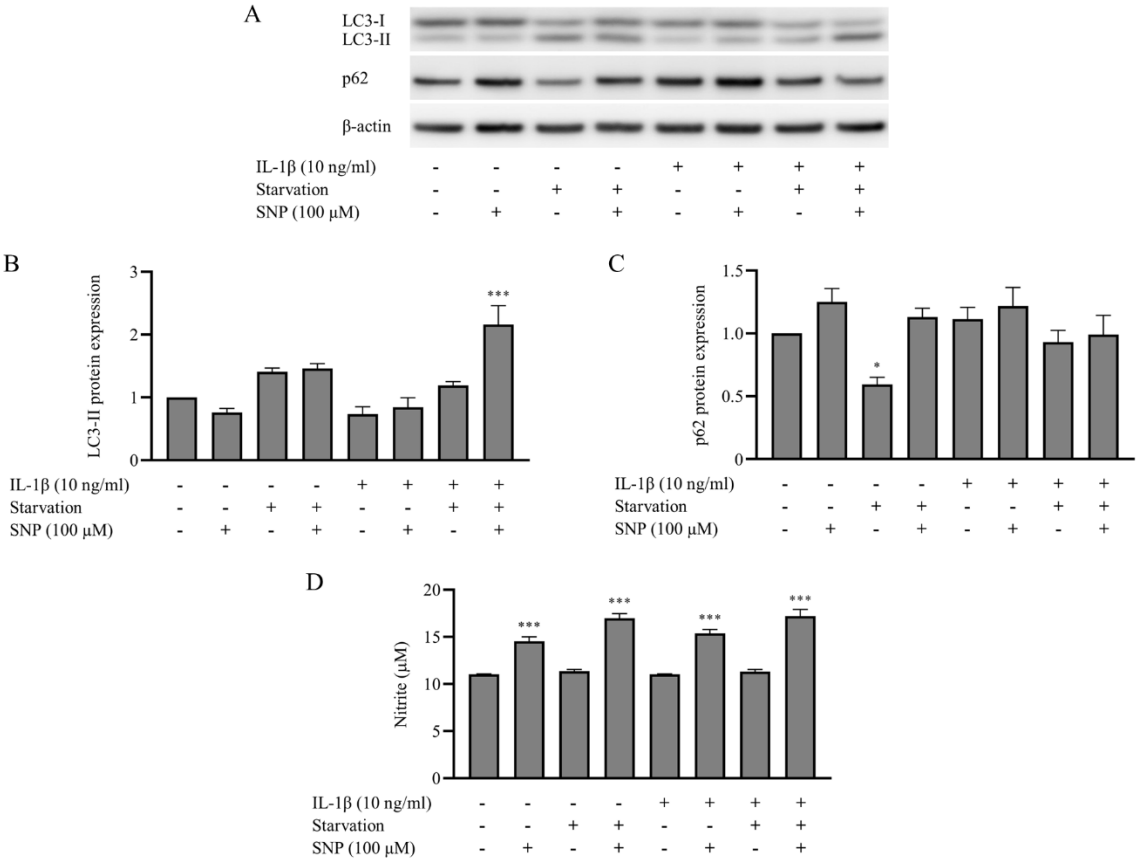

Figure 15. Autophagosome formation was increased in the chondrocytes that pre-treated with IL-1β and stimulated with SNP under nutrient-deprived condition.

Chondrocytes were either not treated or treated with 10 ng/ml IL-1β for 72 h prior to the stimulation of 100 μM SNP in the culture media with the presence or absence of serum supplement for 8 h. **(A)** Total protein was analyzed by Western blot, using an antibody for LC3, p62 and β-actin. **(B and C)** Comparison of the protein expression level normalized to β-actin of LC3-II and p62. **(D)** Comparison of nitrite accumulated in the cell culture supernatants, which determined by the Griess reaction. The data are represented as the mean ± SE. (compared to control: **P* < 0.05 and ****P* < 0.001)

4.4.3 Activation of autophagy by rapamycin reduces cell apoptosis

The cytotoxic effect of SNP on chondrocytes was evaluated by cell apoptosis assay using flow cytometry analysis with annexin V and PI staining. The autophagy inducer, rapamycin and inhibitor, bafilomycin were co-treated with SNP to characterize the interaction between autophagy and apoptosis, and to exclude the possibility of autophagic cell death. As shown in Figure 16A, the results from flow cytometry analysis indicated that cell apoptosis was induced by SNP treatment. The proportion of viable cells were significantly reduced ($P < 0.001$) in all SNP treated chondrocytes (Figure 16B). However, co-treatment with rapamycin reduced the cytotoxic effect of SNP on chondrocytes as indicated by a significant increase in the proportion of live cells ($P < 0.001$), compared to either SNP alone or a combination of SNP and bafilomycin. While the proportion of live cells between chondrocytes that treated with SNP alone and co-treatment with bafilomycin were not significant differences ($P = 0.666$). These results suggested that the cell death observed in this study was not caused by excessive autophagic activity. Conversely, activation of autophagy by rapamycin plays a protective role against NO-induced cell apoptosis.

4.4.4 NO reduces activation of autophagy, autophagic flux and Atg mRNA expression

An increase in autophagosome formation as indicated by high LC3-II protein expression in SNP treated chondrocytes was further distinguish between high autophagic activity and inhibition of subsequent events by blocking the fusion of autophagosomes and lysosomes. The V-ATPase inhibitor, bafilomycin was used to inhibit autophagosome-lysosome fusion by add into the culture media at 4 h prior to the end of the treatment, then analyzed with Western blot (Figure 17A and 17D). At first, our results demonstrated that the protein expression of LC3-II was significantly increased by the treatment with rapamycin ($P = 0.006$),

SNP (P = 0.008) or even a combination of SNP and rapamycin (P < 0.001), compared to untreated chondrocytes (Figure 17B). While the protein expression of p62 was significantly increased by the treatment with rapamycin (P = 0.003) and a combination of SNP and rapamycin (P = 0.039) (Figure 17C). However, treatment with bafilomycin revealed that the protein expression of LC3-II in SNP treated chondrocytes were significantly decreased (P = 0.008), compared to untreated chondrocytes (Figure 17E). Whereas the LC3-II protein expression remained significantly increased in the chondrocytes that treated with either rapamycin alone (P = 0.016) or a combination of SNP and rapamycin (P = 0.006) (Figure 17E). As shown in Figure 17F, the protein expression of p62 was significantly increased only by the co-treatment with SNP and rapamycin (P = 0.032). These results were further confirmed by the presence of cytoplasmic LC3-II puncta formation in chondrocytes using immunocytochemistry (Figure 18). Consistent with Western blot analysis, without bafilomycin, the untreated chondrocytes showed the lowest amount of LC3-II puncta formation in cytoplasm. Whereas the accumulation of LC3-II puncta was reduced by the treatment with SNP under the presence of bafilomycin. In addition, we also investigate the effects of NO on autophagic activity of chondrocytes at the gene transcription level using qPCR analysis. Our finding revealed a marked decrease in mRNA expression of beclin-1 (P < 0.001), Atg7 (P < 0.001) and LC3 (P = 0.003) in chondrocytes treated with SNP alone (Figure 17H-J). Notably, the co-treatment with rapamycin had no effects on these autophagy-related genes. The mRNA expression of beclin-1 (P < 0.001), Atg7 (P < 0.001) and LC3 (P < 0.001) were remained significantly decreased (Figure 17H-J), similar to the chondrocytes that treated with SNP alone. While the expression of Atg5 mRNA was not affected by any treatment conditions in this study (Figure 17G). In addition, the mRNA expression of p62 was significantly increased by the treatment with rapamycin (P = 0.021) and a combination of SNP and rapamycin (P < 0.001) (Figure 17K). Taken together, these results suggest that SNP could reduce the activation of

autophagy, autophagic flux and multiple autophagy-related genes expression of cultured chondrocytes.

4.4.5 NO generated by SNP is not directly related to cell death

The concentration of nitrite accumulated in cell culture supernatants from SNP treated chondrocytes were quantified by Griess reaction. As shown in Figure 15D and 17L, treatment with SNP significantly increased the production of NO in all groups ($P < 0.001$) regardless of the presence of IL-1β, rapamycin or starvation condition. Combining with the cell viability results (Figure 14), we suggest that NO alone was capable of triggering cell death only in high concentration, while the cell viability could be potentially reduced with the combination of IL-1β and nutrient-deprived condition. Nevertheless, rapamycin treated chondrocytes could maintain higher cell viability (Figure 16B) under the same condition.

4.4.6 NO reduces autophagy via promotion of the ERK, Akt and mTOR pathway

The molecular mechanism of NO on autophagy was further investigated on the ERK and Akt pathway. Our results from Western blot analysis indicated that treatment with SNP significantly promotes ($P < 0.001$) the phosphorylation of ERK, Akt, mTOR and p70S6K, compared to untreated chondrocytes (Figure 19B-E). Although the co-treatment with rapamycin potentially inhibits the phosphorylation of mTOR signaling, it had no effect on the phosphorylation of ERK and Akt (Figure 19B-C). These results suggested that the reduction of autophagic activity in SNP treated chondrocytes was due to an increase in phosphorylation levels of ERK, Akt and mTOR.

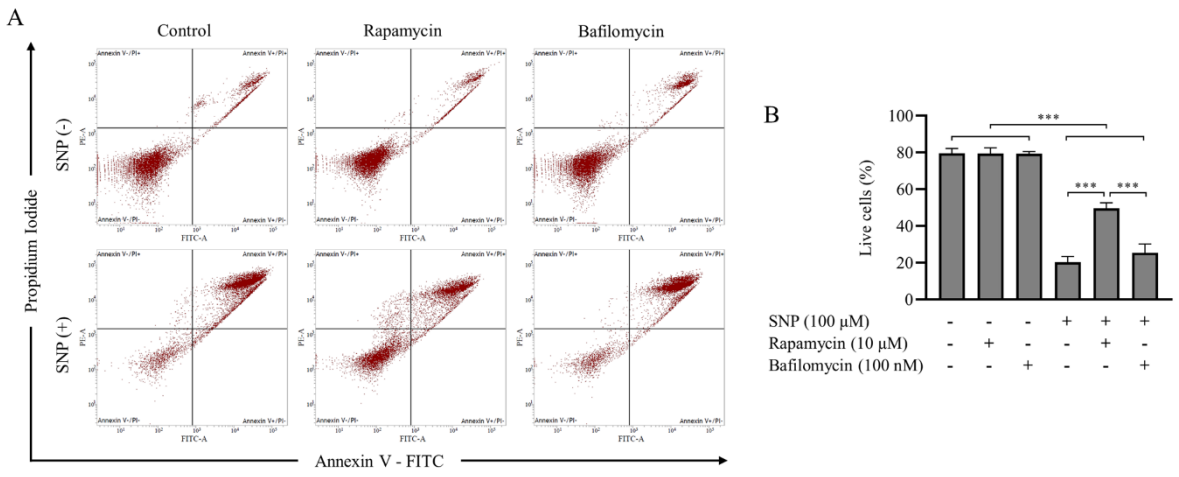

Figure 16. Activation of autophagy by rapamycin reduced cell apoptosis, whereas the inhibition of autophagy by bafilomycin had no effect on cell apoptosis.

Chondrocytes were pre-incubated with IL-1β and either not treated or treated with 100 μM SNP under the nutrient-deprived condition for 8 h. Together with SNP treatment, the chondrocytes were incubated with the presence or absence of autophagy inducer (10 μM rapamycin) or inhibitor (100 nM bafilomycin). **(A)** Flow cytometry detection of chondrocytes apoptosis was evaluated with annexin V and PI staining. The results showed the percentage of cells binding to annexin V and PI. Each quadrant is indicated for: upper left, necrotic cells; upper right, late apoptotic cells; lower left, live cells; and lower right, early apoptotic cells. **(B)** Comparison of the proportion of live cells between each treatment condition. The data are represented as the mean ± SE. (compared to control: ****P* < 0.001)

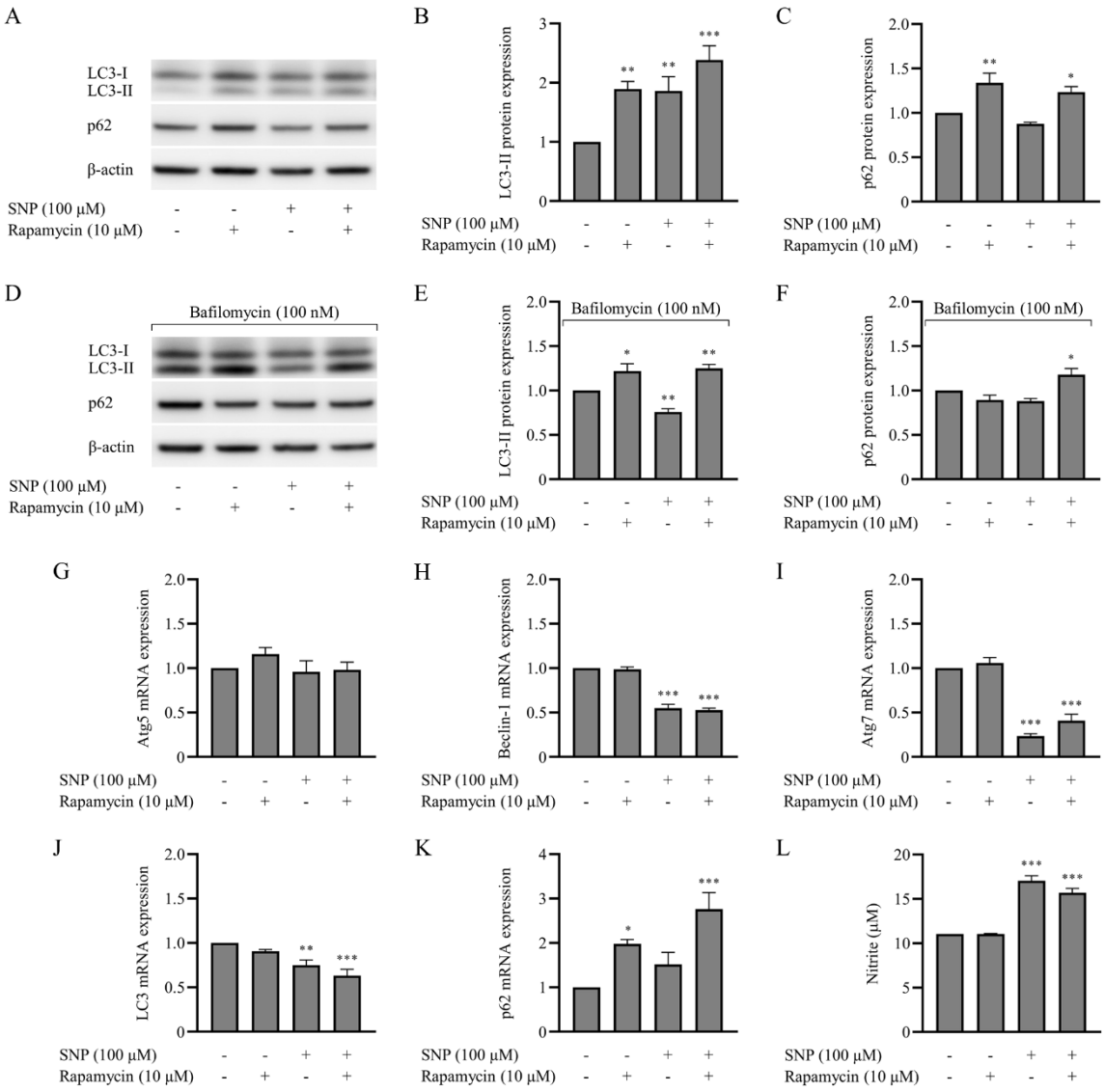

Figure 17. Treatment with SNP resulted in reduction in autophagic activity, autophagic flux and Atg mRNA expression in chondrocytes.

Chondrocytes were pre-incubated with IL-1β and either not treated or treated with 100 μM SNP under the nutrient-deprived condition for 8 h. Together with SNP treatment, the chondrocytes were incubated with the presence or absence of 10 μM rapamycin. In addition, 100 nM bafilomycin was added at 4 h before the end of the treatment to assess the autophagic flux. **(A and D)** Total protein was analyzed by Western blot, using an antibody for LC3, p62 and β-actin. **(B, C, E and F)** Comparison of the protein expression level normalized to β-actin of LC3-II and p62. **(G-K)** Comparison of the relative mRNA expression level normalized to GAPDH of Atg5, beclin-1, Atg7, LC3 and p62. **(L)** Comparison of nitrite accumulated in the cell culture supernatants, which determined by the Griess reaction. The data are represented as the mean ± SE. (compared to control: $*P < 0.05$, $**P < 0.01$ and $***P < 0.001$)

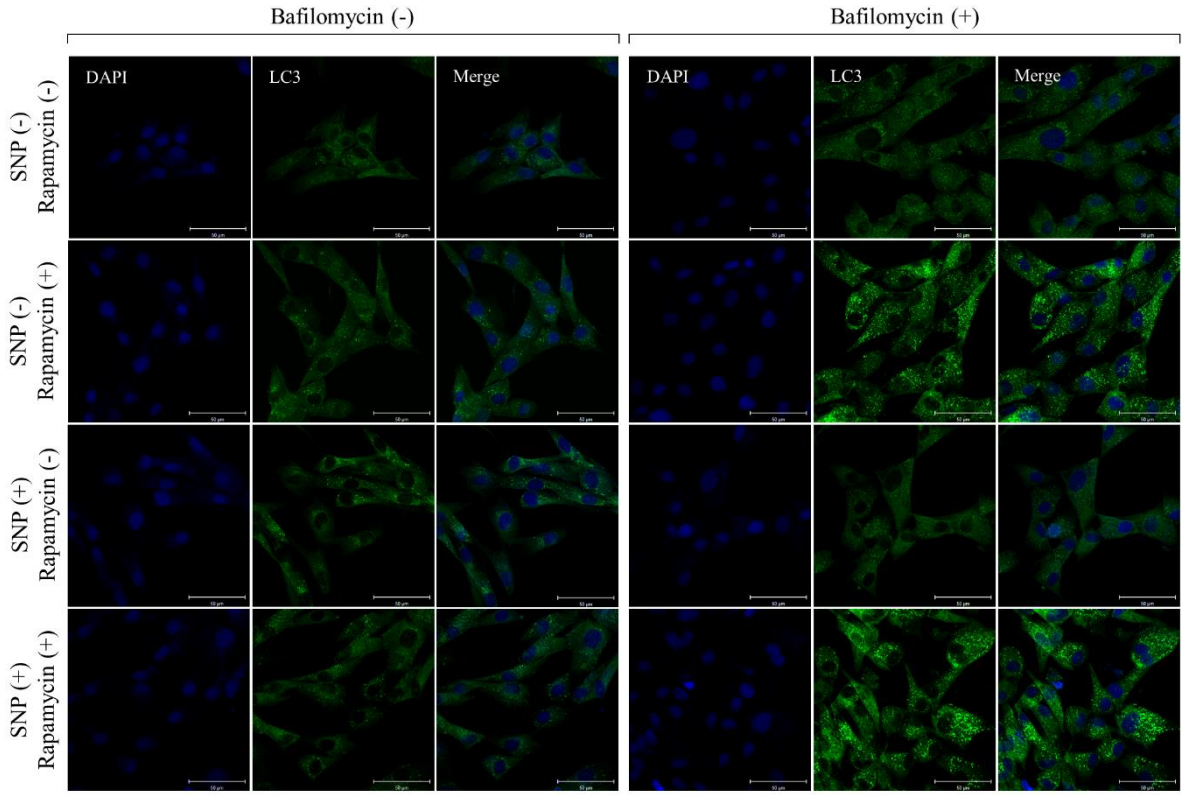

Figure 18. Treatment with SNP resulted in reduction in cytoplasmic LC3-II puncta under the presence of bafilomycin.

Chondrocytes were pre-incubated with IL-1β and either not treated or treated with 100 μM SNP under the nutrient-deprived condition for 8 h. Together with SNP treatment, the chondrocytes were incubated with the presence or absence of 10 μM rapamycin. In addition, 100 nM bafilomycin was added at 4 h before the end of the treatment to assess the autophagic flux. The cytoplasmic LC3-II puncta were detected by immunocytochemistry, using an antibody for LC3 (green). Nuclei were stained with DAPI (blue). Scale bars: 50 μm.

4.4.7 Inhibition of mTOR/p70S6K pathway by rapamycin impairs NO-induced cell apoptosis

The inhibitory effect of rapamycin on mTOR was demonstrated by Western blot analysis. Treatment with rapamycin alone significantly ($P < 0.001$) inhibits the phosphorylation of mTOR and p70S6K compared to untreated chondrocytes (Figure 19D and 19E). Even though the co-treatment with SNP attenuated the effect of rapamycin on mTOR inhibition, the similar results were still observed as indicated by the significant reduction ($P = 0.035$) in mTOR phosphorylation (Figure 19D). Whereas the phosphorylation of p70S6K remained significantly inhibited ($P < 0.001$) despite the presence of SNP (Figure 19E). Taken together with high autophagosome formation (Figure 17E) and the proportion of live cells (Figure 16B), these findings indicate that inhibition of mTOR/p70S6K pathway by rapamycin promotes cell survival through the activation of autophagy in the presence of SNP.

4.4.8 NO-induced cell apoptosis is predominantly through the caspase-independent pathway

Further investigation was focus on the molecular mechanism of NO-induced cell apoptosis by using caspase-3 assay kit and Western blot analysis to evaluate the activation of caspase-3. The results indicated extremely low caspase-3 activity, as evidenced by the low but remained detectable caspase-3 cleavage and PARP cleavage protein expression in all treatment conditions (Figure 20A). Similarly, the results from caspase-3 assay kit showed rather low and no significant difference ($P > 0.05$) of caspase-3 activity between each treatment condition (Figure 20B). Furthermore, an important caspase-independent death regulator AIF protein expression was evaluated by Western blot analysis. As shown in Figure 20C and 20D, the AIF protein expression was significantly increased in both SNP treatment alone ($P = 0.048$) and

SNP co-treatment with rapamycin (P = 0.010) compared to untreated chondrocytes. These results suggest that NO-induced cell apoptosis mainly but not completely through the caspase-independent pathway and the activation of autophagy by rapamycin is not associated with the expression level of AIF.

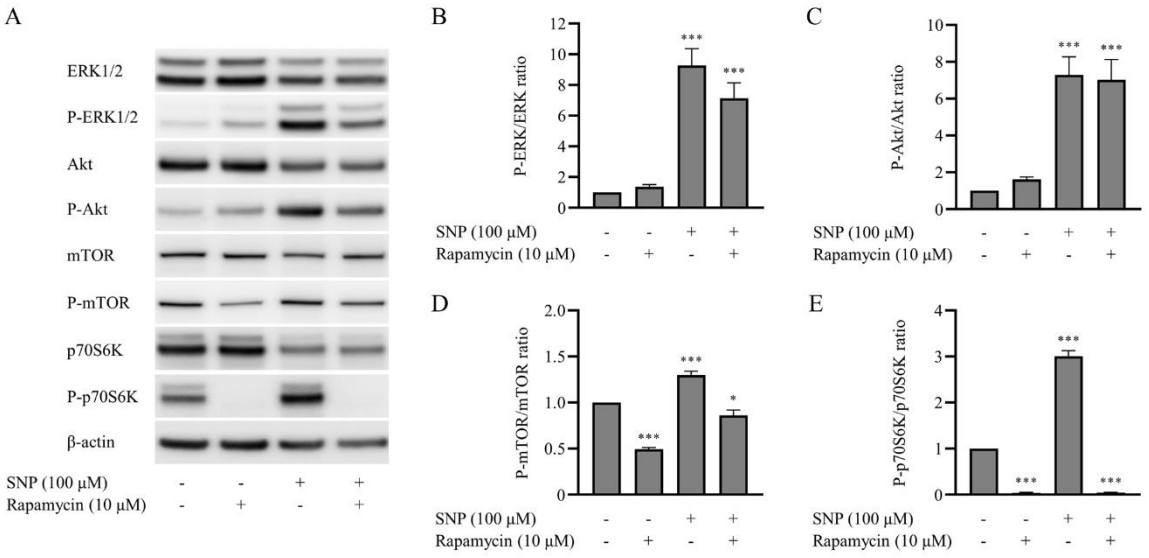

Figure 19. The phosphorylation of ERK, Akt, mTOR and p70S6K were promoted in SNP treated chondrocytes.

Chondrocytes were pre-incubated with IL-1β and either not treated or treated with 100 μM SNP under the nutrient-deprived condition for 8 h. Together with SNP treatment, the chondrocytes were incubated with the presence or absence of 10 μM rapamycin. **(A)** Total protein was analyzed by Western blot, using an antibody for ERK1/2, phospho-ERK1/2, Akt, phospho-Akt, mTOR, phospho-mTOR, p70S6K, phospho-p70S6K, and β-actin. **(B-E)** Comparison of the protein expression level normalized by the corresponding total proteins of phospho-ERK1/2, phospho-Akt, phospho-mTOR and phospho-p70S6K. The data are represented as the mean ± SE. (compared to control: $*P < 0.05$ and $***P < 0.001$)

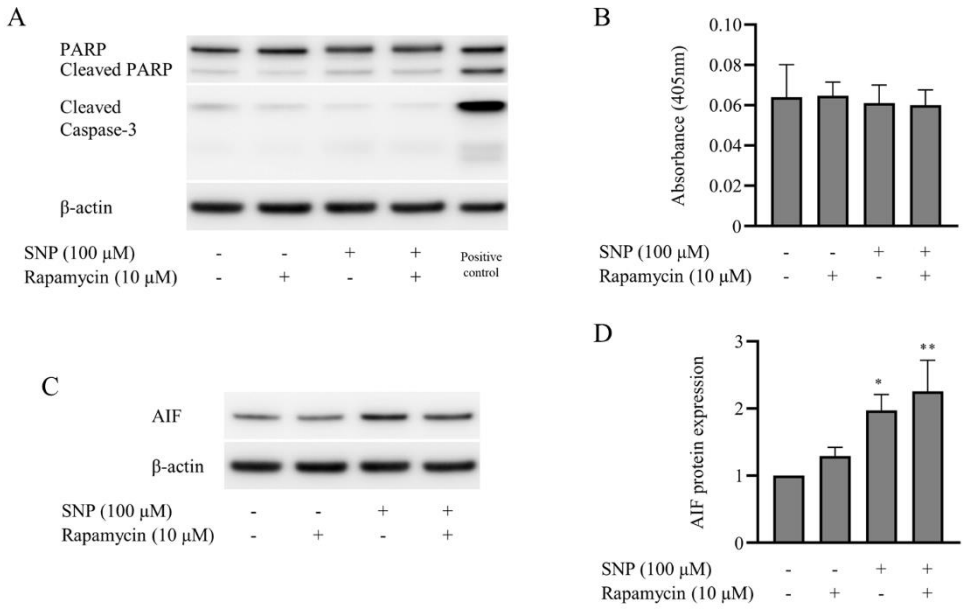

Figure 20. The cleavage of PARP and caspase-3 activation in response to apoptosis was weakly detected, while AIF was highly expressed in SNP treated chondrocytes.

Chondrocytes were pre-incubated with IL-1β and either not treated or treated with 100 μM SNP under the nutrient-deprived condition for 8 h. Together with SNP treatment, the chondrocytes were incubated with the presence or absence of 10 μM rapamycin. **(A and C)** Total protein was analyzed by Western blot, using an antibody for PARP, cleaved caspase-3, AIF and β-actin. **(B)** Comparison of caspase-3 activity in cell lysis, which determined by caspase-3 assay kit. **(D)** Comparison of the protein expression level normalized to β-actin of AIF. The data are represented as the mean ± SE. (compared to control: $*P < 0.05$ and $**P < 0.01$)

4.5 Discussion

The role of NO in articular cartilage may depend on the production rate of chondrocytes. Under physiological conditions, NO is spontaneously and constitutively synthesized in a small amount for maintaining cellular homeostasis and regulating several cellular functions. However, the production rate of NO could be altered under pathological conditions, particularly in osteoarthritic cartilage, where the overproduction of NO has occurred and detectable in the synovial fluid of arthritis patients (Kühn et al., 2004; Abramson, 2008b; DeAndrés et al., 2013; Charlier et al., 2016). An excessive amount of NO acts as a destructive mediator in osteoarthritic cartilage, which involves in disease progression and cartilage degradation (Fermor et al., 2007; Rahmati et al., 2016). Interestingly, previous studies revealed that NO alone is not cytotoxic to cultured chondrocytes, while the protective role of NO was existed and seems to be observed under certain conditions (Stefanovic‐Racic et al., 1993; Del Carlo and Loeser, 2002; Abramson, 2008a). On the other hand, several studies have demonstrated the catabolic effects of NO on articular cartilage and chondrocyte functions, especially the cytotoxic activity of NO that mediates chondrocytes apoptosis (Blanco et al., 1995; Hayashi et al., 1997). The apoptotic rate of chondrocytes in articular cartilage evidently increases with age and positively correlated with the severity of OA (Heraud, 2000). While apoptosis contributes to the development of OA, another form of programmed cell death termed autophagy was associated with cell survivability under pathological conditions. Due to the low regenerative nature of chondrocytes, an appropriate level of autophagy is an essential feature to maintain normal cellular metabolism. Notably, an inadequate level of autophagy was associated with osteoarthritic cartilage and could also be observed in chondrocytes from aging cartilage, whereas the severity of experimental OA could be reduced by activation of autophagy and enhance by inhibition of autophagy (Caramés et al., 2010; Caramés et al., 2012; Hui et al.,

2016; Cheng et al., 2017). In this study, we used canine articular chondrocytes cultured in the monolayer to demonstrates that NO-induced chondrocyte cell death was associated with both apoptosis and autophagy molecular pathways, as the treatment with NO donor resulted in apoptotic cell death and significantly reduced in the autophagic activity.

Pro-inflammatory cytokine IL-1β is the most well-known biochemical mediator that involve in the inflammatory responses. In osteoarthritic cartilage, IL-1β was contributed to the synthesis and activity of several proteolytic enzymes associated with cartilage degradation in both OA and RA. However, IL-1β alone is not enough to induce chondrocyte cell death (Kühn et al., 2004; Vuolteenaho et al., 2007; Charlier et al., 2016). Numerous studies have revealed that overproduction of NO was stimulated by IL-1β through the induction of inducible nitric oxide synthase (iNOS), which enhance disease progression (Blanco et al., 1995; Vuolteenaho et al., 2007). In contrast, an increase in NO production in this study was observed only in chondrocytes treated with either SNP alone or a combination with SNP regardless of the presence of IL-1β. The results from cell viability assay and NO quantification indicate that NO generated by SNP treated chondrocytes was not directly related to cell death. By using the same concentration of SNP, cell death only occurred in the presence of IL-1β and nutrient-deprived conditions. We speculate that the cytotoxicity of NO is dependent on the involvement of other mediators and experimental conditions, while the observed cell death may be related to an impaired autophagic activity.

In this study, our results demonstrated that NO inhibits autophagy in chondrocytes. Although at first, the SNP treated chondrocytes showed high LC3-II protein expression, which indicates an accumulation of autophagosome formation and high autophagic activity. We further confirm the result by using bafilomycin to classify the causes of accumulated autophagosome formation, as bafilomycin could block the fusion of autophagosomes with

lysosomes (Klionsky et al., 2016). Interestingly, our further investigation resulted in significantly reduced autophagic flux. These results are in consistent with the presence of cytoplasmic LC3-II puncta formation observed from immunocytochemistry images. In addition, the results from qPCR analysis further indicated that mRNA expression of autophagy-related genes; beclin-1, Atg7 and LC3 were downregulated. Taken together, we suggest that the activation of autophagy, autophagic flux and Atg mRNA expression in chondrocytes was negatively regulated by the presence of NO. Moreover, the inhibitory effect of NO on autophagy seems to depend on the promotion through mTOR signaling, the key regulator of autophagy in mammalian cells (Rabanal-Ruiz et al., 2017; Paquette et al., 2018). According to Western blot analysis, our finding indicates that NO positively regulates the phosphorylation of ERK and Akt (Notoya et al., 2000; Kim et al., 2002; Mejía-García et al., 2013), whereas the activation of ERK and Akt pathways acts synergistically to promote mTOR/p70S6K signaling (Winter et al., 2011). Our results further reveal that the autophagy inducer rapamycin could attenuate NO-induced cell apoptosis by inhibition of mTOR signaling and reduces phosphorylation of p70S6K, which resulted in an activation of autophagy as indicates by increasing in LC3-II protein expression.

Apoptosis is an active form of programmed cell death, which is defined as a highly regulated process to eliminate itself. The key features of apoptotic cells include nuclear fragmentation, condensation of chromatin, membrane blebbing and cell shrinking (Elmore, 2007). Some studies have described that SNP treated chondrocytes would result in the classical apoptosis pathway, with activation of caspase and the presence of DNA fragmentation (Notoya et al., 2000; Kühn et al., 2004; Hwang and Kim, 2015; Charlier et al., 2016). However, our results indicate that SNP treated chondrocytes expressed a surprisingly low level of both caspase-3 and PARP cleavage protein expression, which corresponded to the result from the

caspase-3 assay kit. These findings were in consistent with the protein expression of key mediators in the caspase-independent apoptosis pathway, upregulation of a mitochondrion-localized flavoprotein AIF (Candé et al., 2004; Sung et al., 2008). Taken together, our findings imply that the mechanism of chondrocyte apoptosis induces by SNP was distinct from the classical apoptosis pathway (Kühn and Lotz, 2003). We suggest that NO donor compound SNP may cause cell apoptosis mainly but not entirely through the caspase-independent pathway. However, according to various outcomes from several studies, we also believe that the mechanisms of NO donor-induced chondrocyte cell death could vary among experimental conditions (Kühn et al., 2004).

In conclusion, the study presented in this chapter demonstrates that NO inhibits autophagy and induces chondrocyte apoptosis mainly, but not entirely through the caspase-independent pathway. While the cytotoxicity of NO on chondrocytes could enhance by the involvement of other inflammatory mediators and experimental conditions. Our data suggest that autophagy is a protective mechanism in the pathogenesis of OA and could be proposed as a valuable therapeutic target for the treatment of degenerative joint diseases, particularly to reduce the toxicity of NO.

CHAPTER 5

General Conclusions

Chondrocytes are the sole resident cell that occupies approximately 1-5% of the total cartilage volume but plays a fundamental role in cartilage homeostasis by maintaining the ECM components. These chondrocytes are highly specialized cells that originate from MSC, undergo various stages of differentiation and finally reside in the cartilage matrix. Under physiological conditions, chondrocytes in articular cartilage are recognized as quiescent cells that present in post-mitotic state and exhibit extremely low synthetic activity. Despite the relatively small proportion and inactive nature of chondrocytes, their existence is an indispensable factor in maintaining cartilage homeostasis. Consequently, as the sole constituent cell, chondrocytes are primarily responsible for the pathological conditions of the cartilage. In osteoarthritic cartilage, metabolic activities of chondrocytes are altered, causing a failure of homeostasis and resulting in an imbalance between anabolic and catabolic pathways. During the course of OA, resting chondrocytes undergo a phenotypic shift and become activated chondrocytes, which results in a transient increase in proliferative activity, phenotypic instability and upregulation of several biochemical mediators associated with disease progression. Therefore, the present study was designed to investigate the cellular biology of canine articular chondrocytes in two aspects. First, we focus on the strategies to maintain phenotypic stability of chondrocytes through the restriction of cell metabolic activity and modification on the extracellular microenvironment. Second, we investigate the molecular mechanisms regulating programmed cell death on chondrocytes stimulated by a particular biochemical mediator. The finding of the present study can be classified into three sections.

In the first section, the unconventional cell culture model was established and used to observe the influence of proliferative activity and microenvironment conditions on the phenotypic stability of chondrocytes during the expansion process. Canine articular chondrocytes were seeded at three different initial seeding densities and maintained in long-

term under monolayer culture conditions without undergoing subculture after confluence. The results demonstrated that long-term monolayer culture condition allows chondrocytes to proliferate to their maximum capacity, leading to extremely high cell density with the stratified condition on culture plates that generally cannot be acquired in conventional culture methods, which subsequently promotes ECM synthesis. The chondrocytes harvested from long-term monolayer culture conditions exhibited apparently high chondrocyte phenotype, as evidenced by mRNA expression and GAGs deposition profile, suggesting that the culture condition which resembles native articular cartilage microenvironment could promote phenotypic stability and enhance the redifferentiation process of chondrocytes. Nevertheless, the redifferentiation process could be considered only partially due to some characteristics of hypertrophic differentiated chondrocytes that were correspondingly observed. These results suggest that the metabolic state of chondrocytes and the extracellular microenvironment condition exert a considerable influence on phenotypic stability and differentiation process.

In the second chapter, the effects of DMOADs named PPS, which has been previously demonstrated as a therapeutic target for OA treatment, on the phenotypic stability and proliferative activity of chondrocytes was evaluated. Canine articular chondrocytes were cultured and treated with PPS at various concentrations. The results showed that PPS reduces cell viability of cultured chondrocytes by reducing proliferative activity during the early stages of culture in a concentration- and time-dependent manner, as evidenced by the higher proportion of cells distributed in G1 phase and a lower proportion of cells distributed in S phase of the cell cycle. The PPS treated chondrocytes exhibited lower cycle regulator genes expression, particularly CDK1 and 4, suggesting that the inhibitory effect of PPS on proliferative activity was modulated through the cell cycle signaling pathway. In addition, the effect of PPS as a chondrocyte phenotype promoter and the safety of PPS on cultured

chondrocytes were confirmed. However, the underlying mechanism and correlation between the degree of inhibition on proliferative activity and phenotypic stability remained unverified in this study. These results further support that the metabolic state of chondrocytes, particularly in proliferative activity, could be a valuable target for both phenotype regulation and therapeutic approach.

In the third chapter, the effects and molecular mechanisms of a biochemical mediator, NO on chondrocyte programmed cell death was investigated. Canine articular chondrocytes were cultured and treated with SNP in several conditions. The results demonstrated that NO inhibits autophagy and induces chondrocyte apoptosis mainly, but not entirely through the caspase-independent pathway. Furthermore, the cytotoxicity of NO on cultured chondrocytes is dependent on the involvement of other inflammatory mediators and experimental conditions. These results suggest that autophagy is a protective mechanism of chondrocytes in the pathogenesis of OA and could be proposed as a valuable therapeutic target for the treatment of degenerative joint diseases. In addition, the effects of each biochemical mediator could be potentially enhanced by the involvement of other mediators, which may cause greater disease severity.

In conclusion, from this dissertation, the cellular biology of canine articular chondrocytes was investigated based on phenotypic stability and programmed cell death. The present investigation demonstrates that the metabolic state of chondrocytes is a key to maintain phenotypic stability, which could be applied for cartilage tissue regeneration and used as a prospective therapeutic target in joint diseases. Furthermore, by revealing the molecular mechanism of biochemical mediators induced programmed cell death on chondrocytes, the findings in this study will undoubtedly provide useful information on both research and clinical aspects for the treatment of joint diseases.

References

Abramson SB. 2008a. Nitric oxide in inflammation and pain associated with osteoarthritis. Arthritis Res Ther. 10(Suppl 2):S2.

Abramson SB. 2008b. Osteoarthritis and nitric oxide. Osteoarthr Cartil. 16(Suppl 2):S15–S20.

Akiyama H, Lyons JP, Mori-Akiyama Y, Yang X, Zhang R, Zhang Z, Deng JM, Taketo MM, Nakamura T, Behringer RR, et al. 2004. Interactions between Sox9 and β-catenin control chondrocyte differentiation. Genes Dev. 18(9):1072–1087.

Akkiraju H, Nohe A. 2015. Role of chondrocytes in cartilage formation, progression of osteoarthritis and cartilage regeneration. J Dev Biol. 3(4):177–192.

Anandacoomarasamy A, March L. 2010. Current evidence for osteoarthritis treatments. Ther Adv Musculoskelet Dis. 2(1):17–28.

Anderson HC. 1967. Electron microscopic studies of induced cartilage development and calcification. J Cell Biol. 35(1):81–101.

Anderson KL, O'Neill DG, Brodbelt DC, Church DB, Meeson RL, Sargan D, Summers JF, Zulch H, Collins LM. 2018. Prevalence, duration and risk factors for appendicular osteoarthritis in a UK dog population under primary veterinary care. Sci Rep. 8(1):1–12.

Archer CW, Francis-West P. 2003. The chondrocyte. Int J Biochem Cell Biol. 35(4):401–404.

Athanasiou KA, Darling EM, DuRaine GD, Hu JC, Hari Reddi A. Articular cartilage, CRC Press, Boca Raton. pp. 1–439, 2013.

Bernstein P, Sticht C, Jacobi A, Liebers C, Manthey S, Stiehler M. 2010. Expression pattern differences between osteoarthritic chondrocytes and mesenchymal stem cells during chondrogenic differentiation. Osteoarthr Cartil. 18(12):1596–1607.

Berridge MJ. 2014. Cell cycle and proliferation. Cell Signal Biol. 6:csb0001009.

Binette F, McQuaid DP, Haudenschild DR, Yaeger PC, McPherson JM, Tubo R. 1998. Expression of a stable articular cartilage phenotype without evidence of hypertrophy by adult

human articular chondrocytes in vitro. J Orthop Res. 16(2):207–216.

Blanco FJ, Ochs RL, Schwarz H, Lotz M. 1995. Chondrocyte apoptosis induced by nitric oxide. Am J Pathol. 146(1):75–85.

Bwalya EC, Kim S, Fang J, Wijekoon HMS, Hosoya K, Okumura M. 2017. Pentosan polysulfate inhibits IL-1β-induced iNOS, c-Jun and HIF-1α upregulation in canine articular chondrocytes.Gualillo O, editor. PLoS One. 12(5):e0177144.

Bwalya EC, Kim S, Fang J, Wijekoon HMS, Hosoya K, Okumura M. 2018. Pentosan polysulfate sodium restores the phenotype of dedifferentiated monolayer canine articular chondrocytes cultured in alginate beads. J Tissue Sci Eng. 09(01):1–10.

Candé C, Vahsen N, Garrido C, Kroemer G. 2004. Apoptosis-inducing factor (AIF): Caspase-independent after all. Cell Death Differ. 11(6):591–595.

Caramés B, Hasegawa A, Taniguchi N, Miyaki S, Blanco FJ, Lotz M. 2012. Autophagy activation by rapamycin reduces severity of experimental osteoarthritis. Ann Rheum Dis. 71(4):575–581.

Caramés B, Taniguchi N, Otsuki S, Blanco FJ, Lotz M. 2010. Autophagy is a protective mechanism in normal cartilage, and its aging-related loss is linked with cell death and osteoarthritis. Arthritis Rheum. 62(3):791–801.

Del Carlo M, Loeser RF. 2002. Nitric oxide-mediated chondrocyte cell death requires the generation of additional reactive oxygen species. Arthritis Rheum. 46(2):394–403.

Caron MMJ, Emans PJ, Coolsen MME, Voss L, Surtel DAM, Cremers A, van Rhijn LW, Welting TJM. 2012. Redifferentiation of dedifferentiated human articular chondrocytes: Comparison of 2D and 3D cultures. Osteoarthr Cartil. 20(10):1170–1178.

Chang J, Wang W, Zhang H, Hu Y, Wang M, Yin Z. 2013. The dual role of autophagy in chondrocyte responses in the pathogenesis of articular cartilage degeneration in osteoarthritis. Int J Mol Med. 32(6):1311–1318.

Charlier E, Deroyer C, Ciregia F, Malaise O, Neuville S, Plener Z, Malaise M, de Seny D. 2019. Chondrocyte dedifferentiation and osteoarthritis (OA). Biochem Pharmacol. 165:49–65.

Charlier E, Relic B, Deroyer C, Malaise O, Neuville S, Collée J, Malaise M, De Seny D. 2016. Insights on molecular mechanisms of chondrocytes death in osteoarthritis. Int J Mol Sci. 17(12):2146.

Cheng NT, Meng H, Ma LF, Zhang L, Yu HM, Wang ZZ, Guo A. 2017. Role of autophagy in the progression of osteoarthritis: The autophagy inhibitor, 3-methyladenine, aggravates the severity of experimental osteoarthritis. Int J Mol Med. 39(5):1224–1232.

Costa E, González-García C, Gómez Ribelles JL, Salmerón-Sánchez M. 2018. Maintenance of chondrocyte phenotype during expansion on PLLA microtopographies. J Tissue Eng. 9:1–9.

D'Angelo M, Yan Z, Nooreyazdan M, Pacifici M, Sarment DS, Billings PC, Leboy PS. 2000. MMP-13 is induced during chondrocyte hypertrophy. J Cell Biochem. 77(4):678–693.

Darling EM, Athanasiou KA. 2005. Rapid phenotypic changes in passaged articular chondrocyte subpopulations. J Orthop Res. 23(2):425–432.

Davies R, Kuiper N. 2019. Regenerative medicine: A review of the evolution of autologous chondrocyte implantation (ACI) therapy. Bioengineering. 6(1):22.

DeAndrés MC, Maneiro E, Martín MA, Arenas J, Blanco FJ. 2013. Nitric oxide compounds have different effects profiles on human articular chondrocyte metabolism. Arthritis Res Ther. 15(5).

DeAndrés MC, Takahashi A, Oreffo ROC. 2016. Demethylation of an NF-κB enhancer element orchestrates iNOS induction in osteoarthritis and is associated with altered chondrocyte cell cycle. Osteoarthr Cartil. 24(11):1951–1960.

DeMara CS, Sartori AR, Duarte AS, Andrade ALL, Pedro MAC, Coimbra IB. 2011. Periosteum as a source of mesenchymal stem cells: The effects of TGF-β3 on chondrogenesis. Clinics. 66(3):487–492.

Dreier R. 2010. Hypertrophic differentiation of chondrocytes in osteoarthritis: the developmental aspect of degenerative joint disorders. Arthritis Res Ther. 12(5):216.

Elmore S. 2007. Apoptosis: A review of programmed cell death. Toxicol Pathol. 35(4):495–516.

Fermor B, Christensen SE, Youn I, Cernanec JM, Davies CM, Weinberg JB. 2007. Oxygen, nitric oxide and articular cartilage. Eur Cells Mater. 13:56–65.

Gao Y, Liu S, Huang J, Guo W, Chen J, Zhang L, Zhao B, Peng J, Wang A, Wang Y, et al. 2014. The ECM-cell interaction of cartilage extracellular matrix on chondrocytes. Biomed Res Int. 2014:1–8.

García-Carvajal ZY, Garciadiego-Czares D, Parra- Cid C, Aguilar-Gaytn R, Velasquillo C, Ibarra C, Castro Carmo JS. Cartilage tissue engineering: The role of extracellular matrix (ECM) and novel strategies. In: Regenerative medicine and tissue engineering. Andrades JA. ed. InTech, Croatia. p. 365–397, 2013.

Gartland A, Mechler J, Mason-Savas A, MacKay CA, Mailhot G, Marks SC, Odgren PR. 2005. In vitro chondrocyte differentiation using costochondral chondrocytes as a source of primary rat chondrocyte cultures: An improved isolation and cryopreservation method. Bone. 37(4):530–544.

Gelse K, Ekici AB, Cipa F, Swoboda B, Carl HD, Olk A, Hennig FF, Klinger P. 2012. Molecular differentiation between osteophytic and articular cartilage - Clues for a transient and permanent chondrocyte phenotype. Osteoarthr Cartil. 20(2):162–171.

Gérard C, Goldbeter A. 2014. The balance between cell cycle arrest and cell proliferation: Control by the extracellular matrix and by contact inhibition. Interface Focus. 4(3):20130075.

Ghosh P. 1999. The pathobiology of osteoarthritis and the rationale for the use of pentosan polysulfate for its treatment. Semin Arthritis Rheum. 28(4):211–267.

Ghosh P, Wu A, Shimmon S, Gronthos S, Zannettino A, Itescu S. 2009. Pentosan polysulfate promotes proliferation and chondrogenic differentiation of adult human bone marrow-derived mesenchymal precursor cells. Osteoarthr Cartil. 17:S101.

Ghouri A, Conaghan PG. 2019. Update on novel pharmacological therapies for osteoarthritis. Ther Adv Musculoskelet Dis. 11:1759720X1986449.

Goldring MB. 2012. Chondrogenesis, chondrocyte differentiation, and articular cartilage metabolism in health and osteoarthritis. Ther Adv Musculoskelet Dis. 4(4):269–285.

Goldring MB, Berenbaum F. 2004. The regulation of chondrocyte function by proinflammatory mediators. Clin Orthop Relat Res.(427):37–46.

Goldring MB, Marcu KB. 2009. Cartilage homeostasis in health and rheumatic diseases. Arthritis Res Ther. 11(3):224.

Gratal P, Mediero A, Sánchez-Pernaute O, Prieto-Potin I, Lamuedra A, Herrero-Beaumont G, Largo R. 2019. Chondrocyte enlargement is a marker of osteoarthritis severity. Osteoarthr Cartil. 27(8):1229–1234.

Hall BK. Bones and cartilage: Developmental and evolutionary skeletal biology, Academic Press, Amsterdam. pp.1–792, 2005.

Hall BK. Cartilage, volume 1: Structure, function, and biochemistry, Academic Press, New York. pp.1–400, 2012.

Hayashi T, Abe E, Yamate T, Taguchi Y, Jasin HE. 1997. Nitric oxide production by superficial and deep articular chondrocytes. Arthritis Rheum. 40(2):261–269.

Hendriks J, Riesle J, Van Blitterswijk CA. 2006. Effect of stratified culture compared to confluent culture in monolayer on proliferation and differentiation of human articular chondrocytes. Tissue Eng. 12(9):2397–2405.

Henrotin Y, Sanchez C, Balligand M. 2005. Pharmaceutical and nutraceutical management of canine osteoarthritis: Present and future perspectives. Vet J. 170(1):113–123.

Heraud F. 2000. Apoptosis in normal and osteoarthritic human articular cartilage. Ann Rheum Dis. 59(12):959–965.

Hui W, Young DA, Rowan AD, Xu X, Cawston TE, Proctor CJ. 2016. Oxidative changes and signalling pathways are pivotal in initiating age-related changes in articular cartilage. Ann Rheum Dis. 75(2):449–458.

Hulth A, Lindberg L, Telhag H. 1972. Mitosis in human osteoarthritic cartilage. Clin Orthop Relat Res. 84.

Hwang HS, Kim HA. 2015. Chondrocyte apoptosis in the pathogenesis of osteoarthritis. Int J

Mol Sci. 16(11):26035–26054.

Hwang S-G, Song S-M, Kim J-R, Park C-S, Song W-K, Chun J-S. 2007. Regulation of type II collagen expression by Cyclin-dependent kinase 6, Cyclin D1, and p21 in articular chondrocytes. IUBMB Life. 59(2):90–98.

Isyar M, Yilmaz I, Yasar Sirin D, Yalcin S, Guler O, Mahirogullari M. 2016. A practical way to prepare primer human chondrocyte culture. J Orthop. 13(3):162–167.

Jhou RS, Sun KH, Sun GH, Wang HH, Chang CI, Huang HC, Lu SY, Tang SJ. 2009. Inhibition of cyclin-dependent kinases by olomoucine and roscovitine reduces lipopolysaccharide-induced inflammatory responses via down-regulation of nuclear factor κb. Cell Prolif. 42(2):141–149.

Joyce D, Albanese C, Steer J, Fu M, Bouzahzah B, Pestell RG. 2001. NF-κB and cell-cycle regulation: The cyclin connection. Cytokine Growth Factor Rev. 12(1):73–90.

Kapoor M. Pathogenesis of osteoarthritis. In: Osteoarthritis: Pathogenesis, diagnosis, available treatments, drug safety, regenerative and precision medicine. Kapoor M, Mahomed NN. eds. Springer International Publishing, Switzerland. pp. 1–28, 2015.

Karlsson C, Brantsing C, Svensson T, Brisby H, Asp J, Tallheden T, Lindahl A. 2007. Differentiation of human mesenchymal stem cells and articular chondrocytes: Analysis of chondrogenic potential and expression pattern of differentiation-related transcription factors. J Orthop Res. 25(2):152–163.

Karuppal R. 2017. Current concepts in the articular cartilage repair and regeneration. J Orthop. 14:13–15.

Katz JN, Earp BE, Gomoll AH. 2010. Surgical management of osteoarthritis. Arthritis Care Res (Hoboken). 62(9):1220–1228.

Kim SJ, Ju NW, Oh C Do, Yoon YM, Song WK, Kim JH, Yoo YJ, Bang OS, Kang SS, Chun JS. 2002. ERK-1/2 and p38 kinase oppositely regulate nitric oxide-induced apoptosis of chondrocytes in association with p53, caspase-3, and differentiation status. J Biol Chem. 277(2):1332–1339.

Klionsky DJ, Abdelmohsen K, Abe A, Abedin MJ, Abeliovich H, Arozena AA, Adachi H, Adams CM, Adams PD, Adeli K, et al. 2016. Guidelines for the use and interpretation of assays for monitoring autophagy (3rd edition). Autophagy. 12(1):1–222.

Krasnokutsky S, Attur M, Palmer G, Samuels J, Abramson SB. 2008. Current concepts in the pathogenesis of osteoarthritis. Osteoarthr Cartil. 16(Suppl 3):S1–S3.

Kühn K, D'Lima DD, Hashimoto S, Lotz M. 2004. Cell death in cartilage. Osteoarthr Cartil. 12(1):1–16.

Kühn K, Lotz M. 2003. Mechanisms of sodium nitroprusside-induced death in human chondrocytes. Rheumatol Int. 23(5):241–247.

Kumagai K, Shirabe S, Miyata N, Murata M, Yamauchi A, Kataoka Y, Niwa M. 2010. Sodium pentosan polysulfate resulted in cartilage improvement in knee osteoarthritis - An open clinical trial. BMC Clin Pharmacol. 10(1):7.

Lawrence RC, Felson DT, Helmick CG, Arnold LM, Choi H, Deyo RA, Gabriel S, Hirsch R, Hochberg MC, Hunder GG, et al. 2008. Estimates of the prevalence of arthritis and other rheumatic conditions in the United States. Part II. Arthritis Rheum. 58(1):26–35.

Lin Z, Fitzgerald JB, Xu J, Willers C, Wood D, Grodzinsky AJ, Zheng MH. 2008. Gene expression profiles of human chondrocytes during passaged monolayer cultivation. J Orthop Res. 26(9):1230–1237.

Loeser RF, Goldring SR, Scanzello CR, Goldring MB. 2012. Osteoarthritis: A disease of the joint as an organ. Arthritis Rheum. 64(6):1697–1707.

López-Alcorocho JM, Guillén-Vicente I, Rodríguez-Iñigo E, Guillén-Vicente M, Fernández-Jaén TF, Caballero R, Casqueiro M, Najarro P, Abelow S, Guillén-García P. 2019. Study of telomere length in preimplanted cultured chondrocytes. Cartilage. 10(1):36–42.

Luo P, Gao F, Niu D, Sun X, Song Q, Guo C, Liang Y, Sun W. 2019. The role of autophagy in chondrocyte metabolism and osteoarthritis: A comprehensive research review. Biomed Res Int. 2019:1–7.

LuValle P. 2000. Cell cycle control in growth plate chondrocytes. Front Biosci. 5(1):d493.

Luyten FP, Vanlauwe J. 2012. Tissue engineering approaches for osteoarthritis. Bone. 51(2):289–296.

Makris EA, Gomoll AH, Malizos KN, Hu JC, Athanasiou KA. 2015. Repair and tissue engineering techniques for articular cartilage. Nat Rev Rheumatol. 11(1):21–34.

Maldonado M, Nam J. 2013. The role of changes in extracellular matrix of cartilage in the presence of inflammation on the pathology of osteoarthritis. Biomed Res Int. 2013:1–10.

Man GS, Mologhianu G. 2014. Osteoarthritis pathogenesis - A complex process that involves the entire joint. J Med Life. 7(1):37–41.

Mao Y, Hoffman T, Wu A, Kohn J. 2018. An innovative laboratory procedure to expand chondrocytes with reduced dedifferentiation. Cartilage. 9(2):202–211.

Maroudas A, Bayliss MT, Uchitel-Kaushansky N, Schneiderman R, Gilav E. 1998. Aggrecan turnover in human articular cartilage: Use of aspartic acid racemization as a marker of molecular age. Arch Biochem Biophys. 350(1):61–71.

Martinez-Sanchez A, Dudek KA, Murphy CL. 2012. Regulation of human chondrocyte function through direct inhibition of cartilage master regulator SOX9 by microRNA-145 (miRNA-145). J Biol Chem. 287(2):916–924.

Mazzetti I, Grigolo B, Pulsatelli L, Dolzani P, Silvestri T, Roseti L, Meliconi R, Facchini A. 2001. Differential roles of nitric oxide and oxygen radicals in chondrocytes affected by osteoarthritis and rheumatoid arthritis. Clin Sci. 101(6):593–599.

Mejía-García TA, Portugal CC, Encarnação TG, Prado MAÔM, Paes-de-Carvalho R. 2013. Nitric oxide regulates AKT phosphorylation and nuclear translocation in cultured retinal cells. Cell Signal. 25(12):2424–2439.

Melero-Martin JM, Al-Rubeai M. 2007. In vitro expansion of chondrocytes. Top Tissue Eng. 3:1–37.

Mhanna R, Kashyap A, Palazzolo G, Vallmajo-Martin Q, Becher J, Möller S, Schnabelrauch M, Zenobi-Wong M. 2014. Chondrocyte culture in three dimensional alginate sulfate hydrogels promotes proliferation while maintaining expression of chondrogenic markers. Tissue Eng Part

A. 20(9–10):1454–1464.

Miller RE, Miller RJ, Malfait A-M. 2014. Osteoarthritis joint pain: The cytokine connection. Cytokine. 70(2):185–193.

Mobasheri A. 2013. The future of osteoarthritis therapeutics: Targeted pharmacological therapy. Curr Rheumatol Rep. 15(10):364.

Mora JC, Przkora R, Cruz-Almeida Y. 2018. Knee osteoarthritis: Pathophysiology and current treatment modalities. J Pain Res. 11:2189–2196.

Musumeci G, Castrogiovanni P, Trovato FM, Weinberg AM, Al-Wasiyah MK, Alqahtani MH, Mobasheri A. 2015. Biomarkers of chondrocyte apoptosis and autophagy in osteoarthritis. Int J Mol Sci. 16(9):20560–20575.

Nam Y, Rim YA, Lee J, Ju JH. 2018. Current therapeutic strategies for stem cell-based cartilage regeneration. Stem Cells Int. 2018:1–20.

Neogi T. 2013. The epidemiology and impact of pain in osteoarthritis. Osteoarthr Cartil. 21(9):1145–1153.

Nishida K, Doi T, Inoue H. 2000. The role of nitric oxide in arthritic joints: a therapeutic target? Mod Rheumatol. 10(2):63–67.

Notoya K, Jovanovic D V., Reboul P, Martel-Pelletier J, Mineau F, Pelletier J-P. 2000. The induction of cell death in human osteoarthritis chondrocytes by nitric oxide is related to the production of prostaglandin E2 via the induction of cyclooxygenase-2. J Immunol. 165(6):3402–3410.

Oakes BW, Handley CJ, Lisner F, Lowther DA. 1977. An ultrastructural and biochemical study of high density primary cultures of embryonic chick chondrocytes. J Embryol Exp Morphol. 38:239–263.

Otero M, Favero M, Dragomir C, Hachem K El, Hashimoto K, Plumb DA, Goldring MB. 2012. Human chondrocyte cultures as models of cartilage-specific gene regulation. Methods Mol Biol. 806(7):301–36.

Ovalle WK, Nahirney PC. Netter's essential histology, Elsevier Health Sciences, Philadelphia. pp. 1–512, 2013.

Paquette M, El-Houjeiri L, Pause A. 2018. mTOR pathways in cancer and autophagy. Cancers (Basel). 10(1).

Patti AM, Gabriele A, Rocca CD. 1999. Human chondrocyte cell lines from articular cartilage of metatarsal phalangeal joints. Tissue Cell. 31(6):550–554.

Phull A-R, Eo S-H, Abbas Q, Ahmed M, Kim SJ. 2016. Applications of chondrocyte-based cartilage engineering: An overview. Biomed Res Int. 2016:1–17.

Poole AR. 2012. Osteoarthritis as a Whole Joint Disease. HSS J. 8(1):4–6.

Puig-Junoy J, Ruiz Zamora A. 2015. Socio-economic costs of osteoarthritis: A systematic review of cost-of-illness studies. Semin Arthritis Rheum. 44(5):531–541.

Rabanal-Ruiz Y, Otten EG, Korolchuk VI. 2017. MTORC1 as the main gateway to autophagy. Essays Biochem. 61(6):565–584.

Rahmati M, Mobasheri A, Mozafari M. 2016. Inflammatory mediators in osteoarthritis: A critical review of the state-of-the-art, current prospects, and future challenges. Bone. 85:81–90.

Responte DJ, Natoli RM, Athanasiou KA. 2007. Collagens of articular cartilage: Structure, function, and importance in tissue engineering. Crit Rev Biomed Eng. 35(5):363–411.

Ripmeester EGJ, Timur UT, Caron MMJ, Welting TJM. 2018. Recent insights into the contribution of the changing hypertrophic chondrocyte phenotype in the development and progression of osteoarthritis. Front Bioeng Biotechnol. 6:18.

Robinson WH, Lepus CM, Wang Q, Raghu H, Mao R, Lindstrom TM, Sokolove J, Centers C, Affairs V, Alto P, et al. 2016. Low-grade inflammation as a key mediator of the pathogenesis of osteoarthritis. Nat Rev Rheumatol. 12(10):580–592.

Rothwell AG, Bentley G. 1973. Chondrocyte multiplication in osteoarthritic articular cartilage. J Bone Joint Surg Br. 55(3):588–594.

Roy S, Meachim G. 1968. Chondrocyte ultrastructure in adult human articular cartilage. Ann

Rheum Dis. 27(6):544–558.

Sandell LJ, Aigner T. 2001. Articular cartilage and changes in arthritis: Cell biology of osteoarthritis. Arthritis Res Ther. 3(2):107.

Sarkar S, Korolchuk VI, Renna M, Imarisio S, Fleming A, Williams A, Garcia-Arencibia M, Rose C, Luo S, Underwood BR, et al. 2011. Complex inhibitory effects of nitric oxide on autophagy. Mol Cell. 43(1):19–32.

Sasaki H, Takayama K, Matsushita T, Ishida K, Kubo S, Matsumoto T, Fujita N, Oka S, Kurosaka M, Kuroda R. 2012. Autophagy modulates osteoarthritis-related gene expression in human chondrocytes. Arthritis Rheum. 64(6):1920–1928.

Schulze-Tanzil G. 2009. Activation and dedifferentiation of chondrocytes: Implications in cartilage injury and repair. Ann Anat - Anat Anzeiger. 191(4):325–338.

Schulze-Tanzil G, Souza P de, Castrejon HV, John T, Merker H-J, Scheid A, Shakibaei M. 2002. Redifferentiation of dedifferentiated human chondrocytes in high-density cultures. Cell Tissue Res. 308(3):371–379.

Shapiro F. Pediatric orthopedic deformities, volume 1, Springer International Publishing, Boston. pp. 1–789, 2015.

Shen C, Yan J, Erkocak OF, Zheng X-F, Chen X-D. 2014. Nitric oxide inhibits autophagy via suppression of JNK in meniscal cells. Rheumatology. 53(6):1022–1033.

Shi S, Wang C, Acton AJ, Eckert GJ, Trippel SB. 2015. Role of Sox9 in growth factor regulation of articular chondrocytes. J Cell Biochem. 116(7):1391–1400.

Sokolove J, Lepus CM. 2013. Role of inflammation in the pathogenesis of osteoarthritis: Latest findings and interpretations. Ther Adv Musculoskelet Dis. 5(2):77–94.

Sophia Fox AJ, Bedi A, Rodeo SA. 2009. The basic science of articular cartilage: Structure, composition, and function. Sport Heal A Multidiscip Approach. 1(6):461–468.

Sørensen HP, Vivès RR, Manetopoulos C, Albrechtsen R, Lydolph MC, Jacobsen J, Couchman JR, Wewer UM. 2008. Heparan sulfate regulates ADAM12 through a molecular switch

mechanism. J Biol Chem. 283(46):31920–31932.

Stefanovic-Racic M, Stadler J, Evans CH. 1993. Nitric oxide and arthritis. Arthritis Rheum. 36(8):1036–1044.

Stewart MC, Saunders KM, Burton-Wurster N, MacLeod JN. 2000. Phenotypic stability of articular chondrocytes in vitro: The effects of culture models, bone morphogenetic protein 2, and serum supplementation. J Bone Miner Res. 15(1):166–174.

Stichtenoth DO, Frölich JC. 1998. Nitric oxide and inflammatory joint diseases. Br J Rheumatol. 37(3):246–257.

Sunaga T, Oh N, Hosoya K, Takagi S, Okumura M. 2012. Inhibitory effects of pentosan polysulfate sodium on MAP-kinase pathway and NF-κB nuclear translocation in canine chondrocytes in vitro. J Vet Med Sci. 74(6):707–711.

Sung WL, Yeon SS, Sang HS, Kyung TK, Young CP, Bong SP, Yun I, Kim K, Sang YL, Won TC, et al. 2008. Cilostazol protects rat chondrocytes against nitric oxide-induced apoptosis in vitro and prevents cartilage destruction in a rat model of osteoarthritis. Arthritis Rheum. 58(3):790–800.

Takahashi T, Ogasawara T, Asawa Y, Mori Y, Uchinuma E, Takato T, Hoshi K. 2007. Three-dimensional microenvironments retain chondrocyte phenotypes during proliferation culture. Tissue Eng. 13(7):1583–1592.

VanderKraan PM, van den Berg WB. 2012. Chondrocyte hypertrophy and osteoarthritis: Role in initiation and progression of cartilage degeneration? Osteoarthr Cartil. 20(3):223–232.

Verzijl N, DeGroot J, Thorpe SR, Bank RA, Shaw JN, Lyons TJ, Bijlsma JWJ, Lafeber FPJG, Baynes JW, TeKoppele JM. 2000. Effect of collagen turnover on the accumulation of advanced glycation end products. J Biol Chem. 275(50):39027–39031.

Villar-Suárez V, Calles-Venal I, Bravo IG, Fernández-Álvarez JG, Fernández-Caso M, Villar-Lacilla JM. 2004. Differential behavior between isolated and aggregated rabbit auricular chondrocytes on plastic surfaces. J Biomed Biotechnol. 2004(2):86–92.

Vuolteenaho K, Moilanen T, Knowles RG, Moilanen E. 2007. The role of nitric oxide in

osteoarthritis. Scand J Rheumatol. 36(4):247–258.

Walsh WR, Walton M, Bruce W, Yu Y, Gillies RM, Svehla M. Part II - Structure and function of bone and cartilage. In: Handbook of histology methods for bone and cartilage. An YH, Martin KL, eds. Humana Press Inc, Totowa. pp. 35–73, 2003.

Watt FM. 1988. Effect of seeding density on dtability of the differentiated phenotype of pig articular chondrocytes in culture. JCell Sci. 89 (Pt 3)(0021–9533):373–378.

Winter JN, Jefferson LS, Kimball SR. 2011. ERK and Akt signaling pathways function through parallel mechanisms to promote mTORC1 signaling. Am J Physiol - Cell Physiol. 300(5):1172–1180.

Xia Y, Momot KI, Chen Z, Chen CT, Kahn D, Badar F. Introduction to cartilage. In: Biophysics and biochemistry of cartilage by NMR and MRI. Xia Y, Momot KI. eds. The Royal Society of Chemistry, Cambridge. pp. 1–43, 2017.

Yamamoto K, Okano H, Miyagawa W, Visse R, Shitomi Y, Santamaria S, Dudhia J, Troeberg L, Strickland DK, Hirohata S, Nagase H. 2016. MMP-13 is constitutively produced in human chondrocytes and co-endocytosed with ADAMTS-5 and TIMP-3 by the endocytic receptor LRP1. Matrix Biol. 56:57–73.

Yu SP, Hunter DJ. 2015. Managing osetoarthritis. Aust Prescr. 38(4):115–119.

Yuan X-Y, Zhang L, Wu Y. Specific proteases for osteoarthritis diagnosis and therapy. In: Osteoarthritis: Progress in basic research and treatment. Chen Q. ed. IntechOpen, Rijeka. pp. 159–178, 2015.

Zhang L, Hu J, Athanasiou KA. 2009. The role of tissue engineering in articular cartilage repair and regeneration. Crit Rev Biomed Eng. 37(1–2):1–57.

Zhang W, Robertson WB, Zhao J, Chen W, Mason D. 2019. Emerging trend in the pharmacotherapy of osteoarthritis. Front Endocrinol (Lausanne). 10(July):1–9.

Zhong L, Huang X, Karperien M, Post J. 2016. Correlation between gene expression and osteoarthritis progression in human. Int J Mol Sci. 17(7):1126.

Abstract of the Dissertation

The Cellular Physiology of Canine Chondrocytes: an in-vitro Study on Phenotype Regulation and Characteristics of Cell Death

Articular cartilage is a thin layer of highly specialized connective tissue that covers the ends of the bones where they articulate with each other and form a joint. The structure of articular cartilage is regulated by chondrocytes, which responsible for cartilage homeostasis by maintaining the extracellular matrix (ECM) components through the formation and degradation process. Alteration in metabolic activities of chondrocytes could lead to homeostasis imbalance and resulting in a degenerative condition of articular cartilage.

Osteoarthritis (OA), which is also referred to as degenerative joint disease, is the most common form of arthritis characterized by the progressive breakdown of articular cartilage. During OA progression, resting chondrocytes undergo a phenotypic shift and become activated chondrocytes, which results in a transient increase in proliferative activity, phenotypic instability and upregulation of several biochemical mediators associated with disease progression. A comprehensive investigation of chondrocyte responses in OA conditions will be beneficial for cartilage degenerative disease treatment.

Therefore, the present study was constructed to investigate the cellular biology of canine articular chondrocytes based on two major purposes. The first objective was to identify the effect of cell metabolic activity and extracellular microenvironment on the phenotypic stability of chondrocytes. The second objective was to investigate the molecular mechanisms regulating programmed cell death on chondrocytes stimulated by a particular biochemical mediator.

The dissertation is structured into three experimental sections: First, the unconventional cell culture model was established and used to observe the influence of proliferative activity and microenvironment conditions on the phenotypic stability of chondrocytes during the expansion process. Second, the effects of disease modifying osteoarthritic drugs (DMOADs) named pentosan polysulfate (PPS) was evaluated on the phenotypic stability and proliferative activity of chondrocytes, particularly in cell cycle modulation. In the last section, the molecular mechanisms regulating apoptosis and autophagy in nitric oxide (NO) -induced chondrocyte cell death were investigated.

Findings of the current study provide evidence that the metabolic state of chondrocytes and the extracellular microenvironment condition exert a considerable influence on phenotypic stability and differentiation process. These results were supported by the inhibitory effect of PPS on cell cycle progression while maintaining the phenotypic stability of chondrocytes. In cartilage, both forms of programmed cell death, apoptosis and autophagy are essential cellular degradation mechanisms that influence the homeostasis and survivability of chondrocytes. The results of the current study confirmed that NO inhibits autophagy and induces chondrocyte apoptosis, while autophagy is a protective mechanism of chondrocytes in the pathogenesis of OA and could be proposed as a valuable therapeutic target for the treatment of degenerative joint diseases.

The main conclusions drawn from this research were that the metabolic state of chondrocytes would be a key to maintain phenotypic stability, which could be applied for cartilage tissue regeneration and used as a prospective therapeutic target in joint diseases. Furthermore, by revealing the molecular mechanism of biochemical mediators induced programmed cell death on chondrocytes, the findings in this study will undoubtedly provide useful information on both research and clinical aspects for the treatment of joint diseases.

Acknowledgements

The completion of this dissertation would not have been possible without the scientific support and kind assistance of many individuals. First and foremost, I would like to express my deep and sincere gratitude to my supervisor Prof. Masahiro Okumura (Graduate School of Veterinary Medicine, Hokkaido University), for giving me a great opportunity to study in the Laboratory of Veterinary Surgery, Hokkaido University, and for his continuous support, immense knowledge, motivation, supervision and attention given to me during the past several years. This dissertation would not have been possible without his guidance and persistent support.

Besides my supervisor, I would like to thank the rest of my co-advisors and thesis committee: Prof. Kazuhiro Kimura, Prof. Takashi Kimura, Associate Prof. Atsushi Kobayashi and Assistant Prof. Takafumi Sunaga for their encouragement, insightful comments and valuable guidance. I am exceptionally thankful to Prof. Takashi Kimura for his immense support and all materials for the electron microscope technique. My sincere thanks also go to Assistant Prof. Sangho Kim and Assistant Prof. Ryosuke Echigo for their constant support on research materials.

I would like to offer my special thanks to Dr. Eugene Bwalya for his critical advice and constructive comments on papers for publication, Dr. Suranji Wijekoon and Jing Fang for the basic experiment skills and technical support at the beginning of my PhD program. Also, special thanks go to all of my laboratory colleagues, Dr. Tatsuya Deguchi, Mijiddorj Tsogbadrakh, Yusuke Murase, Sung Koangyong, Wang Yanlin, Mwale Carol and Mika Sumita for their kind support during the study period and for sharing every unforgettable moment.

I would like to thank Japanese Government, The Ministry of Education, Culture, Sports, Science and Technology (MEXT) for their financial support through the Monbukagakusho Scholarship. In addition, I am thankful to all staff of the leading program office and academic affairs section for all supports during my PhD program.

Finally, I would like to acknowledge with gratitude to my parents, Anant and Busarin Akaraphutiporn, brothers and sister, for supporting me spiritually throughout my life. Last but not least, I would like to thank Achiraya Khamanarong for all her love, encouragement and support. This accomplishment would not have been possible without all these people.

Hokkaido University, 2020

Dr. Ekkapol Akaraphutiporn